

Ocular Onchocerciasis – The Role of Toll-Like Receptor-2 and Interferon- γ

Dissertation

zur

Erlangung des Doktorgrades (Dr. rer. nat.)

der

Mathematisch-Naturwissenschaftlichen Fakultät

der

Rheinischen Friedrich-Wilhelms-Universität Bonn

vorgelegt von

Dr. med. Katrin Gentil

aus Suhl

Bonn 2009

Gedruckt mit Genehmigung
der mathematisch-naturwissenschaftlichen Fakultät
der Rheinischen-Friedrich-Wilhelms-Universität Bonn

Referent: Prof. W. Kolanus
Koreferent: Prof. A. Hoerauf
Tag der mündlichen Prüfung: 23.02.2010
Erscheinungsjahr: 2010

Ocular Onchocerciasis - the Role of Toll-Like Receptor 2 and Interferon- γ

Abstract

by

KATRIN GENTIL

River Blindness is still highly prevalent in subsaharan Africa with millions of people suffering from the infection with *Onchocerca volvulus*. This filarial worm harbors the endosymbiont *Wolbachia* which was found to be essential for worm survival. The immune system of chronically infected individuals is constantly stimulated with worm proteins, lipids, carbohydrates and released *Wolbachia* from dying worms. In this study, I investigated the activation of the adaptive immune system by *O. volvulus* and *Wolbachia* in a mouse model of onchocercal keratitis.

Toll-like receptors (TLRs) are innate immune receptors that are activated by conserved bacterial and viral products. Lately, it was also demonstrated that fungal and helminth products can activate selected TLRs. During filarial infection, stimulation occurs through both bacterial and parasitic products, I therefore focused on the role of TLR2 and TLR4 in the pathogenesis of adaptive immune responses and keratitis development.

Using a mouse model of onchocercal keratitis, I immunized C57BL/6, TLR2^{-/-} and TLR4^{-/-} mice with *O. volvulus* protein extract and examined granulocyte migration to the corneal stroma following local injection of this protein extract. I found that TLR2 was required for IFN γ production by splenocytes, CXC chemokine production in the

cornea and neutrophil migration to the corneal stroma, but not for IL-5 production or eosinophil migration.

IFN γ was shown to increase surface expression of TLR2 on macrophages, priming them for further activation via TLR2 agonists like onchocercal protein extract. The pro-inflammatory cytokines produced by macrophages induced chemokine production by corneal fibroblasts. This is one pathway of IFN γ enhanced neutrophil migration to the corneal stroma.

Other parts of this study showed that pro-inflammatory Th₁ responses were predominantly induced by the endosymbiont *Wolbachia* rather than the filarial worm itself, whereas Th₂ responses were mainly induced by the worm.

One wolbachial protein that has been previously described and acts as immuno-activator is the *Wolbachia* surface protein. I characterized TLR2-dependent activation of primary macrophages and splenocytes and identified the region 121-240 of the protein as the main immunostimulatory domain.

Acknowledgements

For their support of my work during the last four years, I would like to thank the following people:

Eric Pearlman - thank you for accepting me in your lab, providing me with a place to learn about filarial research and giving me the freedom to develop my own ideas. Thank you for useful discussions and scientific support.

Achim Hörauf - thank you for encouraging me to go for a Ph.D. and supporting me through the final stages.

Amy G. Hise - thank you for valuable input on experimental designs, new ideas and for being a great friend all along. Thank you to your family as well.

Michelle Lin and Angela Johnson - thank you for being great labmates, helpfull with discussions and friends outside the lab.

Eugenia Diaconu - thank you for helping with all those mouse injections, I will not count how many we did over the years.

Maria Mackroth, Jose-Andres Portillo-Christen and everyone else at the Department of Ophthalmology and the Center for Global Health and Diseases at Case Western Reserve University - thank you for being a great group to work with.

Meinen Eltern Sabine und Ulrich Dähnel - Danke, dass ihr mir den Freiraum gegeben habt, mich zu dem Menschen zu entwickeln, der ich heute bin. Danke auch, dass ihr meine diversen Auslandsaufenthalte immer unterstützt habt, auch wenn es für euch nicht immer leicht war.

Johannes - Danke für die letzten vier Jahre mit dir! Du bist das Wichtigste, was ich aus Cleveland mit nach Deutschland zurückgebracht habe!

This work was supported in part by a grant by the Deutsche Forschungsgemeinschaft
(DÄ1024/1-1)

Table of Contents

Acknowledgements	v
List of Tables	ix
List of Figures	x
Chapter 1. Introduction	1
River Blindness	1
<i>Wolbachia</i>	2
Cornea	3
Mouse Model of River Blindness	4
Antigen-presenting cells	9
Toll-like Receptors	13
Interferon- γ	16
Aims	17
Chapter 2. Materials and Methods	18
Reagents	18
Mice	22
<i>In vivo</i> studies	22
Cell culture	23
FACS	26
Immunohistochemistry	27
ELISA	29
Statistical analysis	29
	vii

Chapter 3. Results	30
<i>In vitro</i> activation of antigen-presenting cells	30
The role of TLR2 and TLR4 in the generation of adaptive immune responses	40
The role of TLR2 and TLR4 in corneal inflammation	41
The role of IFN- γ in the generation of adaptive immune responses	47
IFN- γ induced cytokine responses in macrophages and fibroblasts	50
Activation of macrophages, neutrophils and fibroblasts by pro-inflammatory cytokines.	55
The role of IL-1R1, IL-6 and TNF α in T cell responses and corneal inflammation	58
<i>In vivo</i> responses to <i>Wolbachia</i>	61
<i>In vitro</i> responses to rWSP	66
Chapter 4. Discussion	73
Activation of antigen-presenting cells	73
TLR2 in the adaptive immune response	75
IFN- γ in the adaptive immune response	77
<i>Wolbachia</i>	80
BmWSP	81
Revised mouse model of Onchocerciasis	85
Chapter 5. Summary	87
References	89

List of Tables

2.1	Primers used in this study.	20
2.2	Antibodies used in this study.	27

List of Figures

1.1	Ocular structure	4
1.2	Corneal structure	5
1.3	Sequence of events	8
3.1	Cytokine Production by Dendritic Cells	31
3.2	Relative Expression of Dendritic Cell Surface Activation Markers	32
3.3	Histogram of Dendritic Cell Surface Activation Markers	33
3.4	Cytokine Production by Macrophages	34
3.5	Release of Myeloperoxide by Neutrophils	35
3.6	Production of MIP-2 by Neutrophils	36
3.7	Production of Nitric Oxide by Neutrophils	37
3.8	Production of Reactive Oxygen Species by Neutrophils	38
3.9	Expression of Neutrophil Surface Activation Markers	39
3.10	Splenocyte responses of C57BL/6, TLR2 ^{-/-} and TLR4 ^{-/-} mice	41
3.11	Levels of IgE in C57BL/6, TLR2 ^{-/-} and TLR4 ^{-/-} mice	42
3.12	Levels of IgG ₁ and IgG _{2c} in C57BL/6, TLR2 ^{-/-} and TLR4 ^{-/-} mice	42
3.13	Cross Section of the Cornea	43
3.14	Neutrophil Migration to the Cornea of C57BL/6, TLR2 ^{-/-} and TLR4 ^{-/-} mice	44
3.15	Eosinophil Migration to the Cornea of C57BL/6, TLR2 ^{-/-} and TLR4 ^{-/-} mice	44

3.16	PECAM-1 Expression on Limbal Vessels	46
3.17	CXC Chemokine Levels in the Cornea	46
3.18	Splenocyte Responses of C57BL/6 and IFN- $\gamma^{-/-}$ Mice	47
3.19	Granulocyte Migration to the Corneas of C57BL/6 and IFN- $\gamma^{-/-}$ Mice	48
3.20	PECAM-1 Expression in the Corneas of C57BL/6 and IFN- $\gamma^{-/-}$ Mice	49
3.21	IFN- γ -induced Activation of Macrophages	51
3.22	Priming of Macrophages by IFN- γ	52
3.23	Chemokine Production by Macrophages	53
3.24	IFN- γ -induced Neutrophil Activation	53
3.25	IFN- γ -induced Activation of MK/T-1 Cells	54
3.26	Surface TLR2 Expression by Macrophages	55
3.27	Macrophage Activation by Pro-inflammatory Cytokines	56
3.28	Neutrophil Activation by Pro-inflammatory Cytokines	57
3.29	Activation of MK/T-1 Cells by Stimulation with Pro-inflammatory Cytokines	57
3.30	Splenocyte Responses of C57BL/6 and IL-1R1 $^{-/-}$ Mice	59
3.31	Splenocyte Responses of C57BL/6 and IL-6 $^{-/-}$ Mice	59
3.32	Splenocyte Responses of C57BL/6 and TNF α R $^{-/-}$ Mice	60
3.33	Granulocyte Migration to the Corneas of C57BL/6 and IL-1R1 $^{-/-}$ Mouse Corneas	61
3.34	Granulocyte Migration to the Corneas of C57BL/6 and IL-6 $^{-/-}$ Mouse Corneas	62

3.35	Granulocyte Migration to the Corneas of C57BL/6 and TNF α R ^{-/-} Mouse	
	Corneas	62
3.36	Granulocyte Migration to the Cornea after Injection of <i>Wolbachia</i>	
	Depleted Extract	64
3.37	Splenocyte Responses to <i>A. viteae</i> and <i>Wolbachia</i>	65
3.38	Granulocyte Migration after <i>A. viteae</i> and <i>Wolbachia</i> Injection	65
3.39	Gene Sequence BmWSP	67
3.40	Amino Acid Sequence BmWSP	68
3.41	HEK Cell Stimulation with rWSP	69
3.42	Macrophage Stimulation with rWSP	70
3.43	Splenocyte Responses to rWSP	71
3.44	BmWSP-Specific IgG ₁ Levels in C57BL/6 Mice	72
4.1	Sequence of Events - Systemic Responses	85
4.2	Sequence of Events - IFN- γ -Dependent Responses	86

1 Introduction

1.1 River Blindness

Filarial nematodes cause the debilitating diseases river blindness and lymphatic filariasis. Lymphatic filariasis is caused by *Brugia malayi* or *Wuchereria bancrofti*. It is characterized by immense swelling of mainly the lower limbs and the scrotum. An estimated 120 million people are affected by this disease, the majority of them in India and Africa (1).

Onchocerca volvulus is the causative agent of river blindness. River blindness is mainly prevalent in Africa and distributed along rivers. *O. volvulus* is transmitted by *Simulium* species. Upon a blood meal on infected individuals, first stage larvae are taken up. The larvae undergo two molting steps before reaching the infectious L3 stage. During the next blood meal, L3 larvae are transmitted into humans. They undergo 2 further moltings and mature into adult male and female worms. Female worms produce L1 microfilariae thus completing the life cycle.

Infections with *O. volvulus* are classically treated with ivermectin, a microfilaricidal drug, which is also used for mass drug administration to decrease transmission of *O. volvulus*. Treatment with the filaricidal drug diethylcarbamazine, especially for mass

drug administration, is now contraindicated due to severe adverse reaction, especially increased corneal inflammation (2, 3).

1.2 *Wolbachia*

Intracellular bacteria in filarial worms were first described by Kozek et al. in 1977 (4). At this time, bacteria showing three distinct developmental forms were found in the lateral chords and larvae, and were suspected to be more closely related to *Chlamydiae* than to *Rickettsiae*. Sironi et al (5) could demonstrate by phylogenetic analysis of 16S rDNA that these bacteria belong to the α -Proteobacteria, order Rickettsiales with *Wolbachia pipientis* of arthropods as the closest relative.

Wolbachia are present in nematodes throughout larval development with microfilariae having the lowest *Wolbachia* load and increasing numbers during development to L4 larvae in the human host (6, 7). The levels of *Wolbachia* in nematodes correlate with severity of disease (8). It has also been shown that neutrophils accumulate around *Wolbachia*-containing worms, but not around worms that are *Wolbachia*-depleted (9).

Treatment with ivermectin or diethylcarbamazine causes microfilarial death. Upon worm death, microfilariae are released into the blood and cause pro-inflammatory immune responses: fever, tachycardia, and hypotension. Exacerbated corneal inflammation was also found during post-treatment reactions (10). These increased inflammatory responses are shown to be correlated with wolbachial DNA in the blood (10, 11).

Alternatives to the traditional treatment with ivermectin and diethylcarbamazine now include tetracyclines that kill *Wolbachia*. It was found that bacterial death is associated with decreased worm fecundity and growth retardation (12). Other studies found

decreased embryogenesis after treatment with rifampicin (13) and macrofilaricidal effects with longer dose regimens of doxycycline (14).

1.3 Cornea

The cornea is the transparent outer part of the eye (Figure 1.1). Together with the lens, it forms the optical apparatus. The cornea consists of three layers: the inner single layer endothelium, the 450 μm thick corneal stroma and the outer multilayer epithelium (Figure 1.2). Corneal transparency is essential for intact vision and depends on the organized structure of the corneal matrix, mainly made up of collagen fibrils. Disruption of the collagen fibril structure results in opacification of the cornea, visual impairment and eventual blindness. Infection or inflammation of the cornea usually leads to the infiltration of inflammatory cells (15). During *O. volvulus* infection, eosinophils and neutrophils migrate to the corneal stroma. The granulocytes release cytokines and granular components, disrupting the corneal structure and leading to visual impairment.

Lipopolysaccharide-induced corneal inflammation has been studied in more detail. Neutrophils extravasate from limbal vessels and migrate through the corneal stroma, depending on the presence of TLR4 and PECAM-1 (16). Migration of neutrophils is depending on the presence of the neutrophil chemokines KC, MIP-2 and LIX with corneal fibroblasts as the most probable source for KC and LIX while resident macrophages are producing MIP-2 (17). Activated neutrophils in the cornea release additional MIP-2 (17). Neutrophils also express MMP-8 to facilitate migration through the corneal stroma as there is no MMP-8 expression in CXCR2^{-/-} corneas where neutrophils are absent following LPS challenge and neutrophil migration to the cornea is decreased in MMP-8^{-/-}

mice (18). MMP-8 induces proteolytic cleavage of the extracellular collagen matrix (18), causing disruption of the organized corneal structure and thus opacification.

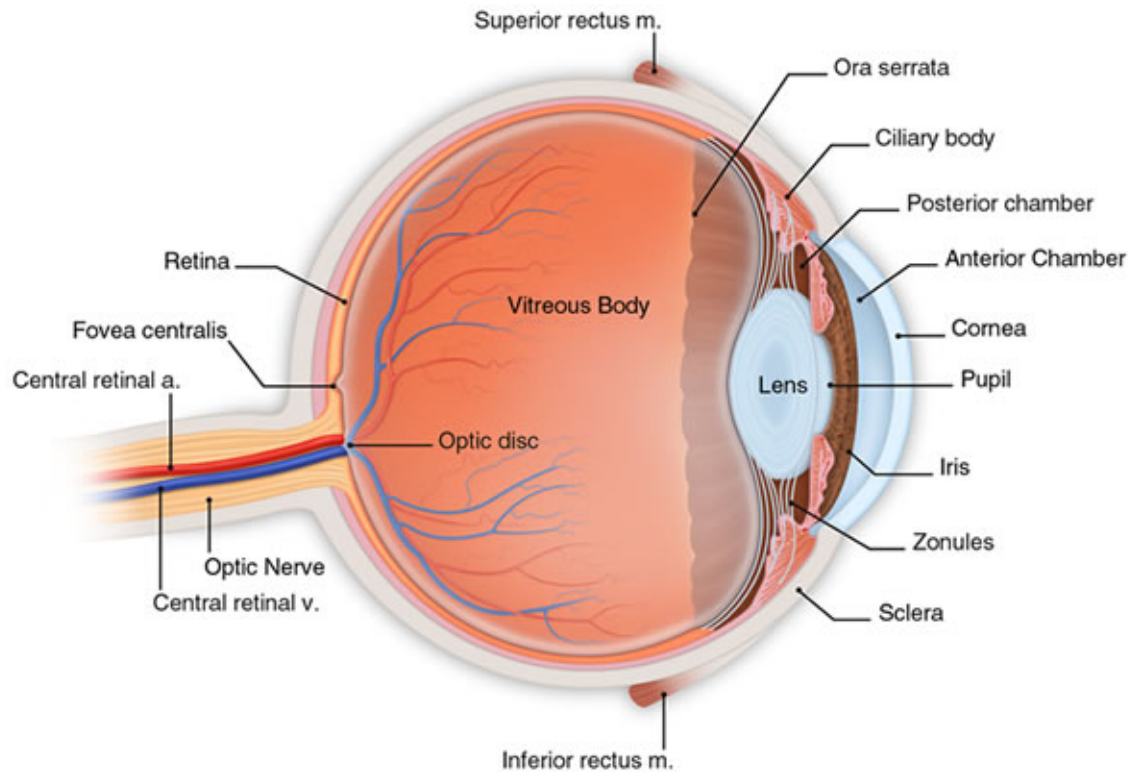


Figure 1.1. Ocular structure (19). The eye consists of the anterior part with the cornea, conjunctiva, anterior chamber and lens and the posterior part with the ciliary body, vitreous, choroidea, sclera and retina.

1.4 Mouse Model of River Blindness

In the 1980s, several groups attempted to establish a mouse model of *O. volvulus* infection. Aoki et al. (21) injected live *O. volvulus* microfilariae in the inguinal region and recovered blood at up to 18 weeks post inoculation to analyze microfilarial counts. After 16 weeks, no live microfilariae were detected. Kozek et al. (22) infected rhesus monkeys, bonnet monkeys, golden spider monkeys, black spider monkeys, galagos, opossums,

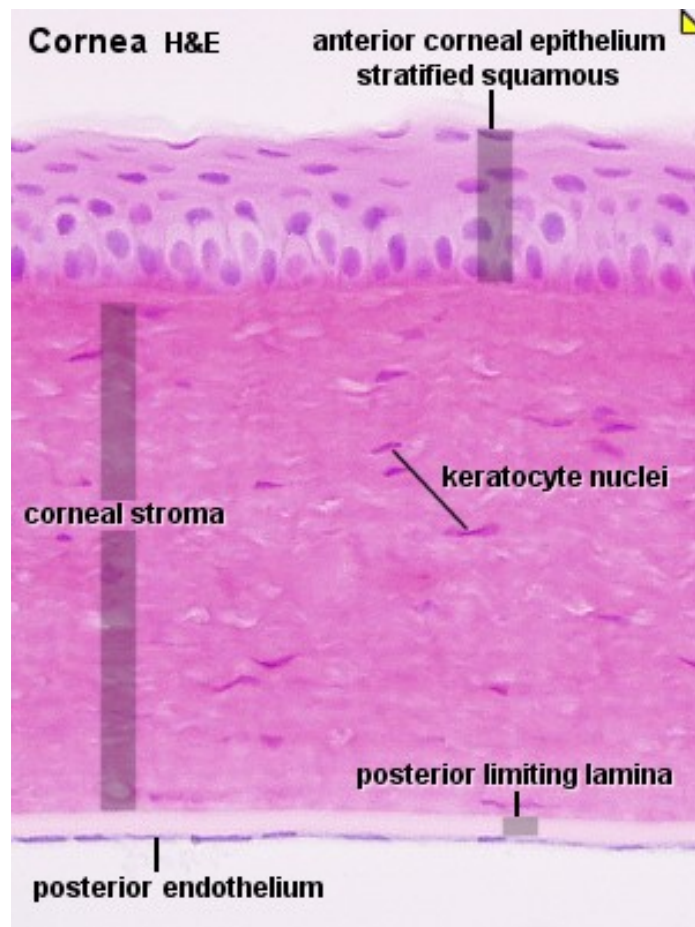


Figure 1.2. Corneal structure (20). The cornea consists of the outer multi layer epithelium, the corneal stroma with well organized fibrils and few cells and the single layered endothelium.

jirds, mice kinkajou, cebus monkeys, rats and calves with live *O. volvulus* microfilariae. They could not detect any adult worms, larvae or patent infection in any of these animals. Other groups attempted to establish infections with related *Onchocerca* worms (23–25). Even though CBA mice are described as relatively susceptible (25), infections terminated without intervention after about 100 days post infection. James et al. (26) injected *Onchocerca cervicalis* microfilariae subcutaneously between the eyes and found microfilariae migrating into the cornea as early as 12 hours post injection. Microfilariae could persist for up to 42 days. However, no inflammatory response was present (27).

Therefore an artificial mouse model of onchocercal keratitis has been developed. Mice immunized with soluble *O. volvulus* extract (OvAg) in either complete Freund's (CFA) or squalene based adjuvant (STP) develop corneal inflammation. The different adjuvants cause differences in cellular corneal infiltrates: CFA-immunized mice show strong neutrophil infiltration whereas in STP-immunized mice eosinophils are predominant (27). Recent studies mainly used STP as adjuvant. In current studies, mice are immunized with OvAg-STP three times in weekly intervals, inducing adaptive immune responses. One week after the third immunization, corneas are injected with OvAg and eyes are excised at various time points. Corneal changes include edema, neovascularization, disruption of the corneal matrix (collagen fibrils) and infiltration of neutrophils and eosinophils (28). Whereas neutrophil migration to the corneal stroma can also be induced by the injection of OvAg into unimmunized mice (29), the migration of eosinophils depends on the presence of adaptive immunity (30).

1.4.1 Immune responses in the mouse model of river blindness

Splenocytes produce increased levels of IL-4, IL-5 and IFN- γ during *in vitro* stimulation with filarial extract when previously immunized with filarial extracts (*Brugia malayi* adult or whole microfilariae, *O. volvulus* extract) (31). Lymph nodes and splenocytes from OvAg immunized mice showed higher levels of IL-4 and IL-5 production upon re-stimulation *in vitro* compared with PPD (*Mycobacterium tuberculosis* purified protein derivative) immunized mice, indicating a preference for Th₂ responses (28). This cytokine profile was found to depend on the presence of CD4⁺ T cells and could be transferred by the adoptive transfer of splenocytes from immunized mice (28).

The preference for Th₂-responses can be skewed by the injection of rIL-12 during the immunization. In this case, IFN- γ production and IgG₁ levels in the serum are increased compared with normally immunized mice (32). The shift towards Th₁ responses is associated with decreased eosinophil infiltration into the lung and expression of major basic protein (32). However, although eosinophil migration to the lung is decreased in IL-12 injected mice, eosinophil infiltration into the corneal stroma is increased after IL-12 injection (33).

Following injection with filarial extracts, neutrophils and eosinophils migrate to the corneal stroma. At seven days post injection, infiltration of inflammatory cells is resolved in unimmunized mice, and the corneas appear normal (28). The infiltration was found to be specific for filarial injection as compared with injections of *Mycobacterium tuberculosis* purified protein derivative (PPD) (28).

Even though eosinophils are usually associated with parasite infections and were found to infiltrate the corneas, studies using IL-5^{-/-} could demonstrate that while eosinophils are absent from the corneas of these mice, the disease manifestations (corneal opacification and neovascularization) are identical to that of wild-type mice (32). This was found to be due to neutrophil infiltration at earlier time points. Neutrophil as well as eosinophil infiltration was dependent on the presence of B cells, antibodies (34) and Fc γ (35). Splenocytes from B cell deficient μ MT mice also showed decreased IL-5 production after OvAg stimulation. However, decreased levels of IL-5 did not correspond to diminished blood eosinophilia (34). Migration of eosinophils to the cornea is depending on the presence of CD4⁺ T cells (36), P-selectin (37) and ICAM-1 (38), while neutrophil migration is decreased in PECAM-1 depleted mouse corneas (38)

and CXCR2^{-/-} mice (39). ICAM-1 expression is regulated by IL-4 and IL-13 (40). Using IL-4^{-/-} mice, it was determined that corneal opacification and neovascularization is dependent on the presence of functional IL-4 (28). IL-4^{-/-} mice also showed reduced number of eosinophils in the corneal stroma (30).

A schematic of the sequence of events is shown in Figure 1.3. To briefly summarize, T cells are responding to filarial extracts by increased production of IL-4 and IL-5 and to a lesser degree IFN- γ and B cells produce increased levels of IgE and IgG₁. In the cornea, IL-4, IL-5 and IL-12 enhance P-Selectin- and ICAM-1-dependent eosinophil migration to the cornea while PECAM-1 and CXCR2 are required for neutrophil migration.

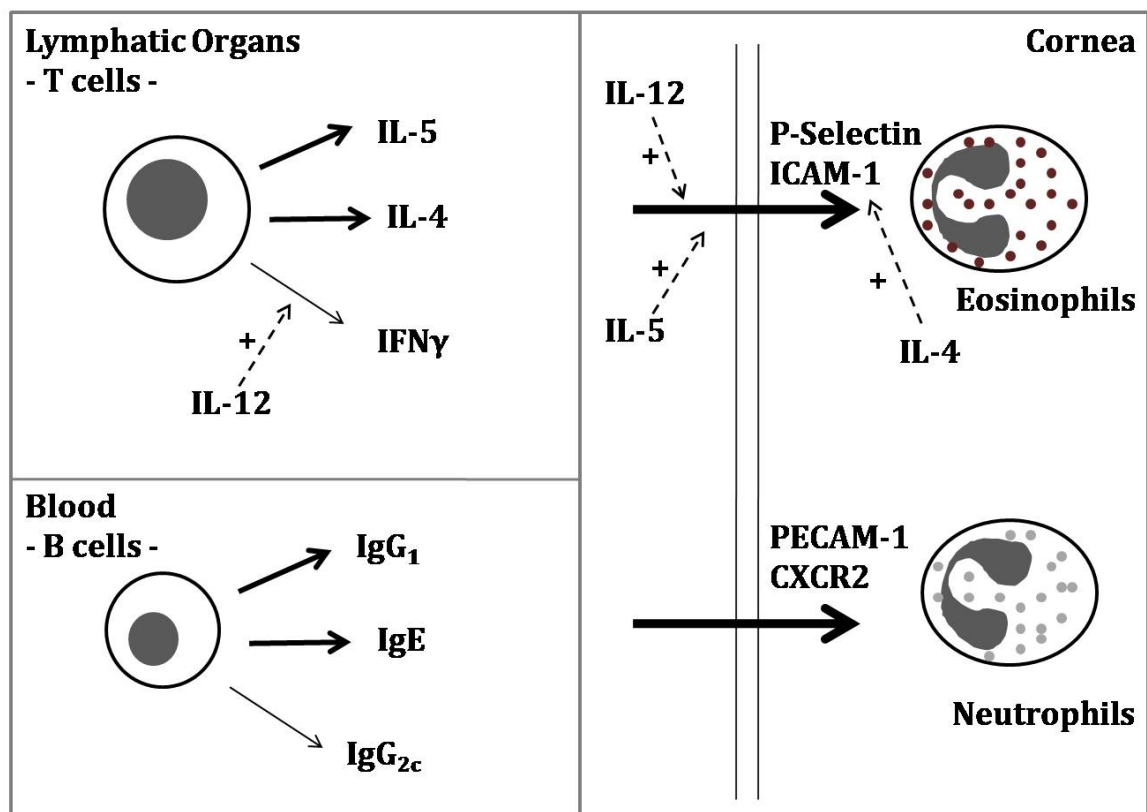


Figure 1.3. Sequence of events (adapted from (41)). The figure is explained in the main text.

1.5 Antigen-presenting cells

Traditionally, only dendritic cells, macrophages and B cells were considered antigen-presenting cells. However, lately it has been shown that neutrophils and eosinophils are capable of presenting antigen to T cells in a contact-dependent manner (42–46). In this section, I will give background information on the cell types relevant for this study: dendritic cells, macrophages and neutrophils.

1.5.1 Dendritic cells

Dendritic cells are the most efficient of the antigen-presenting cells. Upon recognition of microbial products, dendritic cells begin maturation. This is characterized by the upregulation of MHCII and the co-stimulatory molecules CD40, CD80 and CD86 as well as the production of cytokines and chemokines (47). Antigen presented on MHC molecules provides the first specific signal of T cell activation. The co-stimulatory molecules provide the second activatory signal to T cells, thus making dendritic cells efficient antigen-presenting cells (48). A third signal is provided by the cytokines secreted by activated dendritic cells (49).

Depending on the nature of the antigen (bacterial, viral, helminth origin), dendritic cells are primed towards a DC1 cells or DC2 cells type cell. DC1 induce T cells via IL-12 and IL-23 to differentiate towards Th₁ (50, 51). This is mainly found during bacterial and viral infection. During helminth infection, DC2 cells dominate, producing IL-10 and TGF- β (51, 52) and inducing a Th₂ and regulatory T cell response (50, 53).

Typical Th₁ responses include the production of IFN- γ and IL-2, activation of macrophages, IgG₂ antibody production. Neutrophils are also associated with Th₁ immune responses (54). Th₂ responses are characterized by the production of the cytokines IL-4, IL-5 and IL-10 as well as a predominant eosinophil response (55). Interestingly, during filarial infection, we find mixed Th₁ and Th₂ responses. This is thought to be due to the *Wolbachia* endosymbionts inducing Th₁ type responses with the worm itself inducing Th₂ type responses.

1.5.2 Macrophages

Macrophages are important in the innate immune responses as well as for antigen-presentation and induction of adaptive immune responses. Precursor cells are generated in the bone marrow entering the blood stream as monocytes. Following circulation for about 18 hours, monocytes migrate into tissues and differentiate into macrophages (56).

Activation of macrophages is tightly regulated by cytokines. Exposure to Th₁ cytokines IFN- γ , Tumor-necrosis factor (TNF) or lipopolysaccharide induces the classical type 1 activation of macrophages. This pathway is usually activated by intracellular pathogens (56) and is characterized by activation of the interferon regulatory factors (IRF). In response, pro-inflammatory cytokines are produced.

If macrophages are instead activated via the alternative pathway, including exposure to Th₂ cytokines IL-4 and IL-13, type 2 activation occurs and requires mast cell and eosinophil involvement, and granuloma formation. This is usually found in helminth infections or in response to extracellular pathogens (56). Production of macrophage-derived chemokine (MDC) and thymus and activation-regulated chemokine (TARC) is

promoted, while production of reactive oxygen species and pro-inflammatory cytokines is inhibited (56).

Priming of macrophages ensures survival of the cells and prepares the cells for exposure to a secondary signal. Primed macrophages respond to lower doses of antigen, but are not yet activated. Classically, IFN- γ primes macrophages (56).

1.5.3 Neutrophils

For a long time, neutrophils were only regarded as responder cells in the innate immune system. Recent publications have demonstrated a role for neutrophils in antigen-presentation (43), including the expression of MHCII and co-stimulatory molecules on neutrophils (42).

Neutrophils contain secretory vesicles, gelatinase (tertiary) granules, specific (secondary) granules and azurophil (primary) granules. Each granule type shows a specific content: secretory vesicles contain only albumin and heparin binding protein, gelatinase granules contain gelatinase (matrix metalloproteinase 9), specific granules contain CD66b in the granule wall and azurophil granules are characterized by myeloperoxidase content (57). Upon stimulation, granule proteins are released and take part in neutrophil extravasation and migration (gelatinase granules) and antimicrobial activity (specific granules, azurophil granules) (58).

Myeloperoxidase (MPO) is found in neutrophils where it is stored in azurophil granules. It has a central role in the regulation of inflammation. MPO catalyzes the production of hypochlorous acid and serves as a marker for respiratory burst (57, 59). If released by the cell, it contributes to the pathogenesis of the disease (59).

Previous studies demonstrated down-regulation of L-Selectin on the neutrophil surface in response to activation (60). L-Selectin is an adhesion molecule found on leukocytes and functions as homing receptor for leukocytes that are extravasating in lymphoid tissues through the high endothelial venules. L-Selectin expression increases rolling of neutrophils along the endothelium and thus helps extravasation. In addition to adhesion to endothelial cells, L-Selectin also functions in neutrophil activation. Upon L-Selectin activation, neutrophils become less deformable (60, 61). L-Selectin is usually shed by neutrophils in response to stimulation and activation. It is hypothesized that the now soluble L-Selectin can bind to the L-Selectin receptor and prevent neutrophil binding at subacute sites of inflammation (60). Increased serum levels of L-Selectin have been associated with disease, e.g. AIDS (60).

CD18 is found colocalized with L-Selectin (61) but is upregulated upon stimulation. CD11b often forms complexes with CD18. These surface molecules affect aggregation and adhesive properties of neutrophils.

Matrix metalloproteinases (MMPs) are Ca^{2+} -dependent Zn-endopeptidases that degrade the extracellular matrix (62). MMPs are regulated by hormones and cytokines among other factors (63). They are produced as pro-form and stored inside granules (57). Upon activation, they are cleaved and excreted (63). MMP-9 (gelatinase B) and MMP-2 (gelatinase A) are both gelatinases important in corneal remodeling (64). They contain a fibronectin-like domain which binds the gelatin (65). MMP-2 is not expressed by neutrophils, but on keratinocytes (64, 65). MMP-8 (collagenase-2) is expressed by neutrophils, corneal epithelial cells and keratinocytes (among others) (62). In contrast to MMP-2 and MMP-9, it digests a variety of substrates: collagen, chemokines, protease

inhibitors (62). It has been described as a regulator of neutrophil infiltration in LPS-induced keratitis (18).

Neutrophils respond to chemotactic gradients of keratinocyte-derived chemokine (KC, CXCL1), monocyte-inhibitory protein-2 (MIP-2, CXCL2) and LPS-induced chemokine (LIX, CXCL5). Neutrophils only contribute to MIP-2 production, whereas KC and MIP-2 are produced by macrophages and KC and LIX by corneal fibroblasts (17).

1.6 Toll-like Receptors

Pattern recognition receptors (PRRs) recognize pattern associated molecular patterns (PAMPs) in microbes. PAMPs are highly conserved among different microbes, absent from eukaryotes and essential for the survival of the microbe. The family of PRRs consists of Toll-like receptors (TLRs), Dectin-1 (a C-type lectin) and Nod-like receptors (NLRs). Other less studied receptors include NALP3, ISD sensor and RIG-I/MDA5 (66).

TLRs are germ-line encoded receptors recognizing a great variety of microbial products. The receptors were first characterized in *Drosophila*. The family currently consists of at least 10 TLRs in humans (67) and 13 TLRs in mice (68, 69). Some studies refer to 11 human TLRs (70), however the original article identifying the 11th human TLR could not be identified. The receptors recognize conserved microbial PAMPs, although chemical agonists (e.g. imiquimod) have also been described (71, 72). Host proteins like heat-shock proteins were shown to bind TLR2 and TLR4 (73–75). The receptors contain an extracellular leucine-rich repeat domain and an intracellular domain. The intracellular domain is homologous to the IL-1 receptor and therefore referred to as the Toll/IL-1R (TIR) domain (76). Signaling through TLRs recruits the adaptor molecules

myeloid differentiation primary response gene 88 (MyD88) or TIR-domain-containing adapter-inducing interferon- β (TRIF). MyD88 is involved in the signaling of every TLR except TLR3 while only TLR3 and (partly) TLR4 signal through TRIF. MyD88 is recruited by Mal, then signals through IRAK and NF κ B activation to induce production of pro-inflammatory cytokines.

TLR2, TLR4 and TLR9 recognize bacterial products. TLR2 specifically interacts with acylated lipoproteins, TLR4 with lipopolysaccharides and TLR9 with methylated DNA. TLR3, TLR7 and TLR9 are specific receptors for viral products, TLR5 interacts with flagellin. TLR2 is the most promiscuous receptor. Depending on coreceptor usage (TLR1, TLR6 and TLR10) different bacterial products are recognized. TLR1 and TLR2 together specifically interact with triacylated lipoprotein, TLR2 and TLR6 interact with diacylated lipoproteins, ligands for TLR2/TLR10 are not yet described.

TLR2, TLR4 and TLR11 have been implicated in the activation of immune cells by *Leishmania major*, *Trypanosoma cruzi* and *Toxoplasma gondii* (77–79). In contrast to bacterial or viral activation of TLRs, activation via TLRs by eukaryotic parasites prevented immunopathology (77–79).

TLRs are not only important during the generation of innate immune responses, but cells activated via TLR can also induce adaptive immune responses. TLRs have been shown to increase the antigen uptake by dendritic cells (80), induce maturation of and cytokine production by dendritic cells thus increasing the capability to present antigen. B cell proliferation also increases after stimulation with TLR ligands either directly or indirectly via activation of dendritic cells (81). Activation of dendritic cells via Pam₃CSK or LPS induced T cell proliferation and differentiation to Th₁ and Th₂ cells, respectively (82).

1.6.1 Toll-like Receptors in Filarial Infection

Studies examining the role of TLRs in filarial infection focused on TLR2, TLR4 and TLR9. It was reasoned that the most likely agonist for these receptors was not the worm itself but its endosymbiont *Wolbachia*. It was therefore thought that bacteria specific TLRs would be used. In a mouse model of *O. volvulus* keratitis, involvement of *Wolbachia* and MyD88 in corneal inflammation was demonstrated (29). Further investigation identified TLR2 as the receptor activated by *Wolbachia*. No role for TLR4 or TLR9 could be identified (83), although early studies showed TLR4-dependent neutrophil migration to the corneal stroma (84) and TLR4-dependent activation of dendritic cells by *Wolbachia* surface protein (WSP) (85). It was demonstrated that TLR2 required TLR6 as coreceptor in neutrophil and macrophage migration to the cornea in response to *O. volvulus*, *Wolbachia* and recombinant *Wolbachia* lipoprotein (86, 87).

Other groups showed filaria-dependent expression of TLRs. Expression of TLRs was down-regulated in filaria-infected individuals corresponding to decreased cytokine production after stimulation with TLR ligands (88, 89). Repeated exposure to filarial extracts also decreased macrophage responsiveness to *B. malayi* and *Wolbachia* in a TLR2-dependent manner (90). Finally, secreted products of the nematode *Acanthocheilonema viteae* are able to activate dendritic cells in a TLR4-dependent manner (91). Activation of macrophages and dendritic cells via this TLR4 and MyD88-dependent pathway results in decreased responsiveness of these cells to TLR2 and TLR9 agonists (91).

1.7 Interferon- γ

Interferon γ (IFN- γ) is the classical Th₁ cytokine. It is produced only at low levels during filarial infection. It has been described in human biliary epithelial cells and in human monocytes from human rheumatoid arthritis patients that TLR2 is upregulated in response to stimulation with IFN- γ (92, 93). Harada et al. (93) showed upregulation of TLR1-5 by measuring mRNA levels and confirming synergistic effects of IFN- γ and LPS and peptidoglycan stimulation. Similar results were recently shown for murine CD11b⁺ cells where TLR2 expression was increased after IFN- γ stimulation (94).

IFN- γ also affects differentiation of monocytes. It was shown that human precursor cells developed into macrophages rather than dendritic cells if IFN- γ was supplied in addition to the normal growth factors granulocyte-macrophage colony stimulating factor (GM-CSF) and IL-4 used for dendritic cell differentiation. This effect could only be observed in the early differentiation stages and was dependent on the production of macrophage colony stimulating factor (M-CSF) and IL-6 (95).

In addition, as has been described in the section on macrophages, IFN- γ activates macrophages via the classical pathway rather than the alternative pathway that is induced by IL-4 and IL-13.

IFN- γ has been shown to regulate expression of platelet endothelial cell adhesion molecule 1 (PECAM-1) in a mouse model of *Herpes simplex* keratitis. Blockade of IFN- γ reduced neutrophil infiltration into the cornea and expression of PECAM-1 on corneal vessels (96). It has been shown by other groups that PECAM-1 expression enhances directional neutrophil migration (97). Our group previously demonstrated a role for PECAM-1 in neutrophil migration during *O. volvulus* keratitis (38).

Additionally, IFN- γ induces the production of neutrophil chemoattractant CXC chemokines in *Staphylococcus aureus* infected tissues (98).

1.8 Aims

Previous studies described Pam₃CSK and LPS as differential inducers of T cell responses via TLR2 and TLR4, respectively (82). It was also shown that TLR2 and TLR4 are implicated in the recognition of filarial products (84, 85). I therefore reasoned, that filarial products (in addition to *Wolbachia* surface protein) might activate TLR2 and TLR4 and this might lead to a skewing of the adaptive immune responses.

In this study, I first wanted to characterize TLR-dependent activation of dendritic cells by *O. volvulus*. After I demonstrated a role for TLR2 in the activation of dendritic cells, I examined the role of TLRs in the adaptive arm of the immune responses in a mouse model of river blindness. The aim was to show that the initial requirement for TLR2 in the innate immune response was reflected by altered adaptive immune responses. I was interested in the generation of systemic immune responses (T cell activation, serum antibody production) and in the local migration of antigen-presenting cells to the cornea.

With the surprising result of TLR2 being required only for Th₁-like responses IFN- γ production and neutrophil migration, the next goal was to identify a mechanism, linking systemic IFN- γ production to neutrophil infiltration into the cornea.

2 Materials and Methods

2.1 Reagents

2.1.1 OvAg

During previous studies (Eric Pearlman, personal communication), Onchocercomata were excised from patients from the Ivory Coast. Nodules were stored frozen at -80°C until further processing. Then, nodules were thawed overnight at 4°C in digestion solution (HBSS/1 % Penicillin+Streptomycin/50 $\mu\text{g}/\text{ml}$ Gentamicin) and washed with sterile ice cold HBSS. 1 % collagenase, 0.5 % elastase and 0,5 % trypsin were added to the digestion solution (enzyme solution). Nodules were incubated in enzyme solution for 8 hours at 37°C until worms were released from the nodules. Worms were collected in a sterile tube and transferred onto 40 μM filter. Worms were then washed six times with sterile digestion solution, followed by four washes with sterile HBSS. Worms were processed in 1 ml HBSS in glass mortars for 30 minutes. Protein extracts were sonicated three times for 5 minutes, then centrifuged for 10 minutes at 1000 xg. Soluble extract was used for *in vitro* stimulation and *in vivo* intrastromal injection. Insoluble proteins were dissolved in 1 ml HBSS and used for immunizations. Protein concentrations in both extracts were

determined by BCA protein assay (Pierce). WSP and filarial 5S were quantified by quantitative PCR, 40 cycles of 30 seconds extension at 95°C, 30 seconds annealing at 60°C and 30 seconds elongation at 72°C. Primers used in this study are shown in table 2.1.

2.1.2 *Wolbachia*

Wolbachia infected SF9 insect cells were kindly provided by Dr. Mark Taylor (Liverpool School of Tropical Medicine, Liverpool, Great Britain). Cells were maintained under sterile conditions at 27°C, no CO₂. Insect cell medium contained 50 % Mitsuhashi Marmorosh Medium, 50 % Schneider's Insect Medium, 10 % FBS and 1 % Penicillin+Streptomycin. *Wolbachia* infected SF9 cells were harvested, centrifuged at 2000 xg for 10 minutes and the cells were disrupted by sonication for 2 minutes. Cell debris was then pelleted at 600 xg for 5 minutes. Supernatants were transferred into a clean tube and pelleted again. This was repeated four times to remove cellular debris. *Wolbachia* were then pelleted at 16000 xg for 10 minutes. For controls, tetracycline treated SF9 cells were processed identically.

2.1.3 *Wolbachia* Surface Protein

We obtained *Wolbachia* Surface Protein (WSP) cloned into the pET100 TOPO vector from Alan Scott (Johns Hopkins University, Baltimore, MD). The gene was cloned without the signal sequence (first 30 amino acids). Deletion mutants were generated by reverse PCR. Briefly, primers (table 2.1) were designed at both ends of the sequence to be deleted. PCR reactions were run amplifying the full plasmid minus the deleted sequence. PCR amplification consisted of 2 minutes at 95°C, followed by 10 cycles of

Table 2.1. Primers used in this study.

Primer name	Sequence	Annealing temp
5S Fw	GTCTACGACCATAACCACGTTG	60°C
5S Rev	CCCAGGCCGTCTCCGATCC	60°C
12S Fw	AAACTAGGATTAGATACCCTATTAT	60°C
12S Rev	AAGAGCGACGGGCGATGTGT	60°C
WSPovF64	AAGCTTCTTTTATGGCTGGTGG	60°C
WSPovR173	AGCTGTTTCAAATGTATCCCTGC	60°C
WSPAa23qF	TAACGAGCACCAGCATAAAG	60°C
WSPAa23qR	TGCAGCATATATCAGCAATCC	60°C
WSPplasmidF	CACCATGCATTATAAAAAGTTTTTTTCAGC	55°C
WSPplasmidR	TTAGAAATTAAACGCTATTCCAGC	55°C
WSPpetc495	CCCCGGATCCGCTGATGAGGAAACTA	60°C
WSPpetnc385	CCCCGGATCCGGTGAAGGGATGATC	60°C
WSPpetc585	CCCCGGATCCCAAAGGATAGTAAA	60°C
WSPpetnc474	CCCCGGATCCTATTGGACCAACAGGA	60°C
WSPpetc675	CCCCGGATCCGTGGACATTGAAGGAG	60°C
WSPpetnc564	CCCCGGATCCAGCTCCTGTGATACCA	60°C
WSPpetc765	CCCCGGATCCTCAGGACTAGTTAATG	60°C
WSPpetnc651	CCCCGGATCCTCTGATATCATCCATT	60°C
WSPpetc855	CCCCGGATCCAGCAACCCTGCAAAG	60°C
WSPpetnc741	CCCCGGATCCAATTGCTGTAAATTAT	60°C
WSPpetc945	CCCCGGATCCACCCAGAAATTAAAC	60°C
WSPpetnc835	CCCCGGATCCGATATATGCTACACCA	60°C
WSPpetc1035	CCCCGGATCCAGTGAGGATAAAGAA	60°C
WSPpetnc924	CCCCGGATCCTACATCATAGCTAATA	60°C
WSPpetc1125	CCCCGGATCCTAAGGGCGAGCTCAA	60°C
WSPpetnc1011	CCCCGGATCCAGTTCCTTTATTACT	60°C

1 minute at 95°C, 1 minute at 60°C and 7 minutes at 72°C, then 30 cycles of 30 seconds at 95°C, 1 minute at 60°C and 7 minutes at 72°C, followed by final extension at 72°C for 10 minutes. Primers contained a BamH1 site to allow religation after digestion. Circular plasmids were then transformed into competent BL21 cells.

WSP and WSP deletion mutants were purified using the Qiagen NiNTA fast start kit with the native purification protocol. Cells were grown for 3 hours at 37°C on shaking incubator. Cells were then induced with 1 mM IPTG for 5 hours. Cells were harvested at 4000 xg for 20 minutes and frozen overnight at -20°C. Cells were then thawed and lysed in Native Lysis Buffer containing 1 µg/ml lysozyme and 25 U/ml benzonase nuclease for 30 minutes on ice. The lysate was then centrifuged at 14,000 xg for 30 minutes at 4°C. The supernatant was applied to NiNTA Fast Start Column. The column was then washed twice in Native Wash Buffer and the protein was eluted in 1 ml Native Elution Buffer. Purity was determined by Western Blot and Coomassie stain and protein concentration was determined by BCA protein assay (Pierce).

2.1.4 Control reagents

To determine activation of dendritic cells, macrophages, neutrophils, MK/T-1 cells and HEK cells depending on the TLR profile these cells expressed, I used synthetic TLR ligands. For TLR2 activation, I used Peptidoglycan (Invivogen), Pam3CSK (Invivogen) and FSL-1 (Invivogen), for TLR3 activation, Poly(I:C) (Invivogen) was used, for TLR4 activation ultrapure E. coli LPS (Invivogen) and for TLR9 activation CpG-DNA (Invivogen). Positive control for T cell activation was anti-CD3 (kind gift by Dr. Thomas Forsthuber, now at the University of Texas at San Antonio, TX).

2.1.5 Other reagents

STP adjuvant: 10 % squalene (Sigma, St. Louis, MO, USA), 0.4 % Polyoxyethylenesorbitanmonooleate (Tween 80) (Sigma, St. Louis, MO, USA), 1 % Pluronic L (BASF, Germany) in PBS

Recombinant cytokines: IFN- γ , IL-1 α , IL-1 β , IL-6, TNF α , GM-CSF (Peprotech, Rocky Hill, NJ, USA)

2.2 Mice

C57BL/6 mice were bred at the Wolstein Animal Resource Center at Case Western Reserve University (Cleveland, OH) or purchased from Jackson Laboratories (Bar Harbor, ME). TLR2^{-/-}, TLR4^{-/-}, TLR2/4^{-/-}, MyD88^{+/+} and MyD88^{-/-} mice were bred at the Wolstein Animal Resource Center. IFN- γ ^{-/-} mice were a gift by Dr. Tom McCormick (Case Western Reserve University, Cleveland, OH), IL-1R^{-/-} mice were kindly provided by Dr. Susan Mohr (Case Western Reserve University, Cleveland, OH) and TNF α R^{-/-} mice were kindly provided by Dr. Claire M. Doerschuk (Case Western Reserve University, Cleveland, OH). All animal protocols were approved by the IACUC office at Case Western Reserve University.

2.3 *In vivo* studies

2.3.1 Innate immune responses

Mice were anaesthetized with tribromoethanol (TBE). Corneas of mice were rinsed, then carefully scratched with a 27 gauge needle. A 33 gauge needle (Hamilton Company,

Switzerland) was inserted into the cornea through the scratch in the corneal epithelium and 4 μ l of experimental and control reagents were injected. Eyes were taped closed with loosely adherent tape that mice could remove themselves upon awakening. 24 hours post injection, mice were euthanized using CO₂ and corneal haze was examined by confocal microscopy. Whole eyes were removed for sectioning and immunohistochemistry, the corneas were excised carefully with a 2 mm trephine for FACS analysis of the cellular infiltrate or ELISA analysis of chemokines present in the cornea.

2.3.2 Adaptive immune responses

Mice were immunized subcutaneously three times in weekly intervals with 10 μ g insoluble OvAg extract in a 1:1 dilution in STP adjuvant. One week past the final immunization, mice were immunized and injected into the corneal stroma as described under innate immune responses. Mice were then euthanized at 24 or 72 hours post intrastromal injection and eyes removed for sectioning and immunohistochemistry. In some experiments, corneas were excised for ELISA analysis of chemokines.

2.4 Cell culture

2.4.1 Dendritic cells

C57BL/6, TLR2^{-/-}, TLR4^{-/-}, TLR2/4^{-/-}, MyD88^{+/+} and MyD88^{-/-} mice were euthanized. Femurs and tibias were dissected aseptically. Bones were cleaned under sterile conditions, then opened at the distal and proximal ends. For harvesting bone marrow cells, the opened bones were centrifuged for 30 seconds at 6000 xg in a sterile 0.5 ml tube with a hole in the bottom, set into a sterile 1.5 ml tube. Cells were resuspended in HBSS.

Red blood cells were lysed with RBC lysis buffer (eBioscience, San Diego, CA, USA). Cell numbers and viability were determined under trypan blue exclusion. Viability was generally greater than 90 %. Cells were plated at a concentration of 1×10^6 per ml in six-well plates. DC medium contained RPMI (BioWhittaker), 10 % fetal bovine serum (Cellgro, Herndon, VA, USA), 1 % sodium pyruvate (BioWhittaker), 1 % HEPES (BioWhittaker), 1 % L-glutamine (BioWhittaker), 1 % 50/50 penicillin/streptomycin (BioWhittaker) and 1 mM 2-mercaptoethanol (Sigma, St. Louis, MO, USA). Medium was supplemented with GM-CSF (Peprotech, Rocky Hill, NJ, USA) at a final concentration of 20 ng/ml. Fresh medium was added on days 3 and 5. Cells were harvested on day 7 by carefully removing non-adherent cells (dead cells and mature dendritic cells) and then dislodging loosely adherent cells with HBSS (immature dendritic cells). Viability was greater than 90 %.

Dendritic cells were purified with CD11c magnetic beads according to the manufacturer's instructions (MACS, Miltenyi Biotech, Auburn, CA, USA). Dendritic cells were enriched to about 90-95 %.

1×10^6 cells were plated in 96-well plates and stimulated for 24 hours with the following antigens: OvAg at different concentrations, 50 μ g/ml Pam3CSK (InvivoGen, San Diego, CA, USA), 100 ng/ml lipopolysaccharide (LPS) (Invivogen, San Diego, CA, USA) or 20 μ g/ml CpG-DNA (Invivogen, San Diego, CA, USA). Supernatants were analyzed for cytokine production by ELISA and cells were examined by flow cytometry.

2.4.2 Macrophages

C57BL/6 and TLR2^{-/-} mice were injected intraperitoneally with 4 % thioglycollate (Remel, Lenexa, KS, USA) at 4-5 days prior to euthanization. Mice were euthanized by CO₂. The peritoneum was lavaged with 10 ml HBSS. Red blood cells were lysed with

RBC lysis buffer (eBioscience, San Diego, CA, USA) and cells were plated at 1×10^5 per well. After overnight rest, cells were stimulated with medium, OvAg, Pam3CSK, IFN- γ and OvAg + IFN- γ .

2.4.3 Neutrophils

9 % Casein solution was prepared in 0.9 mM CaCl₂ and 0.5 mM MgCl. 1 ml Casein solution was injected at 18 hrs and 3 hours prior to euthanizing the mice. Cells were harvested from the peritoneal cavity, washed with HBSS and purified on 90 % Percoll gradient at 32000 xg for 20 minutes. Neutrophil fraction was harvested and washed to remove residual Percoll. 1×10^5 cells were stimulated with medium, OvAg and Pam3CSK.

2.4.4 MK/T-1 cells

The corneal fibroblast cell line MK/T-1 (99) was maintained by the Ophthalmology Tissue Culture Core Facility at Case Western Reserve University. Cells were maintained in DMEM(high glucose), 10 % FBS and 50 μ g/ml hygromycine. Cells were stimulated at 70 % confluency for 18 hours with medium, OvAg, rIFN- γ , rIL-1 α , rIL-1 β , rIL-6, rTNF α and Pam3CSK.

2.4.5 HEK cells

HEK293/hTLR2 8.10 CFP, HEK293/hTLR3 flag and HEK/hTLR4 MD2 1.6 were a kind gift by Dr. Amy G. Hise (Case Western Reserve University, Cleveland, OH). Cells were maintained in DMEM (high glucose), 10 % low endotoxin FBS, 10 μ g/ml ciprofloxacin with 5 μ g/ml geneticin added every 4th passage. HEK293/hTLR1/hTLR2

and HEK293/hTLR2/hTLR6 were a kind gift by Dr. Clifford Harding (Case Western Reserve University, Cleveland, OH). These cells were maintained in DMEM (high glucose), 10 % FBS, 10 $\mu\text{g/ml}$ blasticidin (Invivogen). 1×10^5 cells were stimulated with medium alone, OvAg, rWSP, Pam3CSK, Poly(I:C) or LPS for 18 hours. Activation was determined by hIL-8 ELISA.

2.4.6 T cells

Spleens were dissected from C57BL/6, TLR2^{-/-}, TLR4^{-/-}, TLR2/4^{-/-}, IFN- γ ^{-/-}, IL-6^{-/-}, IL-1R1/2^{-/-} and TNF α R^{-/-} mice. Single cell suspensions were prepared and 1×10^6 cells were stimulated with medium, OvAg, BmAg or anti-CD3 for 72 hours. For measuring mIL-4 production, soluble anti-IL-4 was added to prevent re-uptake of mIL-4 by the splenocytes. Cell activation was measured by mIL-4, mIL-5 and mIFN- γ ELISA.

2.5 FACS

Following stimulation, cells were harvested and washed with FACS buffer (HBSS without Ca²⁺ or Mg²⁺, 1 % FBS, 1 mM EDTA) and blocked with Fc γ for 30 minutes on ice. Cells were then stained with 1 μg antibody per 1×10^6 cells. Antibodies used are shown in table 2.2.

Table 2.2. Antibodies used in this study.

Name	Clone	Company
CD11b	M1/70	eBioscience
CD11c	N418	eBioscience
CD3	17A2	eBioscience
MCHII	M5/114.15.2	eBioscience
CD40	HM40-3	eBioscience
CD80	16-10A1	eBioscience
CD86	GL1	eBioscience
PECAM	MEC13.3	eBioscience
TLR2	6C2	eBioscience
F4/80	BM8	eBioscience
NIMP/R14	N/A	hybridoma supernatant
L-Selectin	MEL-14	eBioscience
CD18	M18/2	eBioscience
CD21/35	eBio8D9	eBioscience
Major Basic Protein	N/A	James Lee

2.6 Immunohistochemistry

2.6.1 Cell staining

Eyes were enucleated, embedded in OCT compound (Sakura Finetek U.S.A., Torrance, CA) and frozen at -20°C . $5\ \mu\text{m}$ sections were cut at -20°C and dried at room temperature overnight. Sections were stored at -20°C . Prior to staining, sections were brought to room temperature and fixed in 4 % formaldehyde for 30 minutes. Slides were then washed with PBS pH 7.6 and blocked for 30 minutes at room temperature in PBS/1 %

fetal bovine serum (PBS/1 % FBS). Generally, sections were stained with primary antibody diluted 1:100 in PBS/1 % FBS for 2 hours at room temperature in a humid chamber. Slides were washed in PBS and stained with 1:1000 dilution of Alexa Fluor 488 labeled secondary antibody (except for eosinophil staining where FITC labeled secondary antibody at 1:200 dilution was used) at room temperature in a humid chamber in the dark. After the final wash, slides were mounted in anti-fade medium (Vector Laboratories, Burlingame CA). The number of cells per section was determined by counting stained cells on a fluorescence microscope in a 400x magnification from limbus to limbus.

Primary antibody for neutrophil staining was anti-NIMP-R14 and for eosinophil staining anti-major basic protein (anti-MBP). Secondary antibody for neutrophil staining was rabbit-anti-rat antibody in PBS/1 % FBS, goat-anti-rabbit antibody for eosinophil staining.

For staining with PECAM-1, I used FITC-conjugated PECAM-1 antibody.

2.6.2 PECAM-1 analysis

Images of PECAM-1 stained corneal sections were taken and vessels identified. Intensity of PECAM-1 staining was analyzed using ImagePro software. Vessels were marked with this software and the intensity of fluorescence per vessel was calculated and based on these numbers, the average fluorescent intensity of vessels per eye as described (38). Average vessel fluorescent intensity per eye was graphed and analyzed for statistical differences.

2.7 ELISA

2.7.1 Cytokine ELISA

All cytokine ELISA kits were commercially obtained from R&D Systems and used according to the manufacturer's direction. Briefly, Immulon4 plates were coated with primary antibody in PBS overnight at 4 °C, then blocked in PBS/5 % bovine serum albumin (BSA). Standards and samples were applied overnight at 4 °C, followed by 2 hours incubation with detection antibody and 20 minutes with HRP-streptavidin. HRP was detected with 3,3',5,5'-tetramethylbenzidine (TMB), the reaction was stopped with 20 % H₂SO₄ and absorption measured at 450 nm.

2.7.2 Antibody ELISA

Immulon4 plates were coated with 10 µg/ml filarial extract in carbonate buffer overnight at 4 °C. Plates were blocked with PBS/1 % FBS for 2 hours. Serum dilutions ranging from 1:100 to 1:100 000 were then incubated for 2 hours at room temperature, followed by 1 hour detection with biotinylated anti-IgG₁ or anti-IgG_{2c} antibodies. Antibodies were detected with HRP-streptavidin and TMB. The color reaction was stopped with 1 N HCl and absorption was measured at 450 nm.

2.8 Statistical analysis

Experiments were analyzed by student's t-test and p-values of less than 0.05 were considered significant. Data are shown as mean with standard error of the mean.

3 Results

3.1 *In vitro* activation of antigen-presenting cells

3.1.1 Dendritic cells

Bone marrow was harvested from C57BL/6, TLR2^{-/-}, TLR4^{-/-} and TLR2/4^{-/-} mice and myeloid dendritic cells were differentiated in GM-CSF enriched culture for 7 days. Cells were purified with anti-CD11c magnetic beads and purity was generally greater than 90 % compared with dendritic cells without CD11c enrichment, that were 70 % CD11c positive cells. I then stimulated dendritic cells to determine which TLRs are involved in activation by filarial extracts.

1x10⁶ cells were stimulated for 24 hours with *O. volvulus* extract (OvAg), or with defined TLR agonists, peptidoglycan (PGN) (TLR2), Pam₃CSK (TLR2), LPS (TLR4), and CpG-DNA (TLR9); and IL-6 and RANTES were measured by ELISA. I could not show IL-6 or RANTES production in response to Poly(I:C). Other groups also showed only absent or low levels of IL-10, IL-12p40, IL-12p70 and TNF α upon stimulation with Poly(I:C) (100). Surprisingly, no increased levels of mIL-12p70 were detected after stimulation with worm antigen or TLR ligands (data not shown). Association of IL-12p70 with Th₁ responses and IL-6 with Th₂ responses were shown previously (50).

Figure 3.1 shows OvAg stimulated IL-6 production by DCs from C57BL/6 and TLR4^{-/-} mice, but not from TLR2^{-/-} or TLR2/4^{-/-} mice, which is similar to the effect of the TLR2 ligand Pam₃CSK. As controls, the TLR4 ligand LPS induced cytokine production by C57BL/6 and TLR2^{-/-} DCs, but not by DCs from TLR4^{-/-} or TLR2/4^{-/-} mice, and the TLR9 ligand CpG-DNA induced IL-6 by DCs from all TLR knockout mice. Similar results were found with BmAg (data not shown), and with RANTES production by OvAg stimulated DCs (Figure 3.1). Together, these findings clearly demonstrate that filaria-induced IL-6 and RANTES production by dendritic cells is TLR2-dependent. Decreasing doses of OvAg did not alter the requirement of TLR2 for the activation of dendritic cells (data not shown).

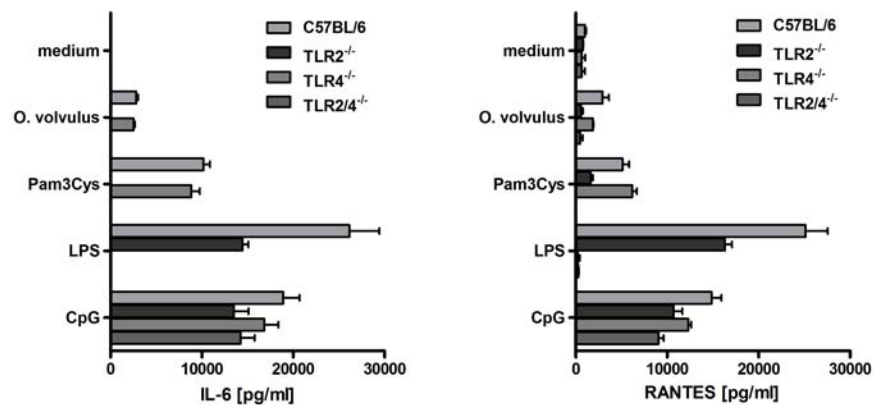


Figure 3.1. Dendritic cells were purified from C57BL/6, TLR2^{-/-}, TLR4^{-/-} and TLR2/4^{-/-} mice and stimulated with OvAg for 24 hours. As controls, dendritic cells were stimulated with Pam₃CSK, LPS and CpG. IL-6 and RANTES were produced by dendritic cells in response to filarial extracts in a TLR2-dependent manner.

As an additional indicator of dendritic cell activation, I examined CD40 expression on enriched CD11c⁺ DCs from C57BL/6, TLR2^{-/-}, TLR4^{-/-} and TLR2/4^{-/-} mice. Cells were incubated with OvAg or TLR ligands for 24 hours, and mean fluorescence intensity for

CD40 was determined on the gated CD11c⁺ CD3⁻ CD11b⁺ MHCII⁺ cells. As shown in Figure 3.2, OvAg increased CD40 surface expression on dendritic cells from C57BL/6 mice and TLR4^{-/-} mice, but not from TLR2^{-/-} mice or TLR2/4^{-/-} mice, which was similar to Pam3CSK activation. LPS-induced CD40 expression was TLR4-dependent, and CpG-DNA up-regulated CD40 expression in DCs from all mouse strains. To further illustrate these findings, representative profiles are shown in Figure 3.3, with stimulation shown as the clear peak. These findings support the cytokine data and demonstrate further that filaria-induced activation of DCs as measured by CD40 surface expression is dependent on the expression of TLR2, but not TLR4.

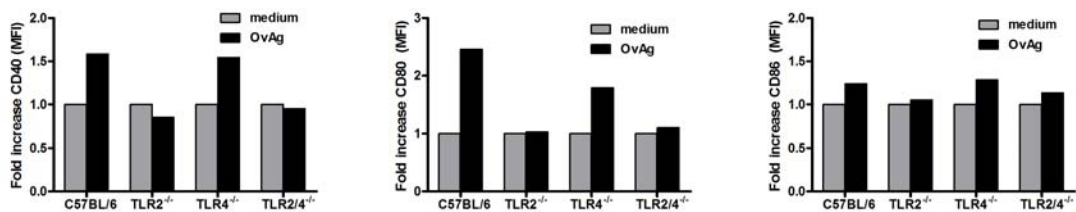


Figure 3.2. Dendritic cells were purified from C57BL/6, TLR2^{-/-}, TLR4^{-/-} and TLR2/4^{-/-} mice and stimulated with OvAg for 24 hours. As controls, dendritic cells were stimulated with Pam₃CSK, LPS and CpG. CD40, CD80 and CD86 are upregulated following OvAg stimulation in a TLR2-dependent manner.

As additional activation markers, I also analyzed upregulation of CD80 and CD86 on filaria stimulated dendritic cells and found, similar to CD40 expression, increased expression only on C57BL/6 and TLR4^{-/-} dendritic cells (Figure 3.2 and Figure 3.3).

3.1.2 Macrophages

Peritoneal macrophages were stimulated with OvAg and cytokine production was determined by ELISA. I measured MIP-2, KC, TNF α , IL-1 α , IL-1 β and IL-6 production.

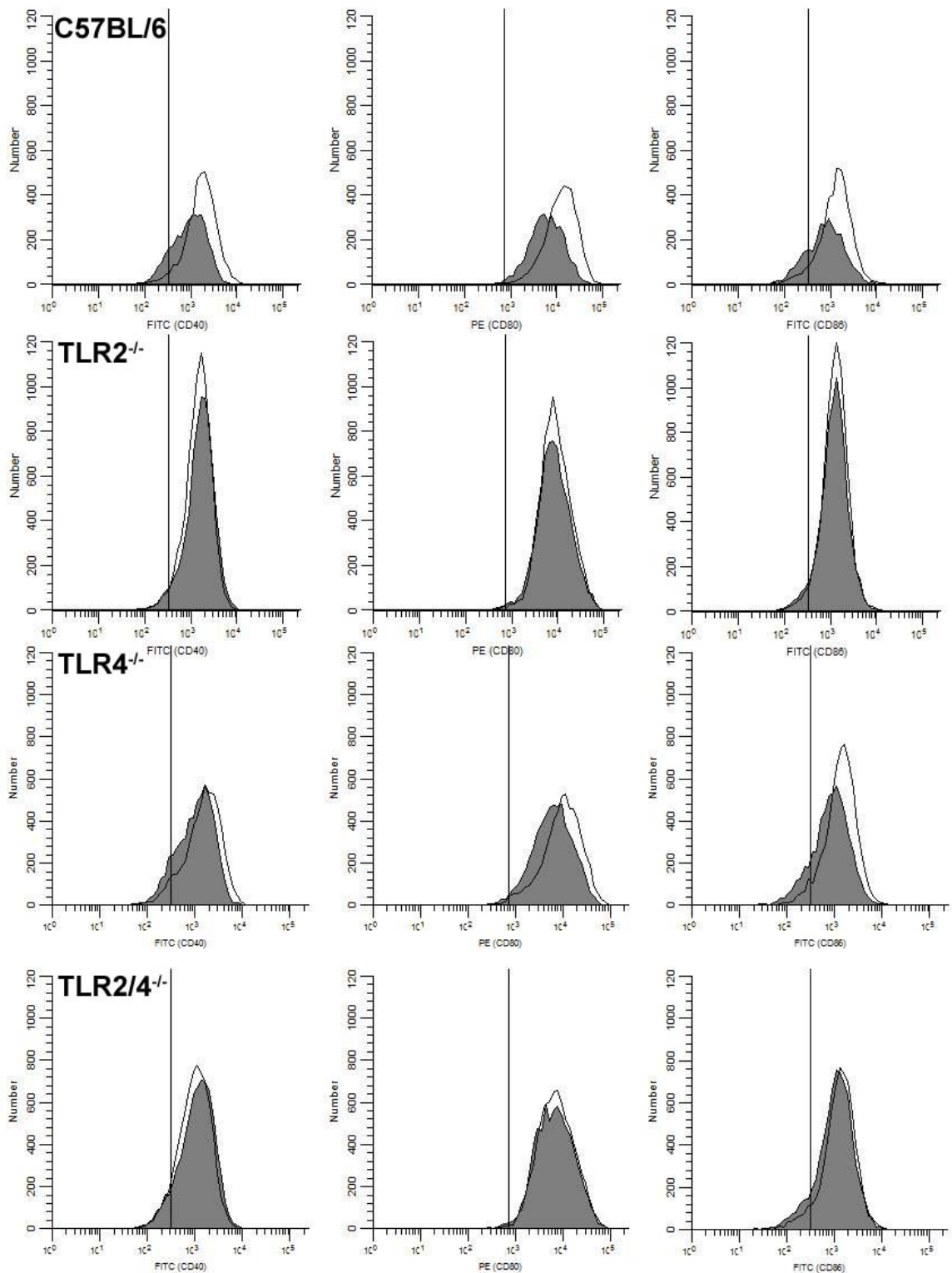


Figure 3.3. Dendritic cells were purified from C57BL/6, TLR2^{-/-}, TLR4^{-/-} and TLR2/4^{-/-} mice and stimulated with OvAg for 24 hours. Shaded peaks correspond to medium stimulation, black lines to OvAg stimulation. CD40, CD80 and CD86 are upregulated in response to OvAg stimulation in C57BL/6 and TLR4^{-/-} dendritic cells, but not in TLR2^{-/-} and TLR2/4^{-/-}.

I found increased levels of all cytokines in response to OvAg stimulation (Figure 3.4). Our results agreed with the previous work by Hise et al. (86). In this study TLR2- and TLR6-dependent macrophage activation by *O. volvulus* as measured by IL-6, TNF α and RANTES production was demonstrated.

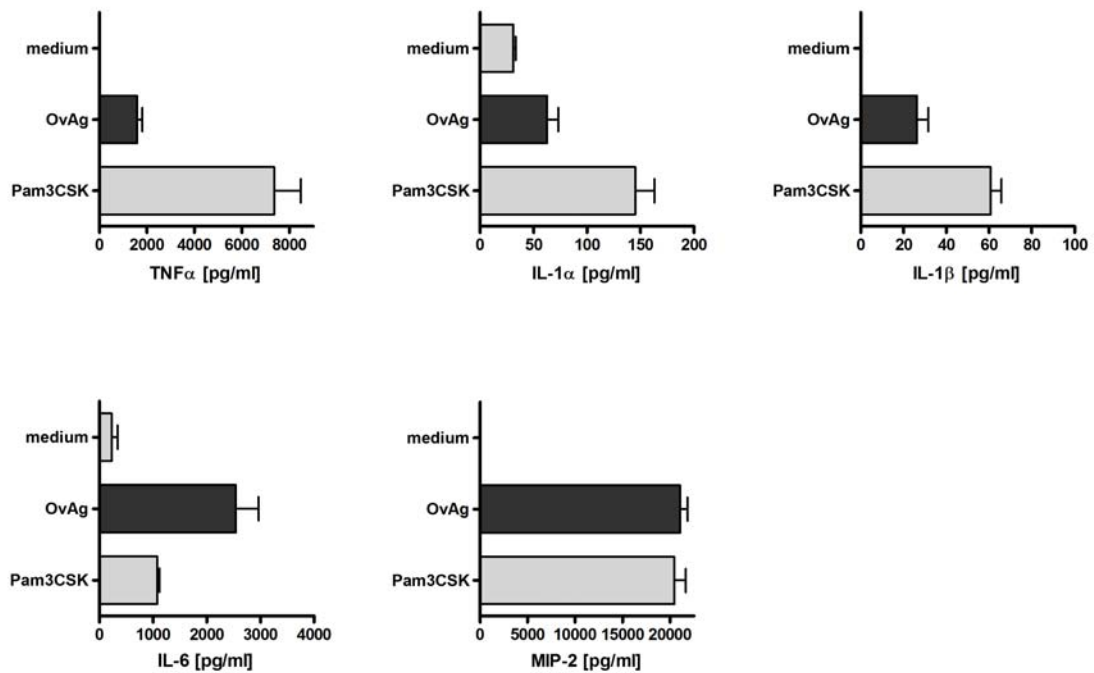


Figure 3.4. Macrophages were purified from C57BL/6 mice and stimulated for 18 hours with OvAg. Production of MIP-2, KC, TNF α , IL-1 α , IL-1 β and IL-6 were measured by ELISA. All cytokines are upregulated in response to OvAg.

3.1.3 Neutrophils

It was previously demonstrated that neutrophils are responsible for corneal opacification following injection of filarial extracts, *Wolbachia*, LPS and others (17, 29, 101). I therefore investigated neutrophil activation in addition to neutrophil infiltration into

the corneal stroma. Neutrophils were purified from the peritoneal cavity of Casein injected mice. Cells were purified over a 90 % Percoll gradient. Purity was generally greater than 95 %. 1×10^5 cells were stimulated with OvAg or TLR ligands for 18 hours unless otherwise noted. Cells and supernatants were analyzed for activation parameters.

Release of myeloperoxidase (MPO) was measured following stimulation of neutrophils with OvAg and Pam₃CSK for up to 6 hours. A slight increase in MPO production could be demonstrated for OvAg stimulation as early as one hour (Figure 3.5). After one hour of stimulation, no further increase in MPO release could be detected for six hours, when the remaining MPO was released by all cells independent of the stimulus. Neither Pam₃CSK nor LPS could induce MPO release by neutrophils.

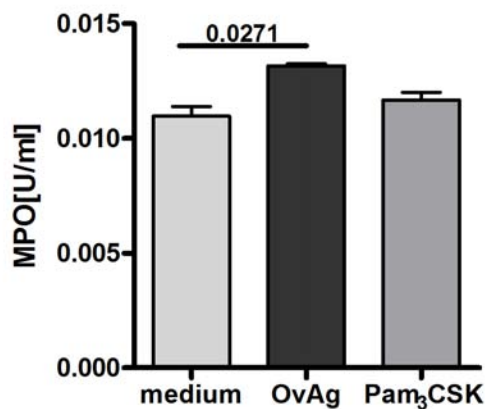


Figure 3.5. Neutrophils were purified from C57BL/6 mice and stimulated for 6 hours with OvAg. Neutrophils release myeloperoxidase in response to OvAg stimulation. Numbers given are p-values calculated by student's t-test.

MIP-2 (CXCL2) production was determined by sandwich ELISA (Figure 3.6). A dose-dependent increase in MIP-2 production could be demonstrated.

TLR2-dependent production of chemokines by neutrophils in response to stimulation with *O. volvulus* was shown by Gillette-Ferguson et al. (83).

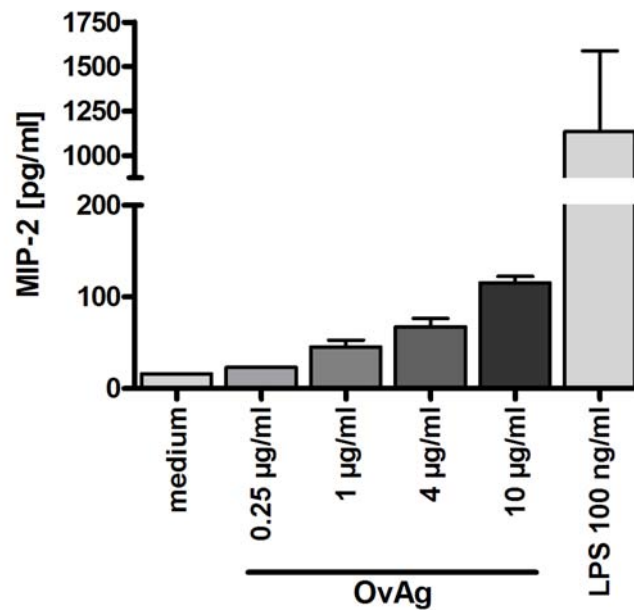


Figure 3.6. Neutrophils were purified from C57BL/6 mice and stimulated for 18 hours with OvAg. Neutrophils produce MIP-2 in response to OvAg in a dose-dependent manner.

Nitric oxide production was determined by fluorescence analysis using 4-amino-5-methylamino-2',7'-difluorofluorescein diacetate (DAF-FM). DAF-FM permeates the cell membrane. Upon contact with nitric oxide, DAF-FM forms a fluorescent product. Cells were incubated with DAF-FM for 1 hour to allow penetration of DAF-FM. Remaining dye was then washed off and cells were stimulated with OvAg and Pam₃CSK. Fluorescent measurements were taken for a total of 24 hours, with 1 minute intervals for the first 10 minutes, followed by 10 minute intervals for 1 hour and then 1 hour intervals for 24 hours. No NO production above background level was detected upon stimulation with OvAg or Pam₃CSK (Figure 3.7).

Reactive oxygen species (ROS) were detected using carboxylated dichlorodihydrofluorescein diacetate (carboxy-H₂DCFDA). By this method, hydrogen peroxide, peroxy

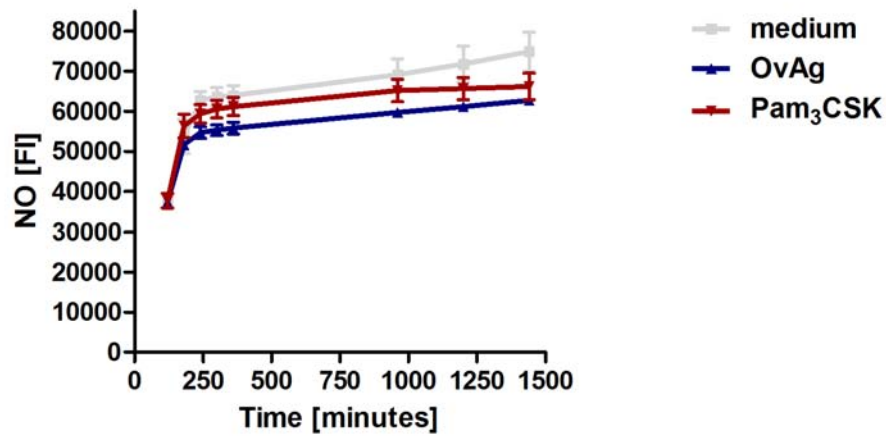


Figure 3.7. Neutrophils were purified from C57BL/6 mice and stimulated with OvAg. Production of nitric oxide was measured at different time points. Neutrophils do not produce increased levels of nitric oxide upon stimulation with OvAg or Pam₃CSK.

radicals and peroxynitrite anions can be detected. The fluorescent dye permeates the neutrophil membrane and, in the presence of reactive oxygen, intermediates undergoes oxidation to 2',7'-dichlorofluorescein. The cells were primed with carboxy-H₂DCFDA for one hour, then the extracellular dye was washed off. Cells were stimulated with OvAg and Pam₃CSK and fluorescence measurements commenced immediately, at 1 minute intervals for 10 minutes, followed by 10 minutes intervals for 1 hour and then hourly measurements for 24 hours (Figure 3.8). Increase in ROS production could be detected within the first 10 minutes with the highest increase during the first six hours. Interestingly, activation of ROS occurred independent of TLR2 and the TLR2 agonist Pam₃CSK could not induce ROS production in neutrophils.

I investigated surface expression of L-Selectin and CD18 by flow cytometry. Neutrophils were stimulated with filarial extracts and control reagents for 18 hours. In addition to L-Selectin and CD18 expression, I also examined CD11b and CD21/CD35 expression.

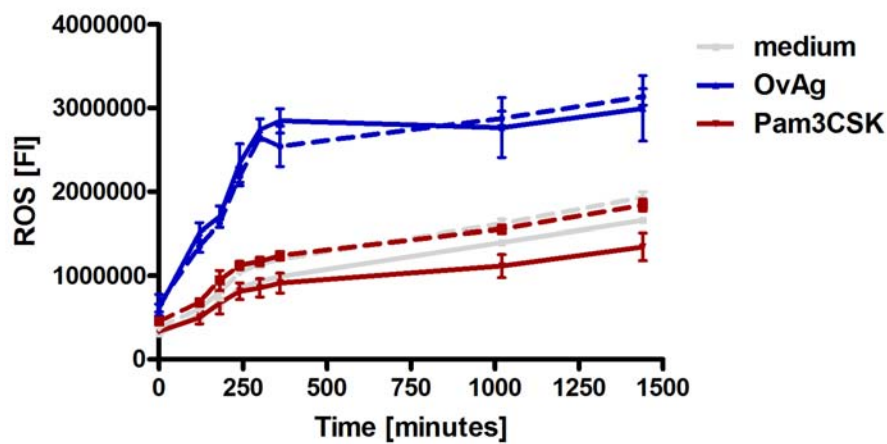


Figure 3.8. Neutrophils were purified from C57BL/6 and TLR2^{-/-} mice and stimulated with OvAg. ROS release was measured at different time points. Neutrophils produce ROS in response to stimulation with OvAg in a TLR2 independent manner. TLR2^{-/-} neutrophil stimulations are shown as dotted lines.

As expected I found a significant increase in CD11b and CD18 expression following stimulation with the TLR2 agonist Pam₃CSK and a significant down-regulation of L-Selectin. Stimulation with OvAg increased the expression of CD11b. The expression of CD18 and L-Selectin was not significantly altered, although a trend to higher expression of CD18 and decreased expression of L-Selectin could be observed. Up- and down-regulation of these surface markers was TLR2-dependent. Neutrophils from TLR2^{-/-} showed an unaltered expression of CD11b, CD18 and L-Selectin expression following stimulation with OvAg or Pam₃CSK. The expression of CD21/35 remained unaffected after the different stimulations (Figure 3.9).

Finally, I also examined the release of matrix metalloproteinases 2 and 9 by zymography. Both are gelatinases and would degrade the gelatin matrix of the protein gel, then be visualized by Coomassie blue staining. Several experiments revealed a multitude of bands of different sizes, however, some of it was shown to be due to gelatinase

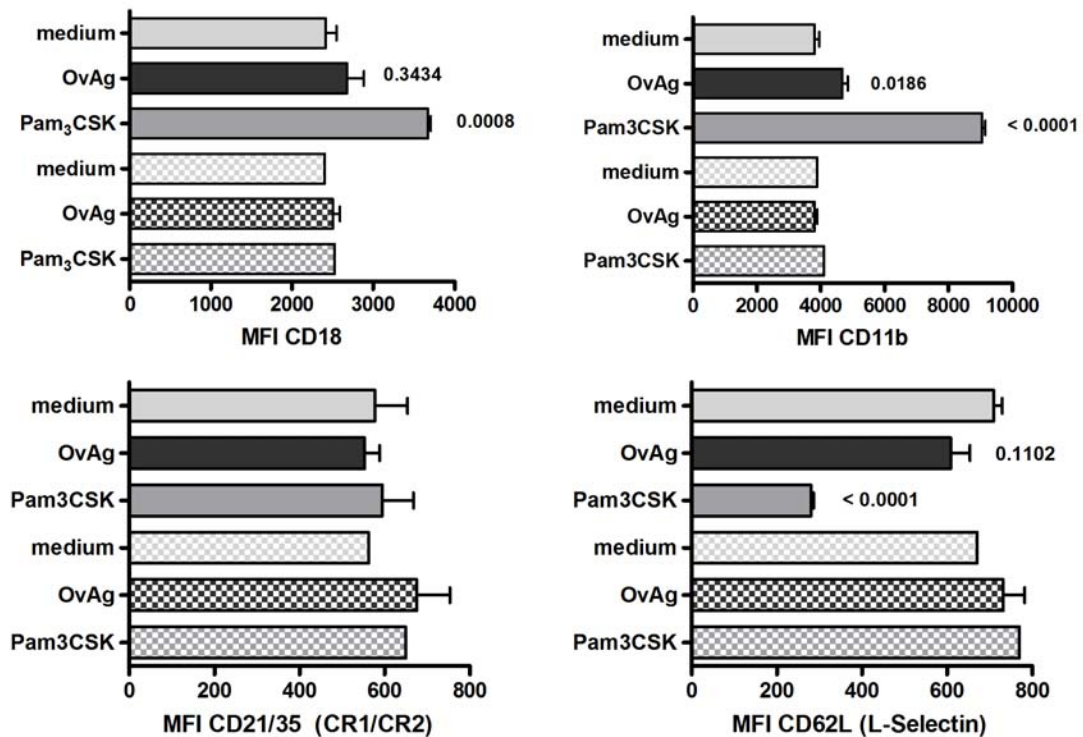


Figure 3.9. Neutrophils were purified from C57BL/6 and TLR2^{-/-} mice and stimulated with OvAg. Upon stimulation with OvAg, CD11b and CD18 were upregulated in a TLR2 dependent manner, whereas L-Selectin is downregulated in a TLR2 dependent manner as shown by mean fluorescent intensity (MFI). CR1 expression remained unaffected. The full bars correspond to responses by C57BL/6 neutrophils, checked bars correspond to responses by TLR2^{-/-} neutrophils. Numbers given are p-values calculated by student's t-test comparing stimulation with medium background.

activity of filarial extracts (data not shown). No clear conclusion could be drawn from that data.

3.2 The role of TLR2 and TLR4 in the generation of adaptive immune responses

3.2.1 T cell activation

Previous studies demonstrated that immunization with BmAg or *B. malayi* microfilariae, or with OvAg induced a predominant, but not exclusive Th₂-like response (28, 102). To examine the role of TLRs on the development of T cell phenotype, C57BL/6, TLR2^{-/-}, and TLR4^{-/-} mice were immunized subcutaneously three times over three weeks with OvAg. One week after the last immunization, mice were euthanized, splenocytes were stimulated *in vitro* with OvAg, and IL-5 and IFN- γ were measured by ELISA. Figure 3.10 shows IFN- γ production by splenocytes from OvAg immunized C57BL/6 and TLR4^{-/-} mice, but not by TLR2^{-/-} mice, indicating that filaria-induced IFN- γ production is TLR2-dependent. In contrast, IL-5 production was similar in splenocytes from all mouse strains. My findings indicate that TLR2 has a critical role in filaria-induced production of Th₁-associated IFN- γ , but not Th₂-associated IL-5.

3.2.2 Antibody production

Previous studies demonstrated that Th₂-associated isotypes IgE and IgG₁ are predominant after immunization with filarial extracts (34, 39). To determine the role of TLR2 and TLR4 on production of these isotypes, C57BL/6, TLR2^{-/-}, and TLR4^{-/-} mice were immunized as described above, and total serum IgE and filaria-specific IgG₁ were measured by ELISA. IgE was elevated in immunized C57BL/6 mice compared with unimmunized mice (Figure 3.11); however, there was no decrease in IgE levels among immunized TLR2^{-/-} and TLR4^{-/-} mice compared to C57BL/6 wildtype mice as shown in Figure 3.11.

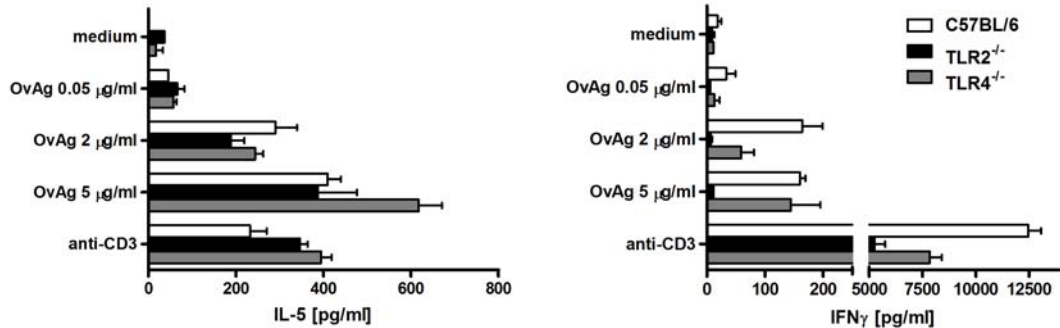


Figure 3.10. Splenocytes from immunized C57BL/6, TLR2^{-/-}, and TLR4^{-/-} mice were stimulated for 72 hours with medium, OvAg and anti-CD3 and IL-5 and IFN- γ production was measured by ELISA. Splenocytes from TLR2^{-/-} mice produced significantly less IFN- γ when stimulated with OvAg.

The only difference I detected were increased levels of IgE in TLR2^{-/-} mice. Similarly, filaria-specific IgG₁ in immunized C57BL/6 mice was detected at up to 1:100,000 dilution (filaria-specific IgG₁ in unimmunized mice was undetectable); however, as with IgE, there were no significant difference between C57BL/6 and TLR2^{-/-} or TLR4^{-/-} mice (Figure 3.12). Previous studies also demonstrated that filaria-specific IgG_{2a}, which is associated with IFN- γ production (103–105), is produced at low levels compared with IgG₁ (106). Filaria-specific IgG_{2c} levels were low in C57BL/6 mice, and there was no difference between these and TLR2^{-/-} and TLR4^{-/-} mice. These findings indicate that TLR2 and TLR4 have no major role in production of filaria-specific antibodies.

3.3 The role of TLR2 and TLR4 in corneal inflammation

Previous studies showed that neutrophils and eosinophils are recruited to the corneas of immunized mice in a biphasic manner after injection of parasite extracts to the corneal

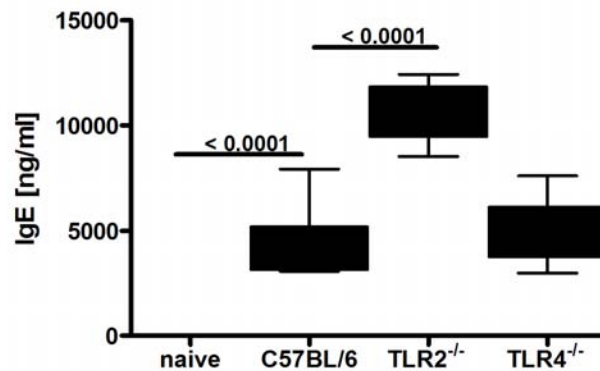


Figure 3.11. Serum levels of IgE in immunized C57BL/6, TLR2^{-/-} and TLR4^{-/-} mice were measured by ELISA. IgE was increased in immunized mice compared with naive mice. TLR2^{-/-} showed higher levels of IgE compared with C57BL/6 mice. Numbers given are p-values calculated by student's t-test.

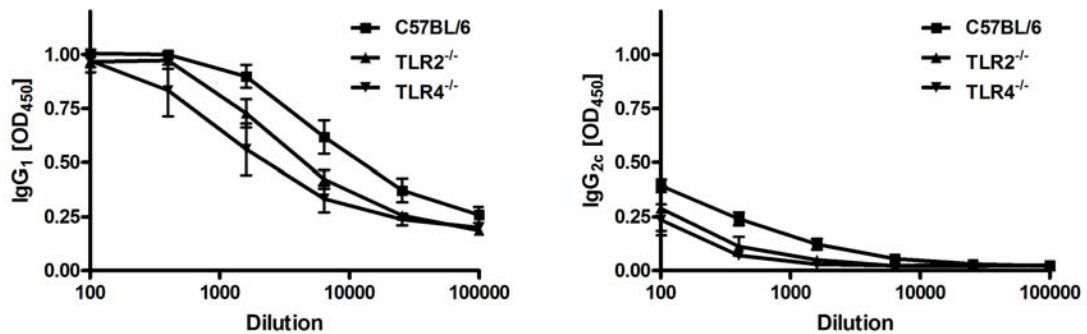


Figure 3.12. Serum levels of antigen-specific IgG₁ and IgG_{2c} in immunized C57BL/6, TLR2^{-/-} and TLR4^{-/-} mice were measured by ELISA. No difference in antibody levels was detected in those strains.

stroma. In this model of *Onchocerca* keratitis (river blindness), neutrophil recruitment peaks 24h after injection, whereas eosinophils are the predominant cell type after 72 hours (32, 41). To determine if TLRs regulate neutrophil and eosinophil migration to the corneal stroma, I injected OvAg into the corneal stroma of immunized C57BL/6, TLR2^{-/-},

and TLR4^{-/-} mice, and quantified the number of neutrophils in the corneal stroma after 24 hours, and the number of eosinophils after 72 hours.

3.3.1 Cellular infiltration

A representative figure of neutrophil infiltration in C57BL/6 and TLR2^{-/-} mice can be seen in Figure 3.13. As shown in Figure 3.14, neutrophils are present in the corneas of immunized C57BL/6 mice and TLR4^{-/-} mice after intrastromal injection of OvAg, whereas in TLR2^{-/-} mice, the number of neutrophils was significantly lower than in C57BL/6 mice.

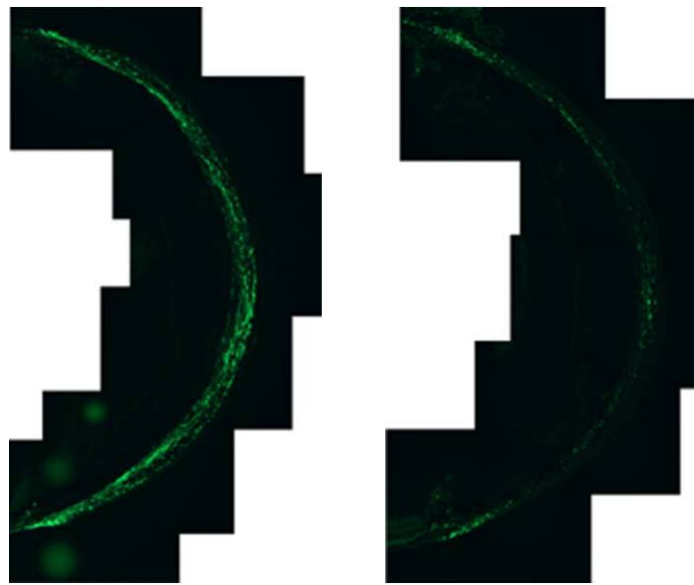


Figure 3.13. Cross section of the cornea: neutrophil infiltration into the corneas of C57BL/6 (left panel) and TLR2^{-/-} (right panel) mice.

In contrast, there was no significant difference in eosinophil numbers among any of the strains (Figure 3.15). If anything, slightly increased levels of eosinophils were found in TLR2^{-/-} mice.

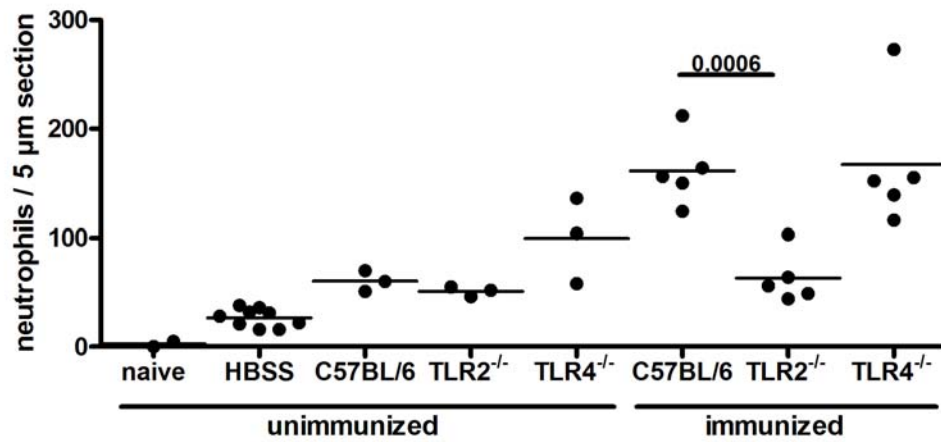


Figure 3.14. Neutrophil infiltration into the corneas of naive and immunized C57BL/6, TLR2^{-/-} and TLR4^{-/-} mice at 24 hours post injection. Neutrophil infiltration was decreased in TLR2^{-/-} mice compared with C57BL/6 mice. Numbers given are p-values calculated by student's t-test.

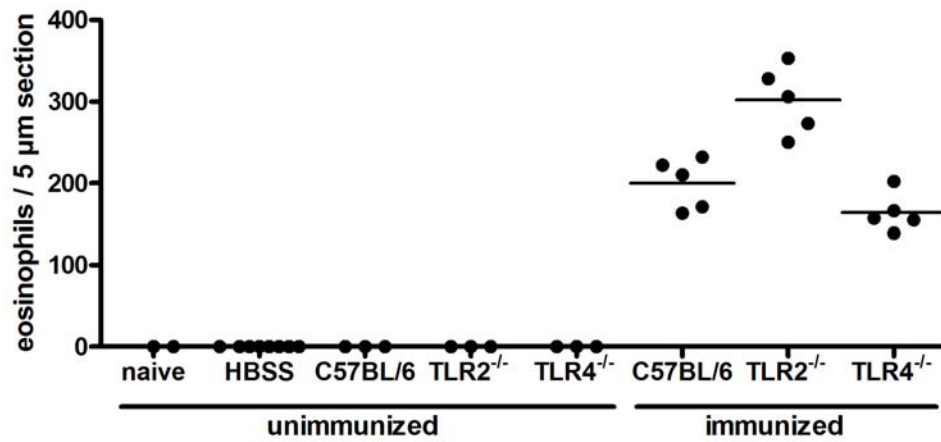


Figure 3.15. Eosinophil infiltration into the corneas of naive and immunized C57BL/6, TLR2^{-/-} and TLR4^{-/-} mice at 72 hours post injection. Eosinophil infiltration was slightly increased in TLR2^{-/-}.

I only found low numbers (50 cells per 5 μm section) of CD4⁺ T cells in the cornea. Those cells mainly remained in the periphery and failed to migrate to the central cornea (data not shown). There were no differences among the different mouse strains.

Macrophage numbers were quantified as F4/80⁺ and CD169⁺ positive cells. F4/80 is expressed on tissue macrophages, whereas CD169 is upregulated on activated macrophages. I found decreased macrophage infiltration into the corneas of TLR2^{-/-} mice one day post injection (data not shown). This corresponds to findings in naive mice injected with filarial extract, where macrophage migration was also dependent on the presence TLR2 (86).

3.3.2 PECAM expression

Previous studies have identified decreased PECAM-1 expression on limbal vessels in the absence of IFN- γ (96). I therefore examined PECAM-1 expression in TLR2^{-/-} mice in comparison to wildtype C57BL/6 to investigate the effect of decreased IFN- γ production in TLR2^{-/-} mice on PECAM-1 expression as a potential mechanism of decreased neutrophil infiltration into the corneas of these mice. Corneal sections were stained with FITC labelled anti-PECAM-1 antibodies and images were recorded and analyzed using ImagePro software. Vessels were marked using this software and the fluorescence intensity per vessel area was calculated. I then averaged the fluorescence intensity per vessel for each eye. As shown in Figure 3.16, no significant differences in PECAM-1 expression were detected, although a trend to reduced PECAM-1 expression was found.

3.3.3 Chemokine production

To determine whether decreased neutrophil infiltration was caused by decreased chemokine production, mice were immunized and injected with filarial extracts as described above. One day post injection, I excised a 2 mm button of the cornea, homogenized the tissue and measured KC, MIP-2 and LIX by ELISA. In TLR2^{-/-} mice no increased

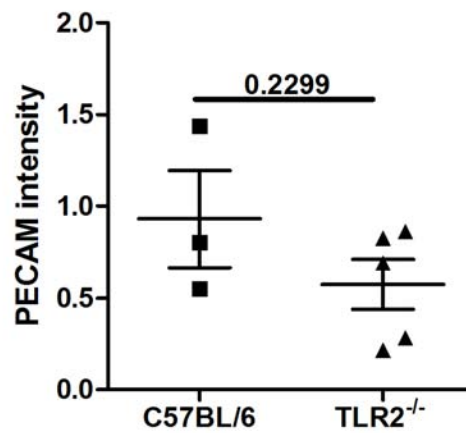


Figure 3.16. Expression of PECAM-1 on the limbal vessels in immunized C57BL/6 and TLR2^{-/-} mice at 24 hours post injection. Numbers given are p-values calculated by student's t-test.

levels of all three chemokines in response to OvAg injection was measured compared to naive, HBSS injected corneas. (Figure 3.17). There was an increased chemokine production in immunized C57BL/6 and TLR4^{-/-} mice with no difference between C57BL/6 and immunized TLR4^{-/-} mice.

Thus decreased chemokine production is one mechanism for reduced neutrophil infiltration into the corneal stroma.

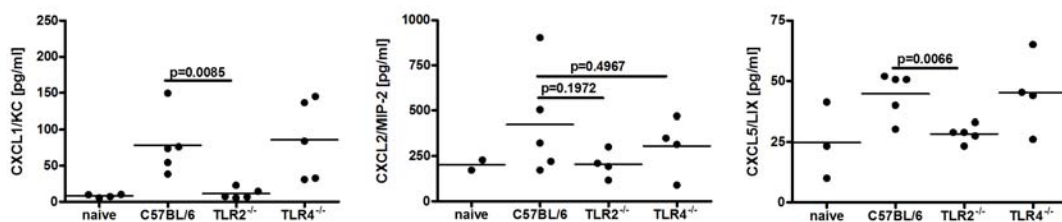


Figure 3.17. CXC chemokine production following HBSS injection (naive) or OvAg injection into immunized mice. CXC chemokine production is decreased in TLR2^{-/-}, but not in TLR4^{-/-} mice. Numbers given are p-values calculated by student's t-test.

3.4 The role of IFN- γ in the generation of adaptive immune responses

3.4.1 T cell activation

C57BL/6 and IFN- γ ^{-/-} mice were immunized as described previously. Splensens were dissected and single cell suspensions prepared. Splenocytes were stimulated for 72 hours with medium, OvAg and anti-CD3. Figure 3.18 shows that anti-CD3 and OvAg treated splenocytes from C57BL/6 produced IFN- γ , while it was absent in cultures from IFN- γ ^{-/-} mice, and that IL-5 production by IFN- γ ^{-/-} mice was not significantly different from IL-5 production by C57BL/6 mice.

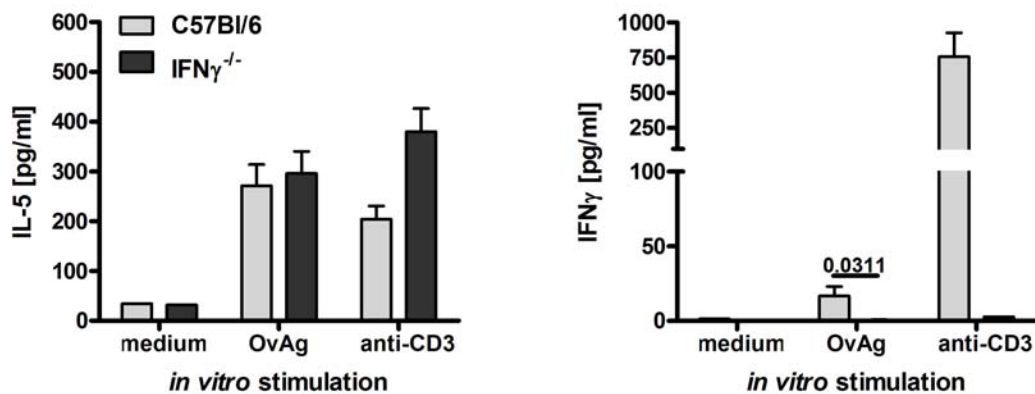


Figure 3.18. Splenocytes of immunized C57BL/6 and IFN- γ ^{-/-} mice were stimulated for 72 hours with OvAg and IL-5 and IFN- γ production were measured by ELISA. There was no IFN- γ production in IFN- γ ^{-/-} mice. IL-5 production did not differ between the two strains. Numbers given are p-values calculated by student's t-test.

3.4.2 Cellular infiltration

Corneas of immunized C57BL/6 and IFN- $\gamma^{-/-}$ mice were injected with OvAg and eyes enucleated at one day post injection. Neutrophil infiltration was determined by immunohistochemistry as described above. As shown in Figure 3.19, the number of neutrophils in the cornea was significantly lower in IFN- $\gamma^{-/-}$ mice compared with C57BL/6 mice, indicating that IFN- γ affects OvAg-induced neutrophil recruitment to the corneal stroma.

I found no significant difference in the number of eosinophils in the corneas of immunized C57BL/6 and IFN- $\gamma^{-/-}$ mice.

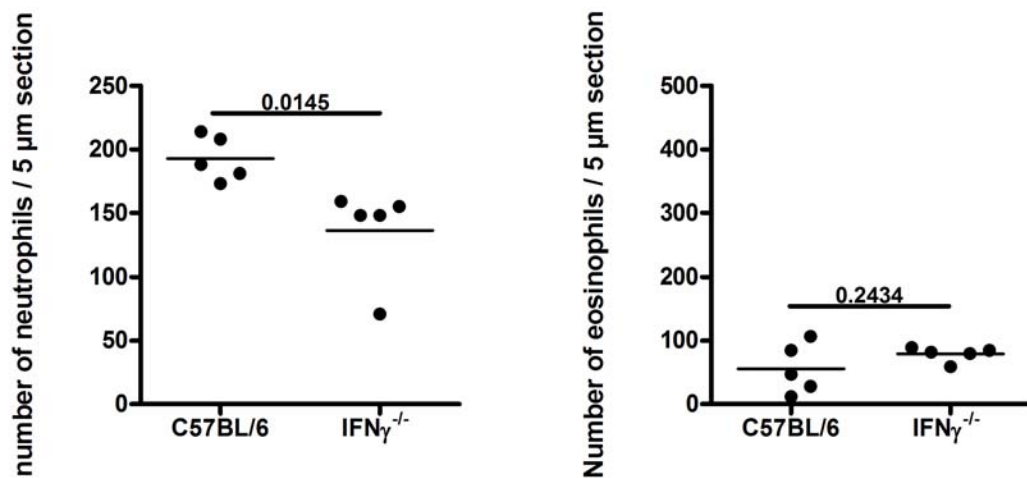


Figure 3.19. Neutrophil and eosinophil migration to the corneas of immunized C57BL/6 and IFN- $\gamma^{-/-}$ mice at 24 hours post injection. Neutrophil infiltration was decreased in IFN- $\gamma^{-/-}$ mice. Numbers given are p-values calculated by student's t-test.

3.4.3 PECAM expression

Studies by other groups showed IFN- γ -dependent PECAM-1 expression in the mouse corneas following injection of *Herpes simplex* virus (96). Therefore I determined the expression of PECAM-1 in C57BL/6 and IFN- $\gamma^{-/-}$ mice. PECAM-1 expression was analyzed as described above. I found no difference in PECAM-1 expression between C57BL/6 and IFN- $\gamma^{-/-}$ mice (Figure 3.20).

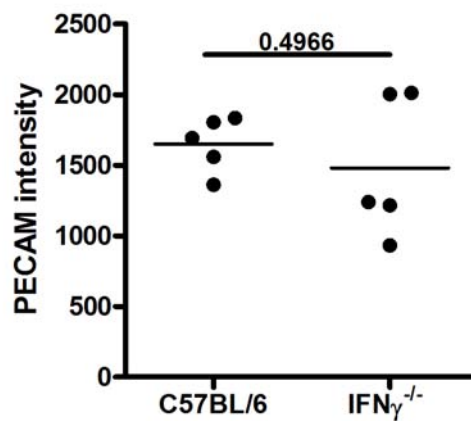


Figure 3.20. PECAM-1 expression on limbal vessels of the cornea was determined at 24 hours post injection. PECAM-1 expression did not differ in the corneas of C57BL/6 and IFN- $\gamma^{-/-}$ mice. Numbers given are p-values calculated by student's t-test.

3.5 IFN- γ induced cytokine responses in macrophages and fibroblasts

3.5.1 Macrophages

To examine whether IFN- γ has a synergistic effect with OvAg on cytokine production, macrophages isolated from the peritoneal cavity were stimulated for 18 hours with either OvAg, rIFN- γ alone, or with both, then IL-1 α , IL-1 β , TNF α and IL-6 were measured by ELISA. Previous studies from our group showed macrophage activation with filaria/*Wolbachia* antigens (86), and I found a dose-dependent increase of cytokine production, and chose 2 μ g/ml OvAg (half maximum cytokine production) as an optimal dose. As shown in Figure 3.21, macrophages incubated with rIFN- γ alone did not induce cytokine production, and incubation with OvAg alone produced increased levels of IL-1 α , IL-1 β , TNF α and IL-6. In marked contrast, rIFN- γ added to macrophages together with OvAg stimulated greatly elevated levels of all four cytokines (Figure 3.21). The synergistic effect of IFN- γ and OvAg was further increased if macrophages were incubated for 6 hours with rIFN- γ prior to stimulation with OvAg (Figure 3.22). Priming was most efficient for production of IL-6 and TNF α . Priming with OvAg followed by IFN- γ stimulation did not have a similar effect.

As CXC chemokines are important for recruitment of neutrophils to the corneal stroma, with macrophages producing CXCL1/KC and CXCL2/MIP-2 (17), I examined if there is a synergistic effect of IFN- γ on OvAg-induced production of these chemokines.

Peritoneal macrophages were stimulated with OvAg, rIFN- γ or both, and CXCL1/KC and CXCL2/MIP-2 were measured by ELISA. As shown in Figure 3.23, OvAg stimulated

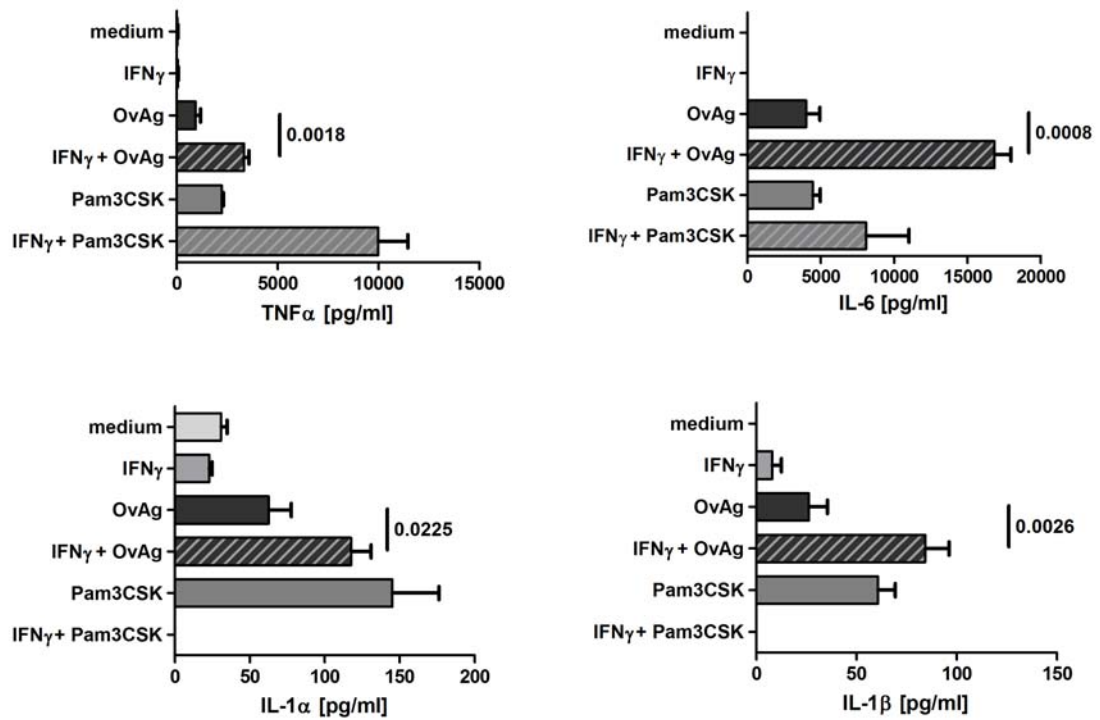


Figure 3.21. Primary macrophages were purified from C57BL/6 mice and stimulated for 18 hours with rIFN- γ . rIFN- γ did not induce cytokine production in primary macrophages. Stimulation with rIFN- γ and OvAg induced increased levels of IL-1 α , IL-1 β , TNF α and IL-6. Numbers given are p-values calculated by student's t-test.

macrophages produced more chemokines than unstimulated cells; however, the addition of IFN- γ did not increase production of any of these chemokines. Therefore, in contrast to pro-inflammatory cytokines, production of CXC chemokines is not enhanced by IFN- γ , and indicate that IFN- γ has a selective effect on macrophage production of pro-inflammatory cytokines.

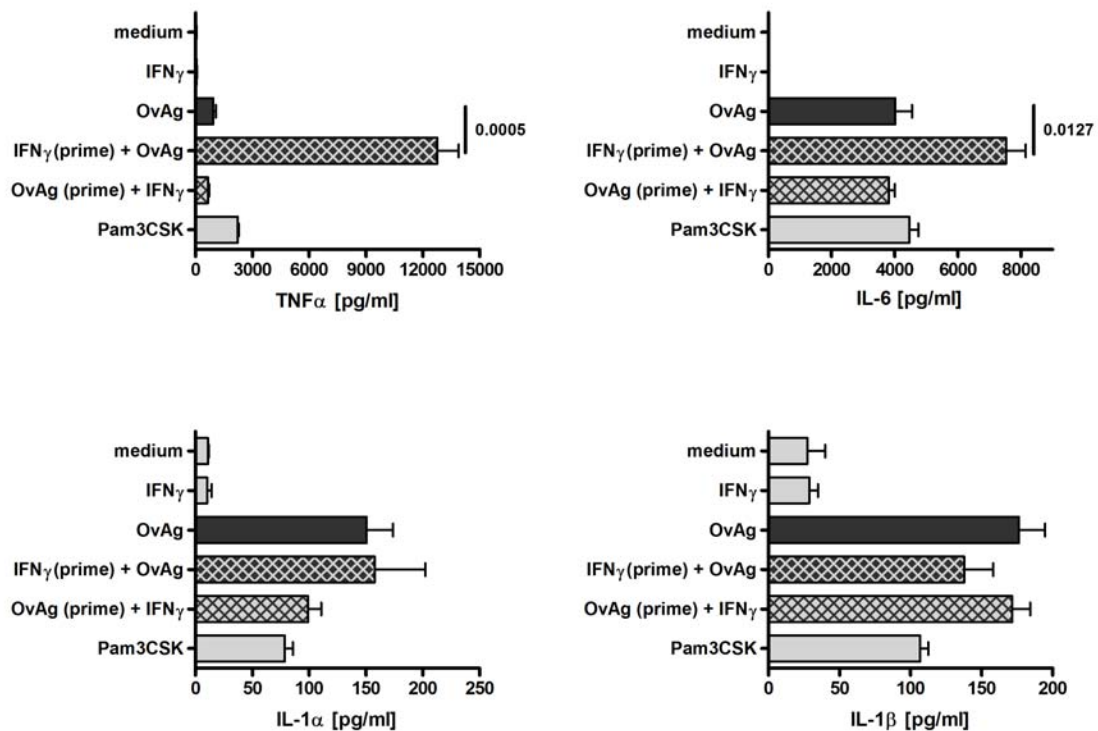


Figure 3.22. Macrophages were purified from C57BL/6 mice and primed with rIFN- γ or OvAg, followed by stimulation with OvAg or rIFN- γ . For controls, cells were incubated with medium only prior to "restimulation". Priming was only effective with rIFN- γ and induced increased cytokine production by macrophages. Numbers given are p-values calculated by student's t-test.

3.5.2 Neutrophils

Neutrophils were shown to be activated by OvAg. Although they do not reside in the corneal stroma, these cells are the first responders upon injection of filarial extract and could enhance further neutrophil migration by CXC chemokine production. I did not find increased production of MIP-2 by neutrophils in responses to stimulation with rIFN- γ and OvAg (Figure 3.24).

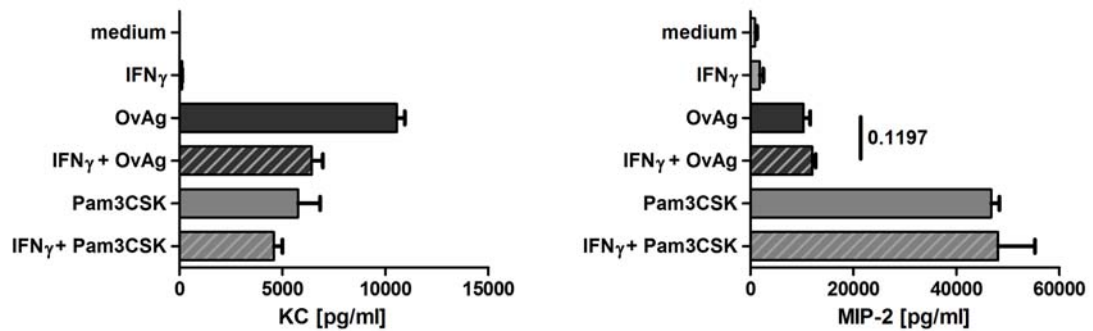


Figure 3.23. Macrophages were purified from C57BL/6 mice and stimulated with rIFN- γ and OvAg. KC and MIP-2 production by macrophages was not increased by costimulation with rIFN- γ and OvAg. Numbers given are p-values calculated by student's t-test.

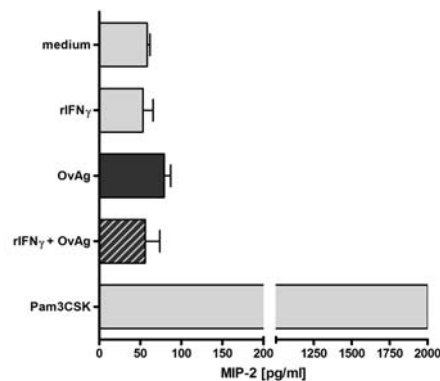


Figure 3.24. Neutrophils were purified from C57BL/6 mice and stimulated with rIFN- γ and OvAg. MIP-2 production following stimulation of neutrophils with rIFN- γ or costimulation with rIFN- γ and OvAg was not increased.

3.5.3 MK/T-1 cells

As CXC chemokines are important for recruitment of neutrophils to the corneal stroma, with corneal fibroblasts producing CXCL1/KC and CXCL5/LIX (17), I examined if there is a synergistic effect of IFN- γ on OvAg-induced production of either chemokine.

MK/T-1 murine corneal fibroblasts were stimulated with OvAg, rIFN- γ or both, and CXCL1/KC and CXCL5/LIX were measured by ELISA. As shown in Figure 3.25, OvAg stimulated corneal fibroblasts produced more chemokines than unstimulated cells; however, the addition of rIFN- γ did not increase production of any of these chemokines by MK/T-1 cells.

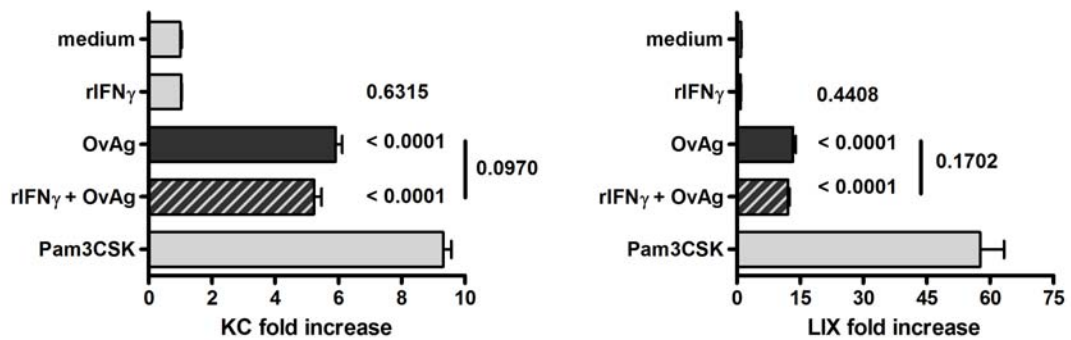


Figure 3.25. The murine fibroblast cell line MK/T-1 was stimulated for 18 hours with rIFN- γ or OvAg or both. rIFN- γ alone did not induce production of CXC chemokines and did not increase CXC chemokine production following stimulation with OvAg. Numbers given are p-values calculated by student's t-test and compared to medium stimulation alone (no bar), or comparing OvAg alone to rIFN- γ +OvAg when marked with a bar.

3.5.4 TLR2 expression on macrophages

As macrophages and dendritic cells are present in the normal corneal stroma (107, 108) and macrophages respond to IFN- γ stimulation, I examined if IFN- γ regulates TLR2 expression by macrophages. Macrophages isolated from the peritoneal cavity were incubated for 6 hours with OvAg, IFN- γ or both, and surface expression of TLR2 was analyzed by flow cytometry. As shown in Figure 3.26, TLR2 surface expression was elevated after stimulation with rIFN- γ . Co-stimulation with rIFN- γ together with either OvAg or

the TLR ligand Pam3CSK further increased TLR2 expression above that of either ligand or IFN- γ alone. These observations indicate that one mechanism of IFN- γ synergism with OvAg is to elevate expression of TLR2 on macrophages.

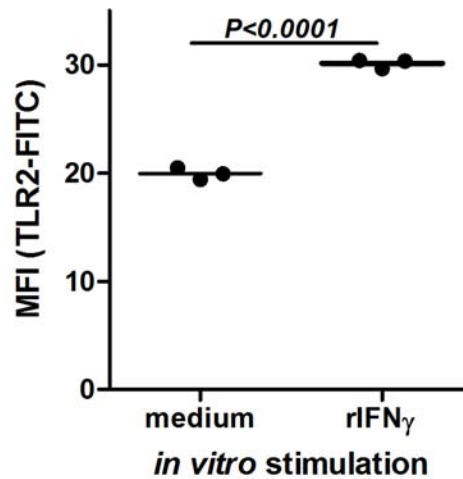


Figure 3.26. Macrophages were purified from C57BL/6 mice and stimulated for 6 hours with rIFN- γ . Stimulation with rIFN- γ increased surface expression of TLR2. Numbers given are p-values calculated by student's t-test

3.6 Activation of macrophages, neutrophils and fibroblasts by pro-inflammatory cytokines.

As I demonstrated that IFN- γ increases production of pro-inflammatory cytokines but not chemokines, I determined whether the pro-inflammatory cytokines rather than IFN- γ affected the production of chemokines by macrophages, fibroblasts and neutrophils.

3.6.1 Macrophages

Peritoneal macrophages were isolated as described above, incubated with rTNF α , rIL-1 α , rIL-1 β or rIL-6. Stimulation with rTNF α and rIL-1 α increased the production of KC and MIP-2 (Figure 3.27), but stimulation with IL-1 β and IL-6 did not.

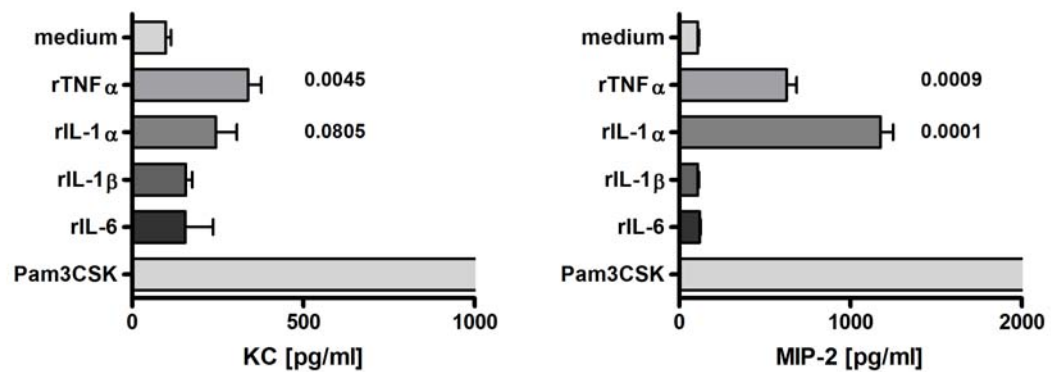


Figure 3.27. Stimulation of C57BL/6 macrophages for 18 hours with TNF α and rIL-1 α , but not with rIL-1 β or rIL-6, increased the production of KC and MIP-2. P-values shown are comparing stimulation with recombinant cytokines to medium stimulation.

3.6.2 Neutrophils

Peritoneal neutrophils were purified as described above. Cells were stimulated with rTNF α , rIL-1 α , rIL-1 β or rIL-6. Low levels of MIP-2 were induced by rIL-1 α , rIL-1 β or rIL-6, but not rTNF α (Figure 3.28). This does not appear to be a major activation pathway.

3.6.3 MK/T-1 cells

Previous studies from our lab showed that corneal fibroblasts secrete high levels of CXCL5/LIX in addition to CXCL1/KC in response to LPS (17); therefore I examined KC

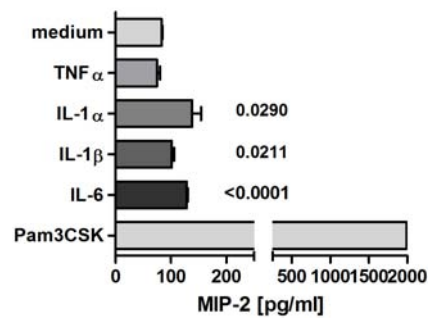


Figure 3.28. Stimulation of C57BL/6 neutrophils for 18 hours with rIL-1 α , rIL-1 β or rIL-6, but not with rTNF α increased the production of MIP-2. P-values shown are comparing stimulation with recombinant cytokines to medium stimulation.

and LIX production by ELISA. As shown in Figure 3.29, corneal fibroblasts produced KC and LIX in response to rTNF α , rIL-1 α and rIL-1 β . rIL-6 did not induce cytokine production by MK/T-1 cells.

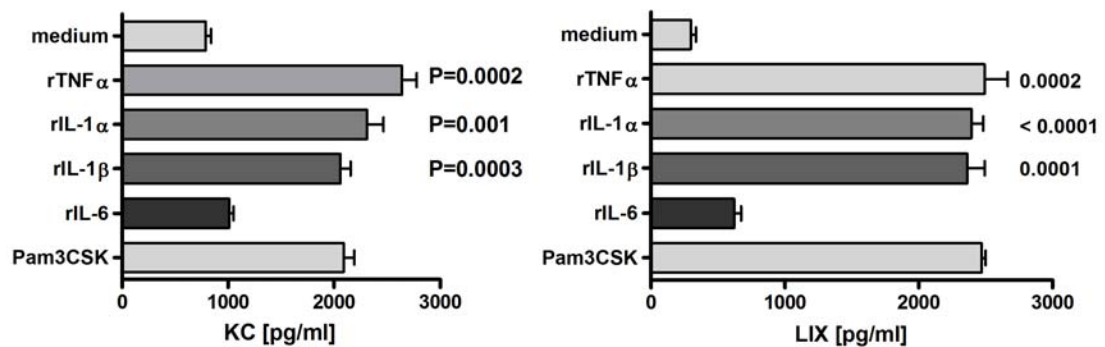


Figure 3.29. Activation of MK/T-1 cells by stimulation with recombinant cytokines was measured by ELISA. rTNF α , rIL-1 α and rIL-1 β induced production of KC and LIX. P-values shown are comparing stimulation with recombinant cytokines to medium stimulation.

3.7 The role of IL-1R1, IL-6 and TNF α in T cell responses and corneal inflammation

With my studies *in vitro* I demonstrated that IL-1, IL-6 and TNF α production are affected by increased levels of IFN- γ . Therefore I examined whether deficiency in these cytokines affected corneal inflammation *in vivo*. C57BL/6, IL-1R1^{-/-}, IL-6^{-/-} and TNF α R^{-/-} mice were immunized as described above and the corneas were injected with soluble OvAg. T cell activation was examined to determine if cytokine deficiency led to insufficient immunization systemically and therefore decreased corneal inflammation.

3.7.1 T cell activation

Following euthanasia, spleens were dissected and splenocyte cultures were incubated with medium, OvAg or anti-CD3 for 72 hours. IL-5 and IFN- γ production was determined by ELISA. In IL-1R1^{-/-} mice, IL-5 and IFN- γ production remained unaffected in comparison to C57BL/6 mice as shown in Figure 3.30. If anything, a slight, but not significant, increase of IL-5 was detected. As I was investigating neutrophil infiltration in response to OvAg stimulation via increased systemic levels of IFN- γ , these experiments were not affected by this increase.

In IL-6^{-/-} mice, IL-5 production remained unaffected in comparison to C57BL/6 mice as shown in Figure 3.31. If anything, a slight, but not significant, increase of IL-5 was detected. IFN- γ levels were undetectable following OvAg stimulation in both C57BL/6 and IL-6^{-/-} mice. However, in this experiment, splenocytes from IL-6^{-/-} mice did not produce similar amounts of IFN- γ in response to anti-CD3 when compared with

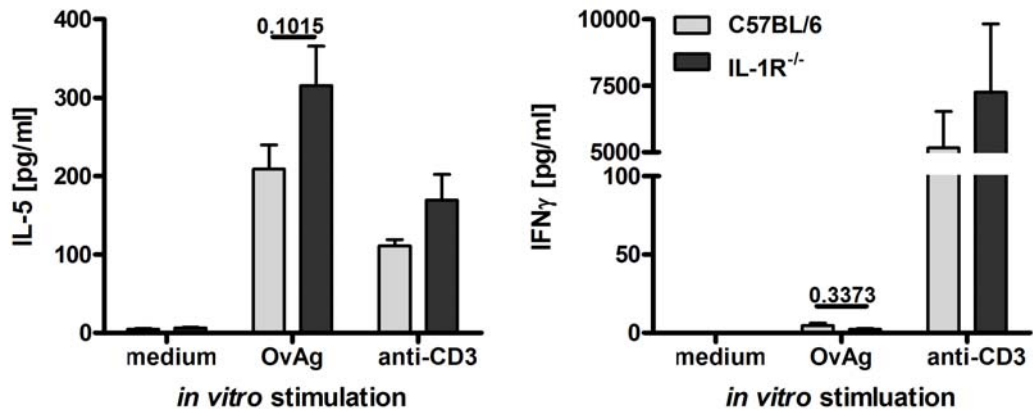


Figure 3.30. IL-5 and IFN- γ production remained unaffected in immunized IL-1R^{-/-} mice compared with C57BL/6 mice. P-values shown are comparing stimulation with OvAg in C57BL/6 and IL-1R^{-/-} mice.

C57BL/6 mice. This was not reproducible in other experiments. Cells were viable as they produced normal amounts of IL-5 in response to anti-CD3.

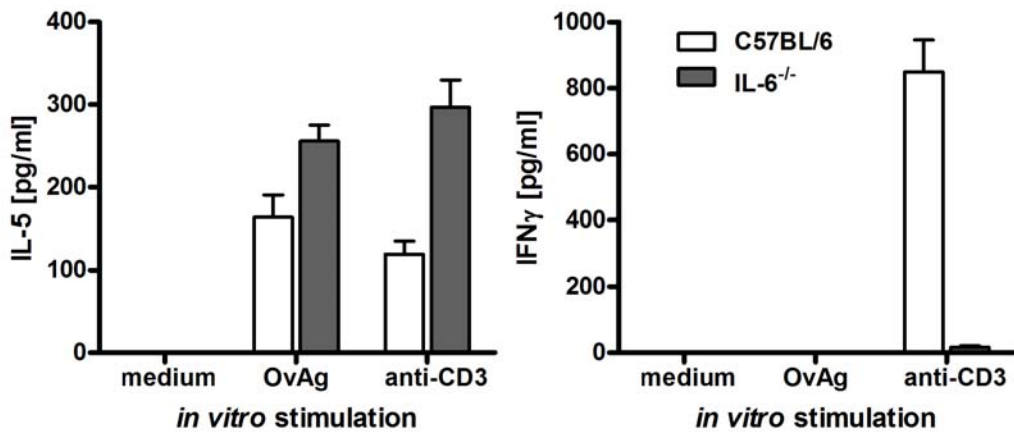


Figure 3.31. IL-5 production remained unaffected in immunized IL-6^{-/-} mice compared with C57BL/6 mice, but IFN- γ production was decreased. Numbers given are p-values calculated by student's t-test.

In $\text{TNF}\alpha\text{R}^{-/-}$ mice, IL-5 and IFN- γ production remained unaffected in comparison to C57BL/6 mice as shown in Figure 3.32. If anything, a slight, but not significant, increase of IL-5 was detected. As I was investigating neutrophil infiltration in response to OvAg stimulation via increased systemic levels of IFN- γ , these experiments were not affected by this increase.

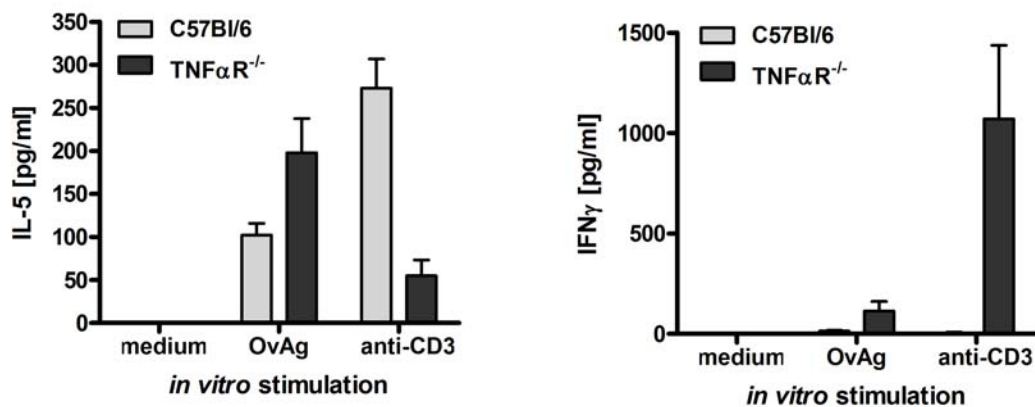


Figure 3.32. IL-5 and IFN- γ production remained unaffected in immunized $\text{TNF}\alpha\text{R}^{-/-}$ mice compared with C57BL/6 mice.

3.7.2 Granulocyte migration into the corneal stroma of cytokine (receptor) knockout mice

Corneas of immunized C57BL/6, $\text{IL-1R1}^{-/-}$, $\text{IL-6}^{-/-}$ and $\text{TNF}\alpha\text{R}^{-/-}$ mice were injected with OvAg and neutrophil infiltration was determined at 24 hours post injection by immunohistochemistry.

In $\text{IL-1R1}^{-/-}$ mice, neutrophil infiltration was significantly reduced compared to C57BL/6 mice (Figure 3.33). In contrast, eosinophil infiltration remained unaffected in these mice (Figure 3.33).

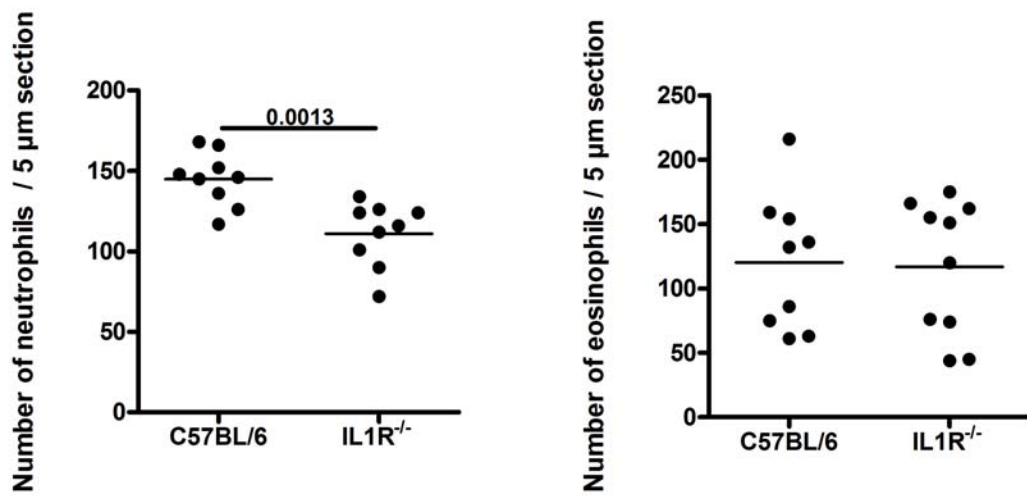


Figure 3.33. Neutrophil infiltration into the corneal stroma is abrogated in immunized IL-1R1^{-/-} mice compared to C57BL/6 mice while eosinophil infiltration remains unaffected. Numbers given are p-values calculated by student's t-test.

In IL-6^{-/-} mice, neutrophil infiltration was significantly reduced compared to C57BL/6 mice (Figure 3.34). In contrast, eosinophil infiltration remained unaffected in these mice, even though there was a slight trend towards decreased levels in IL-6^{-/-} mice (Figure 3.34).

In TNF α R^{-/-} mice, migration of neutrophils and eosinophils to the corneal stroma showed no difference to C57BL/6 mice (Figure 3.35).

3.8 *In vivo* responses to *Wolbachia*

3.8.1 Injection of *Wolbachia* depleted filarial extract into the cornea.

As previous studies suggested that pro-inflammatory immune responses are at least partially induced by the endosymbiont *Wolbachia* (29, 84, 101), I next immunized C57BL/6

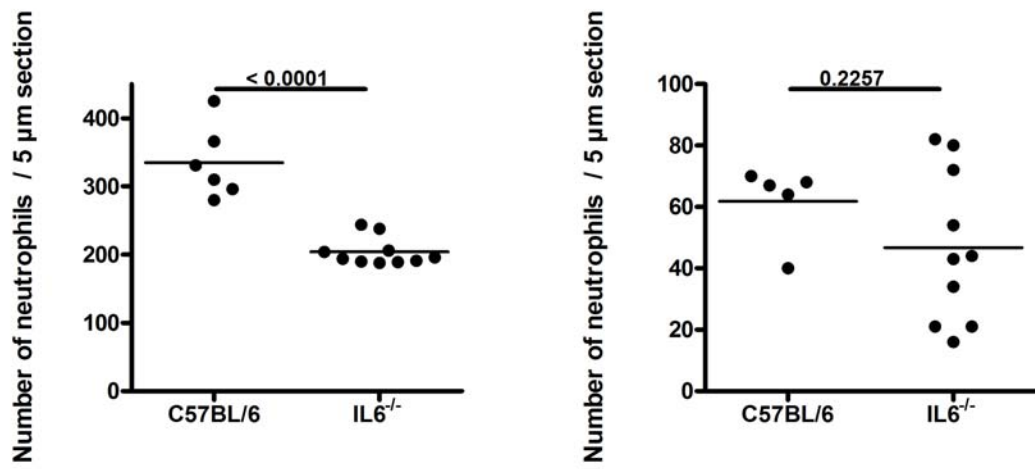


Figure 3.34. Neutrophil infiltration into the corneal stroma is abrogated in immunized IL-6^{-/-} mice compared with C57BL/6 mice while eosinophil infiltration remains unaffected.

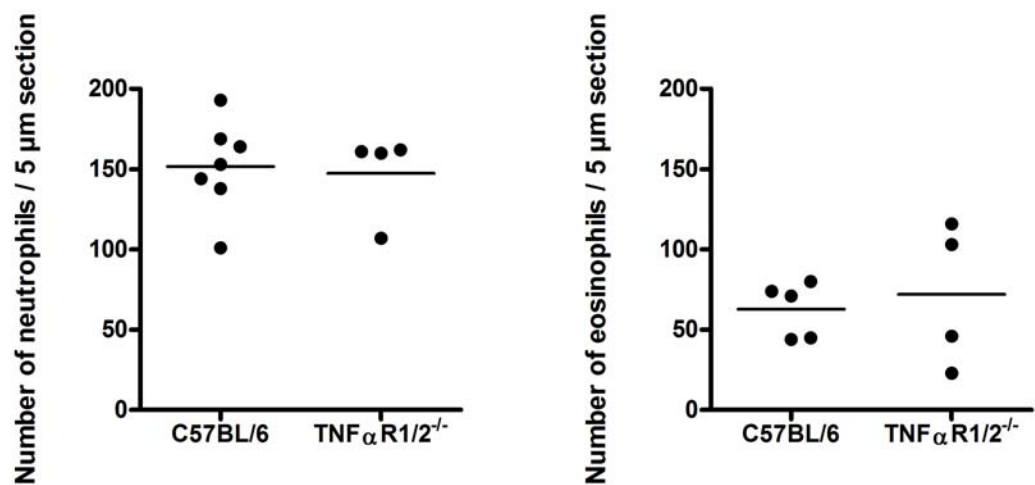


Figure 3.35. No difference in neutrophil and eosinophil infiltration to the corneal stroma between immunized C57BL/6 and TNF α R^{-/-} mice.

mice with 100 000 *B. malayi* microfilariae to induce an adaptive immune response comparable to OvAg immunization. I then injected the corneas with *B. malayi* extract and

extract from *B. malayi* worms that were treated with tetracycline (BmAg^{tet}) for an extended period of time, thus depleting the *Wolbachia*. Following BmAg^{tet} injection into corneas of immunized mice, I found neutrophil infiltration into the corneal stroma similar to that of unimmunized mice injected with BmAg, but significantly decreased compared with immunized C57BL/6 mice injected with BmAg (Figure 3.36). This shows a role for *Wolbachia* in the migration of neutrophils, in the presence of a full adaptive immune response. In contrast to neutrophil infiltration, eosinophil infiltration remained unaffected by the absence of *Wolbachia* from filarial extract.

3.8.2 Adaptive immune responses to *A. viteae* and *Wolbachia*

To determine *Wolbachia*-dependent granulocyte migration to the corneal stroma by a second experimental design, I immunized mice with extract from *A. viteae* worms (AvAg) that are naturally devoid of *Wolbachia* endobacteria or with *Wolbachia* purified from insect cells. I then injected the corneas with AvAg, *Wolbachia* purified from insect cells or a mixture of both.

After euthanasia, spleens were excised and single cell suspensions were stimulated with AvAg, *Wolbachia* or both for 72 hours. IL-5 and IFN- γ production were determined by ELISA. IL-5 production was dependent on the immunization and stimulation being carried out with the same reagent, and AvAg as well as *Wolbachia* could induce similar levels of IL-5. In contrast, IFN- γ was only induced when *Wolbachia* were present during both the immunization and stimulation, indicating *Wolbachia*-dependent priming events during immunization (Figure 3.37).

I then determined neutrophil and eosinophil infiltration into the corneal stroma following injection of AvAg or *Wolbachia*. Eosinophil infiltration was dependent on the

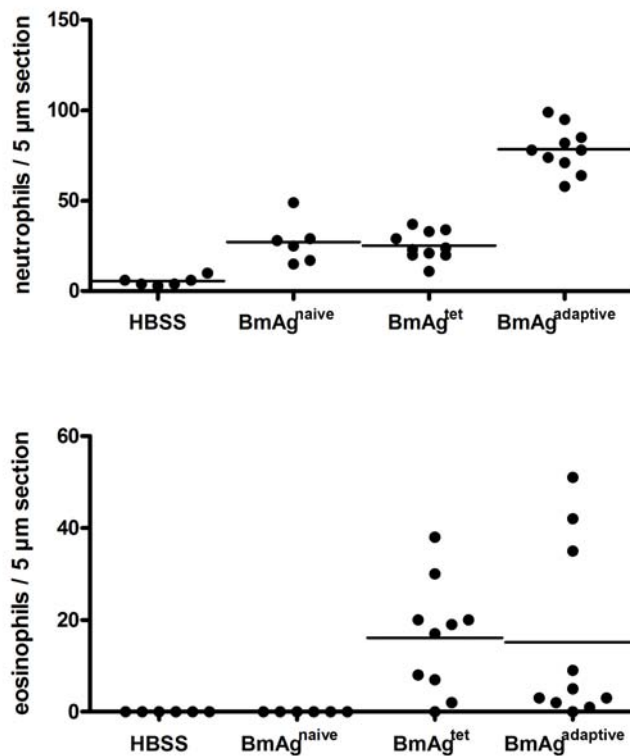


Figure 3.36. C57BL/6 mice were immunized with *B. malayi* microfilariae. Neutrophil infiltration into the corneal stroma of immunized mice was significantly reduced after injection of tetracycline treated *B. malayi* extract in comparison to untreated *B. malayi* extract, whereas eosinophil migration remained unaffected.

The legend corresponds to:

HBSS: naive mice, injected with HBSS,

BmAg^{naive}: naive mice, injected with BmAg,

BmAg^{tet}: immunized mice, injected with *Wolbachia* depleted worm extract,

BmAg^{adaptive}: immunized mice, injected with BmAg.

presence of the same antigens during immunization and stimulation, similar to IL-5 production by splenocytes. AvAg induced eosinophil infiltration when present during the immunization and challenge period, whereas there was hardly any eosinophil migration in the *Wolbachia* injected corneas. Neutrophil infiltration could be induced by

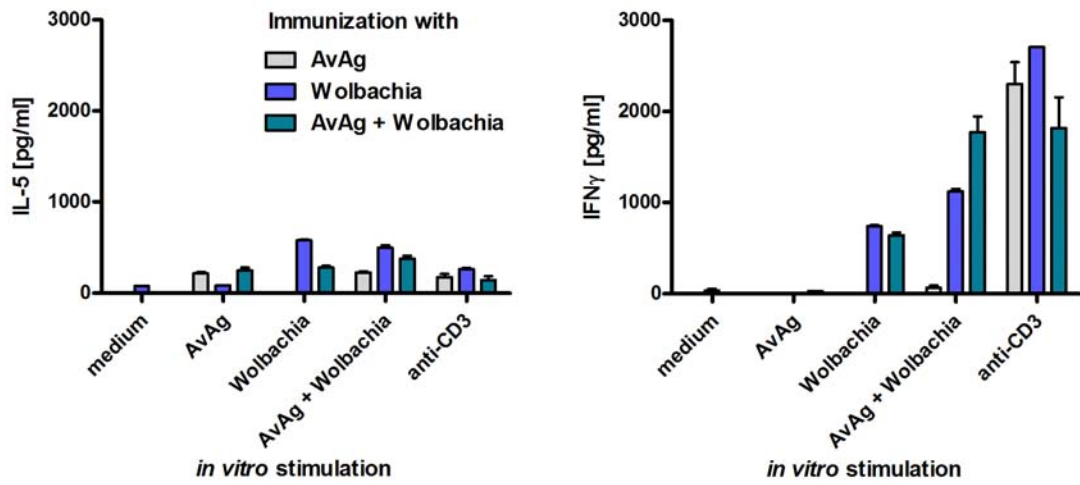


Figure 3.37. C57BL/6 mice were immunized with *AvAg*, *Wolbachia* or both for 3 weeks and spleens were dissected for *in vitro* stimulation. IL-5 and IFN- γ production by splenocytes stimulated with *AvAg* and *Wolbachia* was measured by ELISA.

both, *AvAg* and *Wolbachia* with the highest levels of neutrophils after *Wolbachia* injection (Figure 3.38).

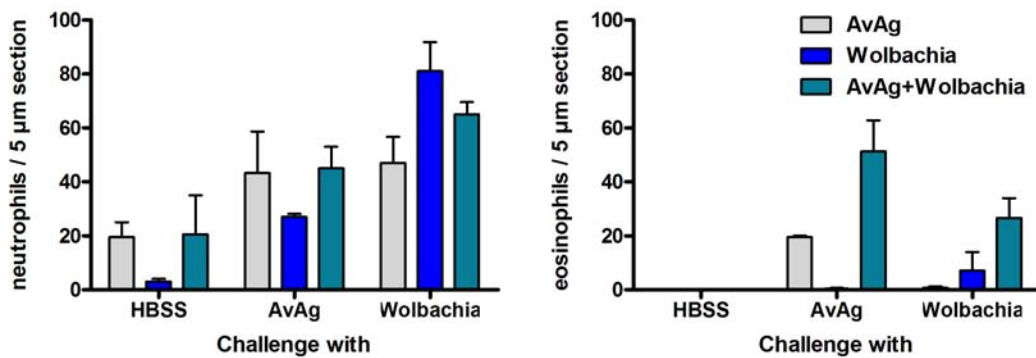


Figure 3.38. C57BL/6 mice were immunized with *AvAg*, *Wolbachia* or both for 3 weeks and corneas were injected with *AvAg*, *Wolbachia* or both. Neutrophil and eosinophil infiltration into the corneal stroma following immunization and intrastromal injection with *AvAg* and *Wolbachia* were determined by immunohistochemistry.

3.9 *In vitro* responses to rWSP

Previous studies indicated a role for the major surface protein of *Wolbachia* in the induction of pro-inflammatory immune responses. Brattig (85) described a role for TLR2 and TLR4 in the activation of dendritic cells and macrophages by rWSP. To further characterize the activation by rWSP, I generated deletion mutants of the surface protein of *B. malayi* (BmWSP). BmWSP cloned into the pet100 vector was obtained from Alan Scott's laboratory (John Hopkins University, Baltimore, MD). The gene sequence of the cloned BmWSP is shown in Figure 3.39. The amino acid sequence is depicted in Figure 3.40. The full sequence contains 240 amino acids (720 base pairs). The 69 base pairs leader sequence (23 amino acids) was previously deleted. I generated sequential deletions from the WSP gene by inverse PCR, replicating the complete plasmid minus the deleted sequence. The following deletion mutants were generated: BmWSP Δ 61-90, BmWSP Δ 91-120, BmWSP Δ 121-150, BmWSP Δ 181-210 and BmWSP Δ 211-240. The wildtype and mutant amino acid sequences are shown in Figure 3.40.

Proteins were purified from *E. coli* under native conditions.

3.9.1 HEK cell responses

To investigate activation of TLR2 by rWSP and deletion mutants, HEK cells transfected with hTLR2 or hTLR3 were stimulated for 18 hours with the different proteins. hTLR4 transfected HEK cells were not used for this experiment as the recombinant proteins were purified from *E. coli* and thus LPS contamination was very likely. For control reagents, I used Pam₃CSK (TLR2), Poly(I:C) (TLR3) and LPS (TLR4). Upon stimulation, hTLR3 transfected HEK cells only produced IL-8 in response to Poly(I:C). All other stimulations were at similar levels to the medium control. Stimulation of hTLR2 transfected

```

ATGCATTATAAAAAGTTTTTTTCAGCAACCGCTTTAGTAATGTTGCTAA
GTTTATCAAACCTGCTTTTTTCAGATCCTGTTGGTCCAATAGCTGATGA
GGAAACTAGTTACTACATTCGCTTGCAGTACAATAGTGAGTTTTTCACCT
TTGAATACAAAGGTTGATGGTATCACAGGAGCTCAAAGGATAGTAAAG
ACACTAATGACCTTTATAAGCCTTCTTTCATGGCTGGTGGTAGTGCATT
TGGTTATAGAATGGATGATATCAGAGTGGACATTGAAGGACTTTATTCA
CAATTAAGTAAAAGTACTCTTTCACGAGCTCCTACTCCAGATATTGTAG
ATAATTTAACAGCAATTTTCAGGACTAGTTAATGTGTATTATGATGTAGT
AATTGAAGATATACCTATTACTCCATATGTTGGTGTGGTCTTGGTGTA
GCATATATCAGCAACCCTGCAAAGGCACAAGTTATTGCTGATCAAAAAC
ATGGGTTTGGTTTTGCTTACCAGGCGAAAGCTGGTATTAGCTATGATGT
AACCCAGAAATTAACCTCTTTGCTGGAGCTCGCTACTTTGGTTCTTAT
GGCGCTAACTTTGATAAAAAGTGAAGAAGTAAATAAAGGAACTAGTGAGG
ATAAAGAAACAAAAGTTACTGCGGGTGCATATAAAGTTCTTTATAGCAC
TATTGGTGCAGAAGCTGGAATAGCGTTTAATTTCTAA

```

Figure 3.39. Gene sequence of BmWSP. The red sequence corresponds to the leader sequence that was previously deleted.

HEK cells yielded IL-8 production in response to rWSP and Pam3CSK. Strikingly, even Poly(I:C) induced IL-8 production, though at much lower levels than in hTLR3 transfected HEK cells. Stimulation with mutant rWSP induced lower levels of IL-8 for the deletion 181-210 (Figure 3.41).

3.9.2 Macrophage responses

To exclude signaling via TLR4, I purified macrophages from TLR4^{-/-} and TLR2/4^{-/-} mice to determine activation via TLR2. Following an overnight rest period, macrophages were

BmWSP minus LP	HHHHHHGMASMTGGQQMGRDLYDDDDKDHPFTMDPVGPIADEETSYYI
BmWSPΔ61-90	HHHHHHGMASMTGGQQMGRDLYDDDDKDHPFTMDPVGPIADEETSYYI
BmWSPΔ91-120	HHHHHHGMASMTGGQQMGRDLYDDDDKDHPFTMDPVGPIADEETSYYI
BmWSPΔ121-150	HHHHHHGMASMTGGQQMGRDLYDDDDKDHPFTMDPVGPIADEETSYYI
BmWSPΔ181-210	HHHHHHGMASMTGGQQMGRDLYDDDDKDHPFTMDPVGPIADEETSYYI
BmWSPΔ211-240	HHHHHHGMASMTGGQQMGRDLYDDDDKDHPFTMDPVGPIADEETSYYI
BmWSP minus LP	RLQYNSEFSPLNKVDGITGAQKDSKDTNDLYKPSFMAGGSAFGYRMD
BmWSPΔ61-90	RLQYNSEFSPLNKVDGITGAG
BmWSPΔ91-120	RLQYNSEFSPLNKVDGITGAQKDSKDTNDLYKPSFMAGGSAFGYRMD
BmWSPΔ121-150	RLQYNSEFSPLNKVDGITGAQKDSKDTNDLYKPSFMAGGSAFGYRMD
BmWSPΔ181-210	RLQYNSEFSPLNKVDGITGAQKDSKDTNDLYKPSFMAGGSAFGYRMD
BmWSPΔ211-240	RLQYNSEFSPLNKVDGITGAQKDSKDTNDLYKPSFMAGGSAFGYRMD
BmWSP minus LP	DIRVDIEGLYSQLSKSTLSRAPTPDIVDNLTAISGLVNVYYDVIEDI
BmWSPΔ61-90	SVDIEGLYSQLSKSTLSRAPTPDIVDNLTAISGLVNVYYDVIEDI
BmWSPΔ91-120	DIRG SSGLVNVYYDVIEDI
BmWSPΔ121-150	DIRVDIEGLYSQLSKSTLSRAPTPDIVDNLTAIG
BmWSPΔ181-210	DIRVDIEGLYSQLSKSTLSRAPTPDIVDNLTAISGLVNVYYDVIEDI
BmWSPΔ211-240	DIRVDIEGLYSQLSKSTLSRAPTPDIVDNLTAISGLVNVYYDVIEDI
BmWSP minus LP	PITPYVGVGLGVAYISNPAKAQVIADQKHGFGFAYQAKAGISYDVTPE
BmWSPΔ61-90	PITPYVGVGLGVAYISNPAKAQVIADQKHGFGFAYQAKAGISYDVTPE
BmWSPΔ91-120	PITPYVGVGLGVAYISNPAKAQVIADQKHGFGFAYQAKAGISYDVTPE
BmWSPΔ121-150	SSNPAKAQVIADQKHGFGFAYQAKAGISYDVTPE
BmWSPΔ181-210	PITPYVGVGLGVAYISNPAKAQVIADQKHGFGFAYQAKAGISYDVG
BmWSPΔ211-240	PITPYVGVGLGVAYISNPAKAQVIADQKHGFGFAYQAKAGISYDVTPE
BmWSP minus LP	IKLFAGARYFGSYGANFDKSEEVNKGTSSEDKETKVTAGAYKVLYSTIG
BmWSPΔ61-90	IKLFAGARYFGSYGANFDKSEEVNKGTSSEDKETKVTAGAYKVLYSTIG
BmWSPΔ91-120	IKLFAGARYFGSYGANFDKSEEVNKGTSSEDKETKVTAGAYKVLYSTIG
BmWSPΔ121-150	IKLFAGARYFGSYGANFDKSEEVNKGTSSEDKETKVTAGAYKVLYSTIG
BmWSPΔ181-210	SSEDKETKVTAGAYKVLYSTIG
BmWSPΔ211-240	IKLFAGARYFGSYGANFDKSEEVNKGTS
BmWSP minus LP	AEAGIAFNF
BmWSPΔ61-90	AEAGIAFNF
BmWSPΔ91-120	AEAGIAFNF
BmWSPΔ121-150	AEAGIAFNF
BmWSPΔ181-210	AEAGIAFNF
BmWSPΔ211-240	SF

Figure 3.40. Amino acid sequence of BmWSP and deletion mutants. Gaps in the amino acid sequence correspond to the deletion in the sequence.

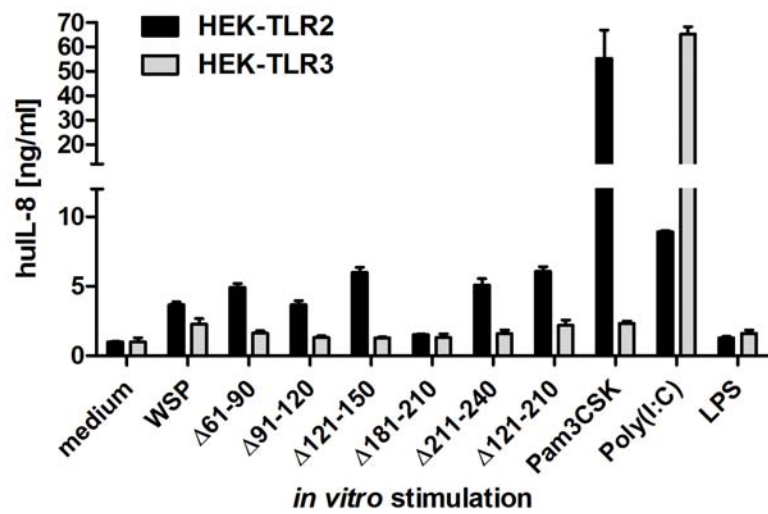


Figure 3.41. HEK-TLR2 and HEK-TLR3 cells were stimulated for 18 hours with rWSP and the deletion mutants. Stimulation with rWSP Δ 181-210 induced lower levels of huIL-8 compared to wildtype rWSP or other deletion mutants. For controls, cells were stimulated with Pam₃CSK (TLR2), Poly(I:C) (TLR3) and LPS (TLR4).

stimulated with BmWSP and the deletion mutants. Pam₃CSK and LPS were used as control reagents. Levels of the pro-inflammatory cytokine TNF α and the chemokine MIP-2 were determined by ELISA. Decreased activation could be detected after stimulation with BmWSP Δ 121-150, BmWSP Δ 181-210 and BmWSP Δ 211-240. No cytokine production was measured in macrophages obtained from TLR2/4^{-/-} mice (Figure 3.42).

3.9.3 Splenocyte responses

TLR4^{-/-} and TLR2/4^{-/-} mice were immunized with BmWSP three times at weekly intervals. One week after the final immunization, mice were euthanized and splenectomized. Splenocyte cultures were incubated with BmWSP and its deletion mutants. Anti-CD3 was used as positive control. TLR2/4^{-/-} cultures showed significantly decreased IFN- γ levels even though levels were already low in TLR4^{-/-} cultures. Stimulation with

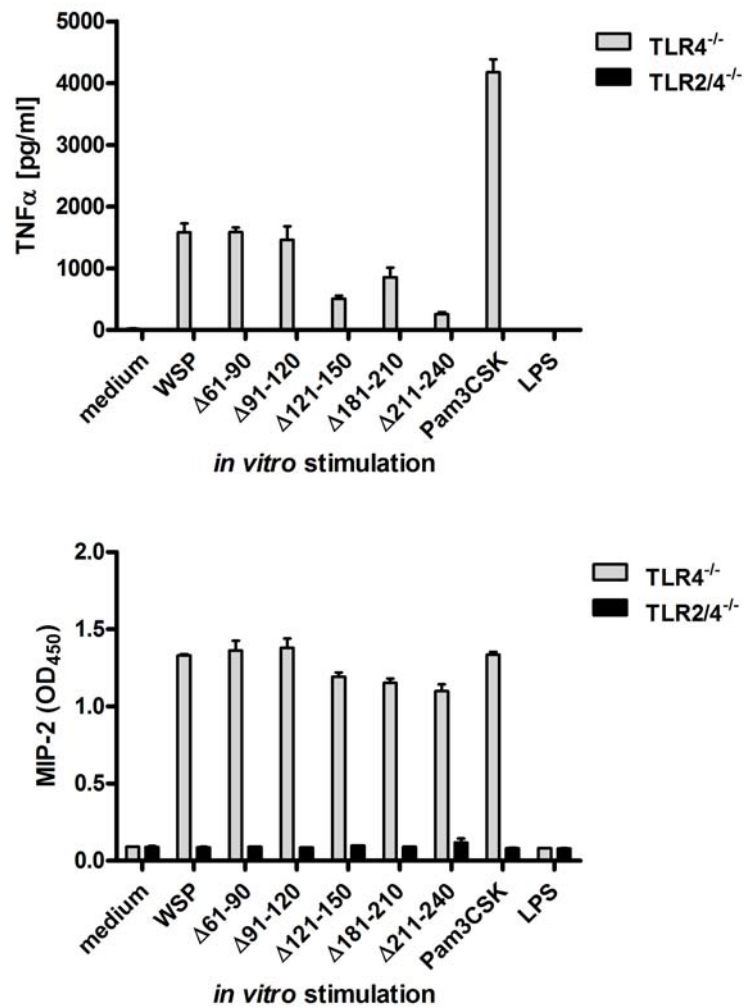


Figure 3.42. C57BL/6 macrophages were stimulated with rWSP and deletion mutants. Decreased levels of cytokine production by macrophages after stimulation with BmWSPΔ121-150, BmWSPΔ181-210 and BmWSPΔ211-240 and in TLR2/4^{-/-} cells were measured by ELISA.

BmWSPΔ121-150, BmWSPΔ181-210 and BmWSPΔ211-240 led to reduced IFN-γ production in TLR4^{-/-} cultures (Figure 3.43). IL-5 levels were undetectable in these experiments (data not shown).

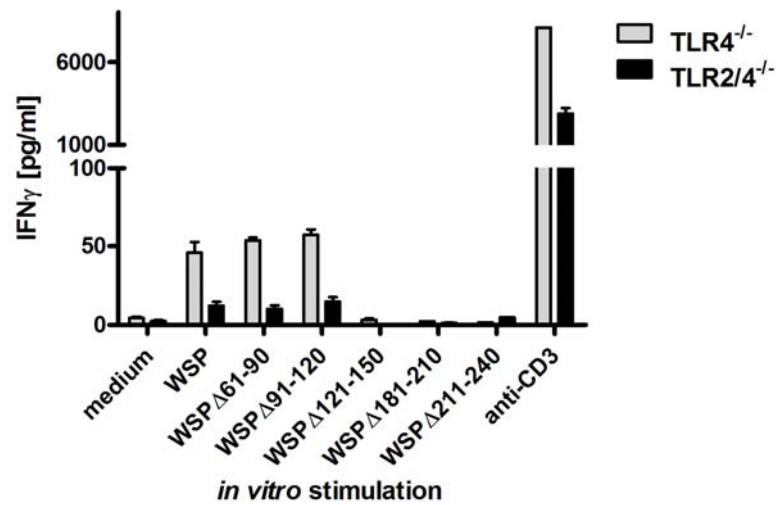


Figure 3.43. TLR4^{-/-} and TLR2/4^{-/-} mice were immunized with rWSP for 3 weeks. Spleens were excised for restimulation *in vitro* with rWSP and the deletion mutants. Decreased levels of IFN- γ after stimulation with BmWSP Δ 121-150, BmWSP Δ 181-210 and BmWSP Δ 211-240 and in TLR2/4^{-/-} cells were measured by ELISA.

3.9.4 Antibody responses

C57BL/6 mice were immunized with BmAg as described before. After three immunizations, mice were bled and serum was obtained for antibody detection. I measured antigen-specific IgG₁ responses by ELISA with WSP as coating antigen. I did not measure IgG_{2c} as the antibody levels were low to begin with. As I measured cross-reactivity from BmAg immunized mice (BmAg containing *Wolbachia* and thus BmWSP) with recombinant BmWSP purified from *E. coli* I expected IgG_{2c} levels below the limit of detection. BmWSP-specific IgG₁ levels were clearly detectable and increased to about 4-fold above background level of unimmunized mice (Figure 3.44). IgG₁ specific for deletion mutants was also clearly detectable for BmWSP Δ 61-90, BmWSP Δ 91-120 and BmWSP Δ 211-240.

Levels were significantly decreased when BmWSP Δ 151-180 and BmWSP Δ 181-210 were used to detect IgG₁.

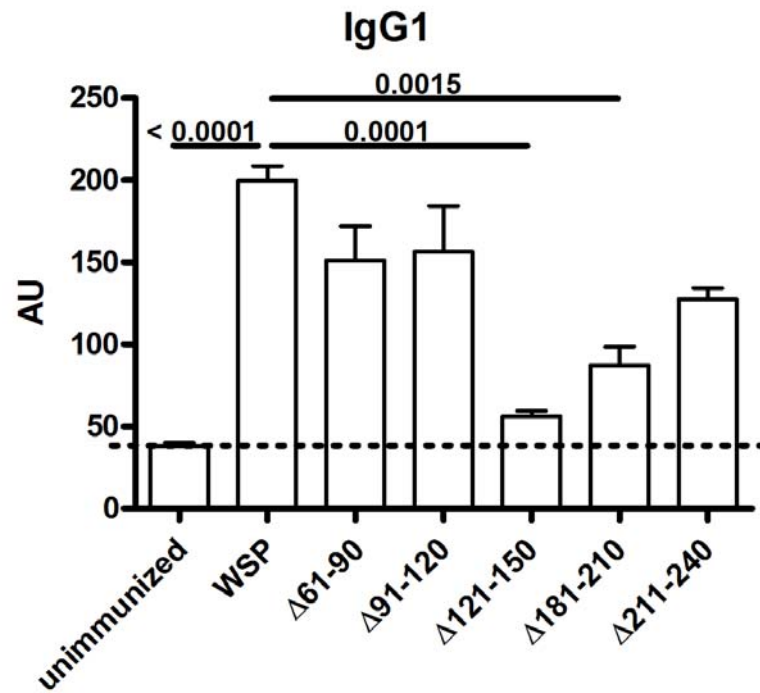


Figure 3.44. C57BL/6 mice were immunized with BmAg and serum was taken after 3 weeks. Decreased levels of BmWSP-specific IgG₁ were measured when detected with BmWSP Δ 181-210 and BmWSP Δ 211-240.

4 Discussion

4.1 Activation of antigen-presenting cells

With the results from this study and the experiments by colleagues, we could demonstrate that dendritic cells, neutrophils and macrophages are all activated by filarial extracts (83, 86). All three cell types require TLR2 expression for activation. For macrophage activation, the requirement of TLR6, MyD88 and Mal was also shown. Expectedly, dendritic cells required MyD88 expression for activation by filarial extracts (data not shown).

Dendritic cell and macrophage activation are essential for efficient induction of adaptive immune responses. Dendritic cells can efficiently activate T cells when previously activated by TLR ligands (80). Upon activation, antigen uptake, membrane transport and antigen presentation are described to be more efficient (80). Typical DC1 cytokines are IL-12, IL-23 and typical DC2 cytokines are IL-10 and TGF- β (51), cytokines more recently associated with the generation of regulatory T cells than in the generation of Th₂ cells, whose generation is characterized by low levels of IL-12 produced by dendritic cells (51). Myeloid dendritic cells in humans are capable of inducing Th₁ or Th₂ responses, depending on the production of IL-12 (109) whereas plasmacytoid dendritic

cells induce Th₁ cells. Initial studies with plasmacytoid dendritic cells did not show consistent cytokine production (data not shown), so I focused on myeloid dendritic cells instead. I initially measured IL-6, IL-12, IP10, TNF α and RANTES and found significant production of IL-6, RANTES and TNF α (data not shown). Missing production of IL-12 implicates differentiation towards Th₂ which is the common pathway during filarial infection. It has also been shown that activation of TLR2 does not induce IL-12 or IP10 production in human monocyte-derived dendritic cells (110).

Activation of the costimulatory molecules CD80 and CD86 will cause CD28 engagement on the T cells (49). Interaction between CD80/CD86 and CD28 in combination with T cell receptor activation via MHCII induces differentiation of naive T cells into Th₁ or Th₂ cells (111). I only found a slight increase of CD86, but higher levels of CD80. However, dendritic cells are differentially regulated and do not express all activation markers upon each stimulation. Similar to cytokine production, the upregulation of costimulatory molecules was TLR2-dependent.

CD40 upregulation has been demonstrated early in the activation of dendritic cells. Increased expression of CD40 can lead to higher MHCII expression upon CD40 ligand engagement and thus more efficient antigen presentation (111). CD40-CD40 ligand interactions were shown to be critical during dendritic cell responses to parasite antigens (112). I found increased CD40 expression on wild-type dendritic cells, that was absent in TLR2^{-/-} cells.

To protect themselves from ROS produced by macrophages, neutrophils and eosinophils, *O. volvulus* and *B. malayi* contain thioredoxin peroxidase (113–115). Increased production of ROS has been related to expulsion of the nematode *Nippostrongylus brasiliensis* (116). Neutrophil activation by filarial extracts was investigated using

several markers: myeloperoxide production, MIP-2 production, generation of nitric oxide and reactive oxygen species, expression of CD11b, CD18 and L-Selectin and release of MMPs. I found production of MPO and MIP-2, generation of ROS and upregulation of CD11b and CD18, while L-Selectin was shed. No generation of NO or release of gelatinases could be clearly demonstrated. Expression of surface activation markers CD11b, CD18 and L-Selectin was regulated TLR2-dependent as was the production of MIP-2. ROS generation occurred independent of TLR2 and could not be induced by TLR2 agonists. This response could therefore be due to the filarial component more than to the *Wolbachia* content of the protein extract. Future experiments may address this question by stimulating neutrophils with the *Wolbachia*-free extract from *A. viteae*.

4.2 TLR2 in the adaptive immune response

This study examined the role of TLRs in the generation of eye disease. Previous studies had shown (i) that neutrophil infiltration into the cornea was dependent on the presence of functional TLR4 and *Wolbachia* (84), and (ii) TLR2- and TLR4-dependent activation by *Wolbachia* surface protein (85). Studies carried out in our lab at the same time could show neutrophil migration to the cornea depending on the presence of MyD88 (29) without previous immunizations. Further investigations revealed requirement of TLR2, but not TLR4 for neutrophil infiltration (83). In this study, it was also shown by using bone-marrow chimeric mice that TLR2 expression on either hematopoietic and resident stromal cells can induce neutrophil infiltration, though not to the same levels as in wildtype reconstituted bone-marrow chimeric mice.

In this study I could also show dependence on TLR2 for neutrophil infiltration in the presence of adaptive immune responses. Systemic responses as characterized by antibody responses were normal in TLR2^{-/-} mice. As previous studies showed a requirement for antibody production for neutrophil migration to the cornea (34), we anticipated normal neutrophil migration and were surprised that the requirement of the innate receptor TLR2 was more important than the presence of antibodies. Neutrophil numbers in the corneas of OvAg-injected immunized TLR2^{-/-} mice were comparable to that of OvAg-injected unimmunized wildtype mice. This indicates a role for the adaptive arm of the immune system in further enhancing neutrophil migration. A potential pathway was presented by TLR2-dependent IFN- γ production by splenocytes. Decreased levels of systemic IFN- γ were hypothesized to affect the expression of PECAM on corneal vessels as shown previously (96) and CXC chemokine production in the cornea.

Taken together, I found requirement for TLR2 at the stages: (i) activation of antigen-presenting cells, (ii) IFN- γ production by splenocytes, (iii) CXC chemokine production and (iv) neutrophil migration to the cornea. While decreased IFN- γ production could be linked to decreased activation of dendritic cells and macrophages and decreased neutrophil migration is caused by decreased chemokine production in the cornea, there is no obvious link between IFN- γ production and CXC chemokine production in the cornea. This surprising finding resulted in the second part of this study, investigating IFN- γ dependent neutrophil migration to the corneal stroma.

4.3 IFN- γ in the adaptive immune response

I could also demonstrate increased neutrophil infiltration into the corneal stroma in the presence of adaptive immune responses and showed that this increased neutrophil infiltration is at least partially caused by IFN- γ .

Previous studies have shown strong IL-5 and weak IFN- γ production by splenocytes in response to restimulation with filarial extracts (32, 117). IFN- γ levels were usually only slightly above the limit of detection. I was therefore surprised that this low response was even further reduced in the absence of TLR2. Previous studies on *Herpes simplex* keratitis have identified IFN- γ as a regulator of PECAM-1 expression in the vascular endothelium of limbal vessels (96). It was shown that the decreased expression of PECAM-1 corresponded to decreased neutrophil infiltration into the corneal stroma (96). Studies by our lab have also shown PECAM-1 expression being important for neutrophil migration during onchocercal keratitis (38). However, I could not show decreased PECAM-1 expression in TLR2^{-/-} mice compared to C57BL/6 mice. I then wanted to investigate if there was a connection between decreased systemical IFN- γ production and neutrophil migration to the cornea. First, I investigated neutrophil migration in IFN- γ ^{-/-} mice and found decreased levels of neutrophil infiltration in the absence of IFN- γ although neutrophil levels were still above background levels. However, neutrophils also migrate to the corneas of naive mice injected into the corneal stroma in the absence of an adaptive immune response (29). It is therefore easily explained that neutrophil migration in IFN- γ ^{-/-} mice reached similar levels compared to neutrophil migration in the absence of adaptive immune responses. However, as in TLR2^{-/-} mice, PECAM-1 expression in the corneas of IFN- γ ^{-/-} mice was not different from C57BL/6 mice.

Therefore I investigated alternative pathways of IFN- γ mediated neutrophil migration to the corneal stroma.

Resident cells in the cornea include keratinocytes (fibroblasts) and macrophages, with a very low number of dendritic cells present (118). The first cells to reach the cornea upon inflammation are neutrophils. I then investigated activation of fibroblasts (using the immortalized mouse corneal fibroblast cell line MK/T-1 (99)), macrophages and neutrophils by IFN- γ and found no activation of either chemokines or pro-inflammatory cytokines. As priming effects of IFN- γ stimulation in macrophages have been demonstrated previously (56), I then investigated costimulation of fibroblasts, macrophages and neutrophils with IFN- γ and filarial extract. I could demonstrate significantly increased production of pro-inflammatory cytokines by macrophages. Neither fibroblasts nor neutrophils showed synergistic responses to IFN- γ and OvAg, nor did macrophages produce increased levels of neutrophil attractant chemokines. However, pro-inflammatory cytokines alone will not increase neutrophil migration to the cornea. I hypothesized autokrin or parakrin effects of those pro-inflammatory cytokines on macrophages, fibroblasts or neutrophils. Stimulating fibroblasts with recombinant IL-1 α , IL-1 β , IL-6 and TNF- α did indeed induce production of chemokines. No significant effect on macrophages or neutrophils was observed.

I examined alternative pathways of macrophage priming by IFN- γ . Regulation of TLR2 expression on biliary epithelial cells (93) and on rheumatoid synovial tissues (92) by IFN- γ was previously shown. I therefore investigated TLR2 expression in macrophages in response to recombinant IFN- γ and could show by Western Blot that total TLR2 expression was increased and by FACS that surface expression of TLR2 was upregulated as well.

I attempted to investigate whether I could substitute the increased systemic levels of IFN- γ that I achieve during immunization by local injection of rIFN- γ or rIL-12 into the cornea. Injection of rIFN- γ had no effect on neutrophil migration (data not shown). As rIFN- γ is known for a short half life, I then injected rIL-12 as an inducer of rIFN- γ . I anticipated that rIL-12 would induce IFN- γ over an extended period of time and thus efficiently prime corneal macrophages. However, repeated experiments produced only inconclusive data with the occasional increase in neutrophil migration or without having an effect on neutrophil migration (data not shown). The reason for this missing response could be fast degradation of the recombinant cytokines or insufficient amounts injected. I calculated the amount injected on other studies using rIL-12, however, injection volume into the cornea is limited and non-physiological, high concentrations of rIL-12 could have side effects like damaging the corneal matrix.

With this part of the study I clearly showed that even though IFN- γ is only produced at low levels by splenocytes, it does play an important role in the priming of pro-inflammatory immune responses and in the development of *Onchocerca* keratitis. Though it does induce higher levels of IL-1 α , IL-1 β , IL-6 and TNF α in macrophages, only IL-1 α and TNF α induce chemokine production in corneal fibroblasts. When examining the role of the two corresponding cytokine receptors, only IL-1R1 could be shown to be involved in neutrophil migration, but not TNF α R1/2. Though I could show that IL-6 affected neutrophil migration to the corneal stroma, this is likely to be due to a different mechanism.

4.4 *Wolbachia*

Previous studies have shown a requirement of *Wolbachia* for neutrophil migration to the corneal stroma (29, 84, 101). However, these studies only examined neutrophil infiltration in the absence of adaptive immune responses. Other studies showed that neutrophil infiltration into onchocercal skin nodules was depending on the presence of *Wolbachia* (9). Yet other studies implicated *Wolbachia* in the development of Th₁ immune responses (119). *Wolbachia* was also shown to cause severe pro-inflammatory responses when released from worms upon treatment with diethylcarbamazine (11). I therefore wanted to test the role of *Wolbachia* in the adaptive phase of the immune response.

I first generated a full adaptive immune response by immunizing mice with *B. malayi* microfilariae. No difference could be detected in the cytokine and antibody responses of mice then treated with BmAg or with BmAg^{tet}. I then injected BmAg and BmAg^{tet} into the corneas. BmAg^{tet} was obtained from worms of tetracycline treated *Meriones unguiculatus*. Migration of neutrophils was found to be decreased in the absence of *Wolbachia* while the migration of eosinophils was not affected. The decreased migration of neutrophils is therefore likely to be due to the lack of *Wolbachia*.

In a second model, I immunized mice with *A. viteae* and/or *Wolbachia*, then injected the corneas with *A. viteae* and/or *Wolbachia*. I used *A. viteae* as *Wolbachia*-free filarial control. As before, the presence of *Wolbachia* increased neutrophil migration. In contrast, there was no eosinophil infiltration in response to *Wolbachia* alone. This all implicates a role for *Wolbachia* in neutrophil migration while at the same time, *Wolbachia* appears dispensable for the migration of eosinophils.

A. viteae also induced neutrophil migration. This is in contrast to the results obtained with *Wolbachia*-depleted *B. malayi* extract, however, this might be due to working with a related, but not identical organism that is naturally void of *Wolbachia*. Literature suggests that *A. viteae* may have harbored the endosymbiont *Wolbachia*, but lost it during evolution (120) and incorporated essential genes into its genome.

Previous studies have shown *Wolbachia* dependent generation of Th₁ immune responses (119). Similarly, I found IFN- γ production only when mice were immunized and splenocytes challenged with *Wolbachia*. In contrast, I found IL-5 production in response to both filarial and bacterial stimulation, but only when mice were previously immunized with the same reagent.

With these findings, *Wolbachia* alone can induce a functional immune response at the splenocyte level and neutrophil infiltration into the cornea. However, eosinophil infiltration is caused by filaria alone.

4.5 BmWSP

BmWSP has been previously cloned by other laboratories (85, 121). I obtained the plasmid from Alan L. Scott (John Hopkins University, Baltimore).

Porksakorn et al. (121) demonstrated activation of the murine cell line RAW264.7 by recombinant BmWSP. The cells presented increased expression of IL-1 α , IL-1 β , IL-6 and TNF α at the RNA level. To exclude LPS contamination, purified proteins were (1) treated with proteinase K and decreased macrophage activation was shown, implying a role for the protein component in activating macrophages; and (2) treated with polymyxin B. Treatment of LPS with polymyxin B decreased cytokine expression to background levels,

while there was only a slight reduction of cytokine expression when BmWSP was treated with polymyxin B.

BmWSP was purified under native and denaturing conditions. I obtained higher protein levels from purification under denaturing conditions, however, the activation of HEK cells and macrophages was decreased compared with native BmWSP (data not shown). I therefore continued my studies with native BmWSP. I was especially interested in activation of TLR2 by the recombinant BmWSP. Previous studies have also identified TLR4 as receptor for WSP (85).

As I was purifying the proteins from *E. coli*, I assumed endotoxin contamination and therefore TLR4 activation. For the studies comparing deletion mutants of BmWSP, I then used TLR4^{-/-} macrophages as controls and TLR2/4^{-/-} macrophages as cells of interest. I found activation of TLR4^{-/-} macrophages that was completely abrogated in TLR2/4^{-/-} macrophages, clearly indicating involvement of TLR2 in the activation pathway. I confirmed activation of TLR2 by stimulation of TLR2-transfected HEK293 cells and again found activation of TLR2-transfected HEK293 cells, but not TLR3-transfected HEK293 cells. As expected, TLR4-transfected HEK293 cells were activated (data not shown), attributing this activation to endotoxin contamination.

I also stimulated splenocytes from BmWSP immunized mice and found increased IFN- γ production in response to BmWSP compared with medium stimulation.

I then stimulated the same cells with deletion mutants of BmWSP. I consistently showed wildtype cytokine production when cells were stimulated with BmWSP Δ 61-90 and BmWSP Δ 91-120. Deletion mutants BmWSP Δ 181-210 consistently showed decreased cytokine production in TLR2-transfected HEK293 cells, macrophages and

splenocytes. This sequence is likely to be important for recognition by TLR2. Mutants BmWSP Δ 121-150 and BmWSP Δ 211-240 showed decreased cytokine production in some assays but not all. The role of those sequences will have to be further analyzed.

Finally, I tested antibody responses of BmAg immunized mice against recombinant BmWSP. Serum from immunized mice could recognize recombinant BmWSP, showing homology to the *in vivo* expressed proteins. Again, I could demonstrate clear decrease in antibody responses for the mutants BmWSP Δ 121-150 and BmWSP Δ 181-210.

I extended previous studies to investigate the sole role of TLR2 in the activation process.

When purifying recombinant proteins from *E. coli*, there will always be low level endotoxin contamination. I therefore decided not to investigate the involvement of TLR4 in more detail especially since my previous studies as well as those of colleagues could not identify a role for this receptor in the mouse model of river blindness. While endotoxin effects can be minimized by the addition of polymyxin B, I was more interested in TLR2 activation.

BmWSP lacks signal sequences required for acylation. Usually TLR2 ligands are di- or triacylated lipoproteins, depending on the coreceptor usage (122). There is only one known non-acylated TLR2 ligand: PorinB of *Neisseria meningitidis* (123, 124). Direct interaction between *Neisseria* porin and TLR2 was shown by an ELISA-like assay (124). Coreceptor for activation by this protein is TLR1.

Smaller studies also implicated porin of *Shigella dysenteriae* as a TLR2 ligand (125). However, studies by this group never analyzed TLR2 activation in either TLR2^{-/-} mice or used single TLR-transfected HEK cells. Binding of porin to TLR2 was never demonstrated by co-immunoprecipitation either. The requirement of TLR2 was concluded

from upregulation of TLR2 upon stimulation of B cells and macrophages with porin and from decreased activation (50 %) following anti-TLR2 treatment of macrophages. Following the same reasoning that upregulation of RNA levels of TLRs reflected TLR usage by porins, this group also implicated TLR6 in the activation by *Shigella* porin.

Summarizing studies on those two porins, there is one confirmed TLR2 ligand that requires TLR1 as coreceptor and the second porin might activate TLR2 with TLR6 as coreceptor.

It will therefore be very interesting to confirm TLR2-dependent activation of macrophages by BmWSP. Future studies will focus on purifying the protein from insect cells to prevent LPS contamination. The protein will then be used for interaction studies with TLR2, TLR4, TLR1, TLR6 and CD14. Molecular interactions will be interesting because of the lack of acylation. The binding will then be further analyzed by using the here described deletion mutants. BmWSP is more likely to require TLR6 as coreceptor as I am only showing TLR2- and TLR6-dependent activation when using whole filarial extracts.

In addition to endotoxin contamination, there could also potentially be lipoprotein contamination from *E. coli*. This problem will not be solved by expressing BmWSP in insect cells as insect cells contain large numbers of lipoproteins. Lipoprotein activity can be decreased by incubation of BmWSP with cleanascite.

4.6 Revised mouse model of Onchocerciasis

With findings from this study I revised the previous model of *O. volvulus* induced keratitis. Dendritic cells in the skin take up filarial antigen. Upon activation (TLR2-dependent), dendritic cells migrate to lymphoid tissues where antigen is presented to CD4⁺ T cells. T cells differentiate into IFN- γ producing Th₁ (TLR2-dependent) and IL-5 producing Th₂ cells. Systemically, IL-5 mobilizes eosinophils from bone marrow and other tissues (126). IL-4 induces B cells to produce IgE (127). The IFN- γ induced responses are discussed in the next paragraph. Upon challenge with filarial extract in the cornea, CXC chemokines are produced (TLR2-dependent) that attract neutrophil migration to the corneal stroma. Migration of neutrophils is also dependent on the presence of TLR2. Systemic responses are shown in Figure 4.1.

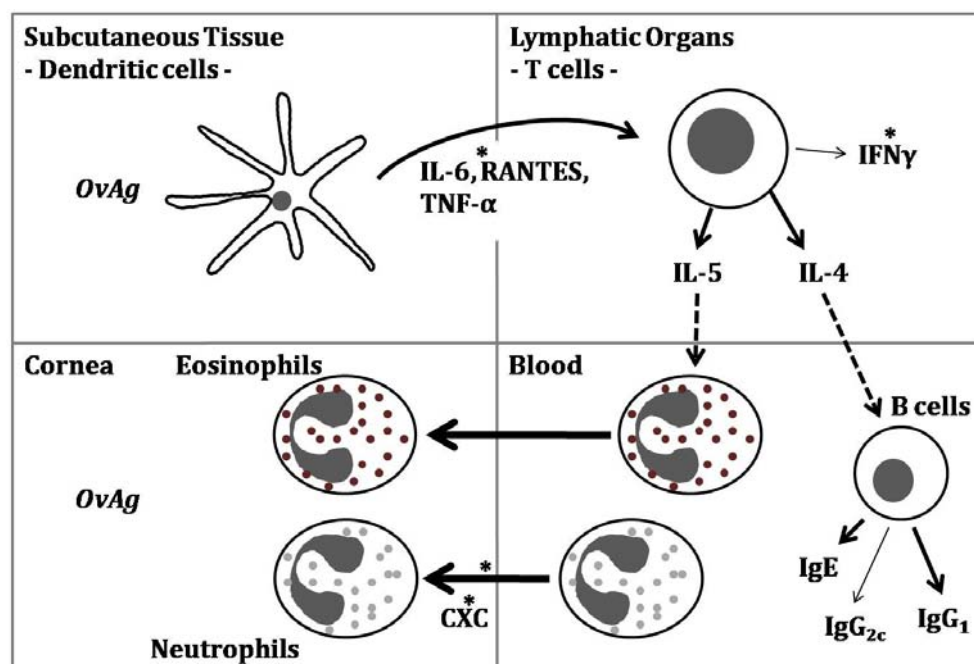


Figure 4.1. Systemic responses to filarial extracts. TLR2-dependent processes are marked with a *. A detailed explanation is given in the main text.

Neutrophil migration is further enhanced by IFN- γ -dependent processes. IFN- γ increases TLR2 expression on macrophages and responsiveness to OvAg. Macrophages increase production of pro-inflammatory cytokines IL-1 α , IL-1 β and TNF α . KC and MIP-2 production by macrophages is induced by filarial extracts, but independent of IFN- γ . Macrophages in the cornea are close to corneal fibroblasts. These cells are activated by IL-1 α , IL-1 β and TNF α and produce high amounts of KC and LIX. All chemokines attract the migration of neutrophils. Activated neutrophils then also start to produce KC, MIP-2 and LIX, further enhancing neutrophil migration. IFN- γ -dependent corneal responses are shown in Figure 4.2.

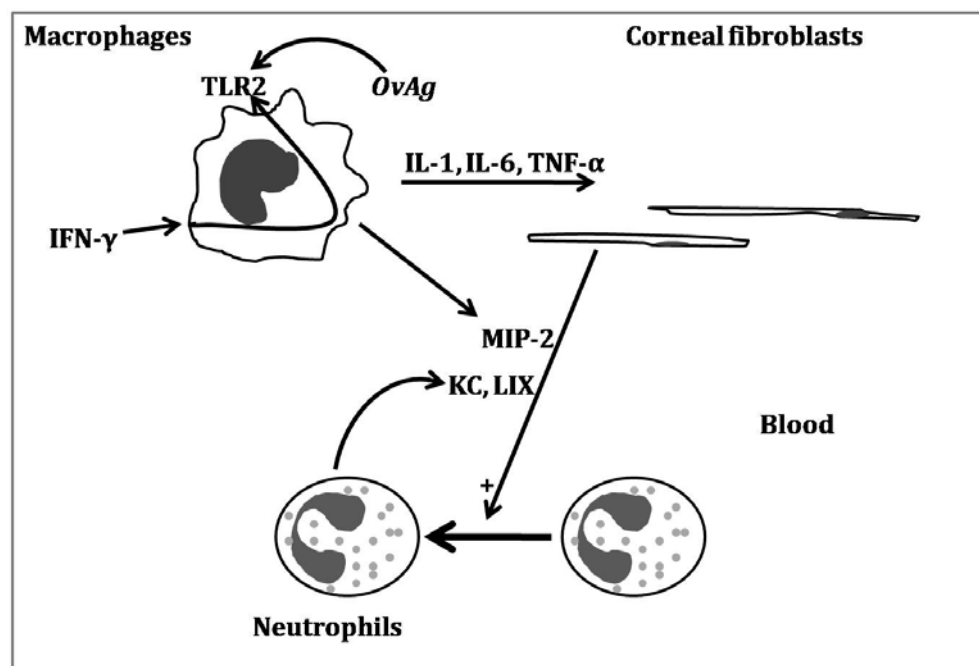


Figure 4.2. IFN- γ -dependent responses to filarial extracts. A detailed description is given in the text.

5 Summary

In this study, I first identified a critical role for TLR2 in Th₁ associated immune responses: decreased dendritic cell activation, decreased IFN- γ production by splenocytes, decreased chemokine production in the cornea, and decreased neutrophil migration to the corneal stroma, whereas TLR4 does not appear to be involved in these steps. Typical anti-helminth responses as IL-5 production and eosinophil migration were independent of TLR2.

Linking the systemic IFN- γ production to neutrophil migration to the corneal stroma, I could show, that IFN- γ increases TLR2 expression and thus responsiveness to the TLR2 ligand OvAg in macrophages. Primed macrophages do not produce increased levels of chemokines, but proinflammatory cytokines that prime chemokine production by corneal fibroblasts. The importance of these cytokines in neutrophil migration could be confirmed *in vivo* where neutrophil migration was decreased in the absence of IL-1R1, TNF α R1/2 and IL-6.

Examining the role of filarial proteins and the endosymbiont *Wolbachia* in the activation of proinflammatory immune responses, I found that IFN- γ was only induced by *Wolbachia*, but not by filarial extracts. Similarly, neutrophil migration to the corneal stroma was induced by *Wolbachia*, although *A. viteae* could induce some neutrophil

migration as well. Eosinophil migration to the corneal stroma, in contrast, was only dependent on the presence of filarial proteins.

Analyzing the recombinant proinflammatory protein BmWSP for its activation potential, I found that I could activate TLR2-transfected HEK293 cells, primary murine macrophages and splenocytes, all in a TLR2-dependent manner. Deletion mutants of BmWSP identified region 121-240 as immunostimulatory part of BmWSP.

Summarizing, I identify Th₂ responses as TLR2-independent, but filaria-dependent, whereas Th₁ responses are TLR2- and *Wolbachia*-dependent, with BmWSP as one candidate protein for the induction of proinflammatory responses via TLR2.

References

- [1] WHO. Fact sheet nr 102: Lymphatic filariasis, 2000.
- [2] Gladys Ozoh, Michel Boussinesq, Anne-Cécile Zoung-Kanyi Bissek, Léon Kobangue, Maryvonne Kombila, Jean-Romain Mourou Mbina, Peter Enyong, Mounkaïla Noma, Azodoga Sékétéli, and Grace Fobi. Evaluation of the diethyl-carbamazine patch to evaluate onchocerciasis endemicity in central africa. *Trop Med Int Health*, 12(1):123–129, Jan 2007.
- [3] Achim Hoerauf. Filariasis: new drugs and new opportunities for lymphatic filariasis and onchocerciasis. *Curr Opin Infect Dis*, 21(6):673–681, Dec 2008.
- [4] W. J. Kozek and H. F. Marroquin. Intracytoplasmic bacteria in onchocerca volvulus. *Am J Trop Med Hyg*, 26(4):663–678, Jul 1977.
- [5] M. Sironi, C. Bandi, L. Sacchi, B. Di Sacco, G. Damiani, and C. Genchi. Molecular evidence for a close relative of the arthropod endosymbiont wolbachia in a filarial worm. *Mol Biochem Parasitol*, 74(2):223–227, Nov 1995.
- [6] Helen F McGarry, Gillian L Egerton, and Mark J Taylor. Population dynamics of wolbachia bacterial endosymbionts in brugia malayi. *Mol Biochem Parasitol*, 135(1):57–67, May 2004.
- [7] Katelyn Fenn and Mark Blaxter. Quantification of wolbachia bacteria in brugia malayi through the nematode lifecycle. *Mol Biochem Parasitol*, 137(2):361–364, Oct 2004.
- [8] Tarig B Higazi, Anthony Filiano, Charles R Katholi, Yankum Dadzie, Jan H Remme, and Thomas R Unnasch. Wolbachia endosymbiont levels in severe and mild strains of onchocerca volvulus. *Mol Biochem Parasitol*, 141(1):109–112, May 2005.
- [9] N. W. Brattig, D. W. Büttner, and A. Hoerauf. Neutrophil accumulation around onchocerca worms and chemotaxis of neutrophils are dependent on wolbachia endobacteria. *Microbes Infect*, 3(6):439–446, May 2001.
- [10] Paul B Keiser, Stacey M Reynolds, Kwablah Awadzi, Eric A Ottesen, Mark J Taylor, and Thomas B Nutman. Bacterial endosymbionts of onchocerca volvulus in the pathogenesis of posttreatment reactions. *J Infect Dis*, 185(6):805–811, Mar 2002.
- [11] H. F. Cross, M. Haarbrink, G. Egerton, M. Yazdanbakhsh, and M. J. Taylor. Severe reactions to filarial chemotherapy and release of wolbachia endosymbionts into blood. *Lancet*, 358(9296):1873–1875, Dec 2001.

- [12] A. Hoerauf, K. Nissen-Pähle, C. Schmetz, K. Henkle-Dührsen, M. L. Blaxter, D. W. Büttner, M. Y. Gallin, K. M. Al-Qaoud, R. Lucius, and B. Fleischer. Tetracycline therapy targets intracellular bacteria in the filarial nematode *litomosoides sigmodontis* and results in filarial infertility. *J Clin Invest*, 103(1):11–18, Jan 1999.
- [13] Sabine Specht, Sabine Mand, Yeboah Marfo-Debrekyei, Alexander Yaw Debrah, Peter Konadu, Ohene Adjei, Dietrich W Büttner, and Achim Hoerauf. Efficacy of 2- and 4-week rifampicin treatment on the wolbachia of *onchocerca volvulus*. *Parasitol Res*, 103(6):1303–1309, Nov 2008.
- [14] Achim Hoerauf, Sabine Specht, Yeboah Marfo-Debrekyei, Marcelle Büttner, Alexander Yaw Debrah, Sabine Mand, Linda Batsa, Norbert Brattig, Peter Konadu, Claudio Bandi, Rolf Fimmers, Ohene Adjei, and Dietrich W Büttner. Efficacy of 5-week doxycycline treatment on adult *onchocerca volvulus*. *Parasitol Res*, 104(2):437–447, Jan 2009.
- [15] Eric C Carlson, Michelle Lin, Chia-Yang Liu, Winston W-Y Kao, Victor L Perez, and Eric Pearlman. Keratocan and lumican regulate neutrophil infiltration and corneal clarity in lipopolysaccharide-induced keratitis by direct interaction with cxcl1. *J Biol Chem*, 282(49):35502–35509, Dec 2007.
- [16] Saloni Khatri, Jonathan H Lass, Fred P Heinzl, W. Matthew Petroll, John Gomez, Eugenia Diaconu, Carolyn M Kalsow, and Eric Pearlman. Regulation of endotoxin-induced keratitis by pcam-1, mip-2, and toll-like receptor 4. *Invest Ophthalmol Vis Sci*, 43(7):2278–2284, Jul 2002.
- [17] Michelle Lin, Eric Carlson, Eugenia Diaconu, and Eric Pearlman. Cxcl1/kc and cxcl5/lix are selectively produced by corneal fibroblasts and mediate neutrophil infiltration to the corneal stroma in lps keratitis. *J Leukoc Biol*, 81(3):786–792, Mar 2007.
- [18] Michelle Lin, Patricia Jackson, Angus M Tester, Eugenia Diaconu, Christopher M Overall, J. Edwin Blalock, and Eric Pearlman. Matrix metalloproteinase-8 facilitates neutrophil migration through the corneal stromal matrix by collagen degradation and production of the chemotactic peptide pro-gly-pro. *Am J Pathol*, 173(1):144–153, Jul 2008.
- [19] http://www.ohiovalleyeye.com/eyeinfo_anatomy.htm.
- [20] <http://www.lab.anhb.uwa.edu.au/mb140/corepages/eye/eye.htm>.
- [21] Y. Aoki, M. M. Recinos, and Y. Hashiguchi. Life span and distribution of *onchocerca volvulus microfilariae* in mice. *J Parasitol*, 66(5):797–801, Oct 1980.

- [22] W. J. Kozek and H. Figueroa Marroquin. Attempts to establish onchocerca volvulus infection in primates and small laboratory animals. *Acta Trop*, 39(4):317–324, Dec 1982.
- [23] S. Townson and A. E. Bianco. Experimental infection of mice with the microfilariae of onchocerca lienalis. *Parasitology*, 85 (Pt 2):283–293, Oct 1982.
- [24] I. Beveridge, E. Kummerow, and P. Wilkinson. Experimental infection of laboratory rodents and calves with microfilariae of onchocerca gibsoni. *Tropenmed Parasitol*, 31(1):82–86, Mar 1980.
- [25] C. K. Carlow, R. Muller, and A. E. Bianco. Further studies on the resistance to onchocerca microfilariae in cba mice. *Trop Med Parasitol*, 37(3):276–281, Sep 1986.
- [26] E. R. James, B. Smith, and J. Donnelly. Invasion of the mouse eye by onchocerca microfilariae. *Trop Med Parasitol*, 37(4):359–360, Dec 1986.
- [27] E. Pearlman. Experimental onchocercal keratitis. *Parasitol Today*, 12(7):261–267, Jul 1996.
- [28] E. Pearlman, J. H. Lass, D. S. Bardenstein, M. Kopf, F. E. Hazlett, E. Diaconu, and J. W. Kazura. Interleukin 4 and t helper type 2 cells are required for development of experimental onchocercal keratitis (river blindness). *J Exp Med*, 182(4):931–940, Oct 1995.
- [29] Illona Gillette-Ferguson, Amy G Hise, Yan Sun, Eugenia Diaconu, Helen F McGarry, Mark J Taylor, and Eric Pearlman. Wolbachia- and onchocerca volvulus-induced keratitis (river blindness) is dependent on myeloid differentiation factor 88. *Infect Immun*, 74(4):2442–2445, Apr 2006.
- [30] E. Pearlman, J. H. Lass, D. S. Bardenstein, E. Diaconu, F. E. Hazlett, J. Albright, A. W. Higgins, and J. W. Kazura. Onchocerca volvulus-mediated keratitis: cytokine production by il-4-deficient mice. *Exp Parasitol*, 84(2):274–281, Nov 1996.
- [31] E. Pearlman, F. E. Hazlett, W. H. Boom, and J. W. Kazura. Induction of murine t-helper-cell responses to the filarial nematode brugia malayi. *Infect Immun*, 61(3):1105–1112, Mar 1993.
- [32] E. Pearlman, L. R. Hall, A. W. Higgins, D. S. Bardenstein, E. Diaconu, F. E. Hazlett, J. Albright, J. W. Kazura, and J. H. Lass. The role of eosinophils and neutrophils in helminth-induced keratitis. *Invest Ophthalmol Vis Sci*, 39(7):1176–1182, Jun 1998.

- [33] E. Pearlman, J. H. Lass, D. S. Bardenstein, E. Diaconu, F. E. Hazlett, J. Albright, A. W. Higgins, and J. W. Kazura. Il-12 exacerbates helminth-mediated corneal pathology by augmenting inflammatory cell recruitment and chemokine expression. *J Immunol*, 158(2):827–833, Jan 1997.
- [34] L. R. Hall, J. H. Lass, E. Diaconu, E. R. Strine, and E. Pearlman. An essential role for antibody in neutrophil and eosinophil recruitment to the cornea: B cell-deficient (micromt) mice fail to develop th2-dependent, helminth-mediated keratitis. *J Immunol*, 163(9):4970–4975, Nov 1999.
- [35] L. R. Hall, E. Diaconu, and E. Pearlman. A dominant role for fc gamma receptors in antibody-dependent corneal inflammation. *J Immunol*, 167(2):919–925, Jul 2001.
- [36] L. R. Hall, J. T. Kaifi, E. Diaconu, and E. Pearlman. Cd4(+) depletion selectively inhibits eosinophil recruitment to the cornea and abrogates onchocerca volvulus keratitis (river blindness). *Infect Immun*, 68(9):5459–5461, Sep 2000.
- [37] J. T. Kaifi, L. R. Hall, C. Diaz, J. Sypek, E. Diaconu, J. H. Lass, and E. Pearlman. Impaired eosinophil recruitment to the cornea in p-selectin-deficient mice in onchocerca volvulus keratitis (river blindness). *Invest Ophthalmol Vis Sci*, 41(12):3856–3861, Nov 2000.
- [38] J. T. Kaifi, E. Diaconu, and E. Pearlman. Distinct roles for pecam-1, icam-1, and vcam-1 in recruitment of neutrophils and eosinophils to the cornea in ocular onchocerciasis (river blindness). *J Immunol*, 166(11):6795–6801, Jun 2001.
- [39] L. R. Hall, E. Diaconu, R. Patel, and E. Pearlman. Cxc chemokine receptor 2 but not c-c chemokine receptor 1 expression is essential for neutrophil recruitment to the cornea in helminth-mediated keratitis (river blindness). *J Immunol*, 166(6):4035–4041, Mar 2001.
- [40] Ravi B Berger, Nathan M Blackwell, Jonathan H Lass, Eugenia Diaconu, and Eric Pearlman. Il-4 and il-13 regulation of icam-1 expression and eosinophil recruitment in onchocerca volvulus keratitis. *Invest Ophthalmol Vis Sci*, 43(9):2992–2997, Sep 2002.
- [41] E. Pearlman and L. R. Hall. Immune mechanisms in onchocerca volvulus-mediated corneal disease (river blindness). *Parasite Immunol*, 22(12):625–631, Dec 2000.
- [42] Gavin P Sandilands, Zubir Ahmed, Nicole Perry, Martin Davison, Alison Lupton, and Barbara Young. Cross-linking of neutrophil cd11b results in rapid cell surface expression of molecules required for antigen presentation and t-cell activation. *Immunology*, 114(3):354–368, Mar 2005.

- [43] Shauna Culshaw, Owain R Millington, James M Brewer, and Iain B McInnes. Murine neutrophils present class ii restricted antigen. *Immunol Lett*, 118(1):49–54, Jun 2008.
- [44] Huan-Zhong Shi. Eosinophils function as antigen-presenting cells. *J Leukoc Biol*, 76(3):520–527, Sep 2004.
- [45] Udaikumar M Padigel, James J Lee, Thomas J Nolan, Gerhard A Schad, and David Abraham. Eosinophils can function as antigen-presenting cells to induce primary and secondary immune responses to strongyloides stercoralis. *Infect Immun*, 74(6):3232–3238, Jun 2006.
- [46] Udaikumar M Padigel, Jessica A Hess, James J Lee, James B Lok, Thomas J Nolan, Gerhard A Schad, and David Abraham. Eosinophils act as antigen-presenting cells to induce immunity to strongyloides stercoralis in mice. *J Infect Dis*, 196(12):1844–1851, Dec 2007.
- [47] Akiko Iwasaki and Ruslan Medzhitov. Toll-like receptor control of the adaptive immune responses. *Nat Immunol*, 5(10):987–995, Oct 2004.
- [48] J. Banchereau and R. M. Steinman. Dendritic cells and the control of immunity. *Nature*, 392(6673):245–252, Mar 1998.
- [49] Olivier Joffre, Martijn A Nolte, Roman Spörri, and Caetano Reis e Sousa. Inflammatory signals in dendritic cell activation and the induction of adaptive immunity. *Immunol Rev*, 227(1):234–247, Jan 2009.
- [50] Esther C de Jong, Pedro L Vieira, Pawel Kalinski, Joost H N Schuitemaker, Yuetsu Tanaka, Eddy A Wierenga, Maria Yazdanbakhsh, and Martien L Kapsenberg. Microbial compounds selectively induce th1 cell-promoting or th2 cell-promoting dendritic cells in vitro with diverse th cell-polarizing signals. *J Immunol*, 168(4):1704–1709, Feb 2002.
- [51] Yonghai Li, Niansheng Chu, Abdolmohamad Rostami, and Guang-Xian Zhang. Dendritic cells transduced with socs-3 exhibit a tolerogenic/dc2 phenotype that directs type 2 th cell differentiation in vitro and in vivo. *J Immunol*, 177(3):1679–1688, Aug 2006.
- [52] Vinoth K Latchumanan, Mumtaz Yaseen Balkhi, Aprajita Sinha, Balwan Singh, Pawan Sharma, and Krishnamurthy Natarajan. Regulation of immune responses to mycobacterium tuberculosis secretory antigens by dendritic cells. *Tuberculosis (Edinb)*, 85(5-6):377–383, 2005.
- [53] Shivanthi P Manickasingham, Alexander D Edwards, Oliver Schulz, and Caetano Reis e Sousa. The ability of murine dendritic cell subsets to direct t helper

- cell differentiation is dependent on microbial signals. *Eur J Immunol*, 33(1):101–107, Jan 2003.
- [54] Klaas P J M van Gisbergen, Marta Sanchez-Hernandez, Teunis B H Geijtenbeek, and Yvette van Kooyk. Neutrophils mediate immune modulation of dendritic cells through glycosylation-dependent interactions between mac-1 and dc-sign. *J Exp Med*, 201(8):1281–1292, Apr 2005.
- [55] S. L. Constant and K. Bottomly. Induction of th1 and th2 cd4+ t cell responses: the alternative approaches. *Annu Rev Immunol*, 15:297–322, 1997.
- [56] J. Ma, T. Chen, J. Mandelin, A. Ceponis, N. E. Miller, M. Hukkanen, G. F. Ma, and Y. T. Konttinen. Regulation of macrophage activation. *Cell Mol Life Sci*, 60(11):2334–2346, Nov 2003.
- [57] Mikkel Faurschou and Niels Borregaard. Neutrophil granules and secretory vesicles in inflammation. *Microbes Infect*, 5(14):1317–1327, Nov 2003.
- [58] George Lominadze, David W Powell, Greg C Luerman, Andrew J Link, Richard A Ward, and Kenneth R McLeish. Proteomic analysis of human neutrophil granules. *Mol Cell Proteomics*, 4(10):1503–1521, Oct 2005.
- [59] Seymour J Klebanoff. Myeloperoxidase: friend and foe. *J Leukoc Biol*, 77(5):598–625, May 2005.
- [60] T. A. Bennett, B. S. Edwards, L. A. Sklar, and S. Rogelj. Sulfhydryl regulation of l-selectin shedding: phenylarsine oxide promotes activation-independent l-selectin shedding from leukocytes. *J Immunol*, 164(8):4120–4129, Apr 2000.
- [61] S. I. Simon, V. Cherapanov, I. Nadra, T. K. Waddell, S. M. Seo, Q. Wang, C. M. Dorschuk, and G. P. Downey. Signaling functions of l-selectin in neutrophils: alterations in the cytoskeleton and colocalization with cd18. *J Immunol*, 163(5):2891–2901, Sep 1999.
- [62] Philippe Van Lint and Claude Libert. Matrix metalloproteinase-8: cleavage can be decisive. *Cytokine Growth Factor Rev*, 17(4):217–223, Aug 2006.
- [63] Rajeshwar P Verma and Corwin Hansch. Matrix metalloproteinases (mmps): chemical-biological functions and (q)sars. *Bioorg Med Chem*, 15(6):2223–2268, Mar 2007.
- [64] F. J. Ollivier, B. C. Gilger, K. P. Barrie, M. E. Kallberg, C. E. Plummer, S. O'Reilly, K. N. Gelatt, and D. E. Brooks. Proteinases of the cornea and preocular tear film. *Vet Ophthalmol*, 10(4):199–206, 2007.

- [65] G. Opdenakker, P. E. Van den Steen, B. Dubois, I. Nelissen, E. Van Coillie, S. Masure, P. Proost, and J. Van Damme. Gelatinase b functions as regulator and effector in leukocyte biology. *J Leukoc Biol*, 69(6):851–859, Jun 2001.
- [66] Noah W Palm and Ruslan Medzhitov. Pattern recognition receptors and control of adaptive immunity. *Immunol Rev*, 227(1):221–233, Jan 2009.
- [67] S. Akira, K. Takeda, and T. Kaisho. Toll-like receptors: critical proteins linking innate and acquired immunity. *Nat Immunol*, 2(8):675–680, Aug 2001.
- [68] Kiyoshi Takeda and Shizuo Akira. Toll-like receptors in innate immunity. *Int Immunol*, 17(1):1–14, Jan 2005.
- [69] A. Phillip West, Anna Alicia Koblansky, and Sankar Ghosh. Recognition and signaling by toll-like receptors. *Annu Rev Cell Dev Biol*, 22:409–437, 2006.
- [70] Angela C Johnson, Xiaoxia Li, and Eric Pearlman. Myd88 functions as a negative regulator of tlr3/trif-induced corneal inflammation by inhibiting activation of c-jun n-terminal kinase. *J Biol Chem*, 283(7):3988–3996, Feb 2008.
- [71] Osamu Takeuchi, Shintaro Sato, Takao Horiuchi, Katsuaki Hoshino, Kiyoshi Takeda, Zhongyun Dong, Robert L Modlin, and Shizuo Akira. Cutting edge: role of toll-like receptor 1 in mediating immune response to microbial lipoproteins. *J Immunol*, 169(1):10–14, Jul 2002.
- [72] Sheila J Gibson, Jana M Lindh, Tony R Riter, Raymond M Gleason, Lisa M Rogers, Ashley E Fuller, JoAnn L Oesterich, Keith B Gorden, Xiaohong Qiu, Scott W McKane, Randy J Noelle, Richard L Miller, Ross M Kedl, Patricia Fitzgerald-Bocarsly, Mark A Tomai, and John P Vasilakos. Plasmacytoid dendritic cells produce cytokines and mature in response to the tlr7 agonists, imiquimod and resiquimod. *Cell Immunol*, 218(1-2):74–86, 2002.
- [73] R. M. Vabulas, P Ahmad-Nejad, C. da Costa, T. Miethke, C. J. Kirschning, H. Häcker, and H. Wagner. Endocytosed hsp60s use toll-like receptor 2 (tlr2) and tlr4 to activate the toll/interleukin-1 receptor signaling pathway in innate immune cells. *J Biol Chem*, 276(33):31332–31339, Aug 2001.
- [74] Ramunas M Vabulas, Sibylla Braedel, Norbert Hilf, Harpreet Singh-Jasuja, Sylvia Herter, Parviz Ahmad-Nejad, Carsten J Kirschning, Clarissa Da Costa, Hans-Georg Rammensee, Hermann Wagner, and Hansjorg Schild. The endoplasmic reticulum-resident heat shock protein gp96 activates dendritic cells via the toll-like receptor 2/4 pathway. *J Biol Chem*, 277(23):20847–20853, Jun 2002.
- [75] Ramunas M Vabulas, Parviz Ahmad-Nejad, Sanghamitra Ghose, Carsten J Kirschning, Rolf D Issels, and Hermann Wagner. Hsp70 as endogenous stimulus of

- the toll/interleukin-1 receptor signal pathway. *J Biol Chem*, 277(17):15107–15112, Apr 2002.
- [76] Shizuo Akira and Hiroaki Hemmi. Recognition of pathogen-associated molecular patterns by tlr family. *Immunol Lett*, 85(2):85–95, Jan 2003.
- [77] Michael J de Veer, Joan M Curtis, Tracey M Baldwin, Joseph A DiDonato, Adrienne Sexton, Malcolm J McConville, Emanuela Handman, and Louis Schofield. Myd88 is essential for clearance of leishmania major: possible role for lipophosphoglycan and toll-like receptor 2 signaling. *Eur J Immunol*, 33(10):2822–2831, Oct 2003.
- [78] Andre Bafica, Helton Costa Santiago, Romina Goldszmid, Catherine Ropert, Ricardo T Gazzinelli, and Alan Sher. Cutting edge: Tlr9 and tlr2 signaling together account for myd88-dependent control of parasitemia in trypanosoma cruzi infection. *J Immunol*, 177(6):3515–3519, Sep 2006.
- [79] Felix Yarovinsky, Sara Hieny, and Alan Sher. Recognition of toxoplasma gondii by tlr11 prevents parasite-induced immunopathology. *J Immunol*, 181(12):8478–8484, Dec 2008.
- [80] Michele A West, Robert P A Wallin, Stephen P Matthews, Henrik G Svensson, Rossana Zaru, Hans-Gustaf Ljunggren, Alan R Prescott, and Colin Watts. Enhanced dendritic cell antigen capture via toll-like receptor-induced actin remodeling. *Science*, 305(5687):1153–1157, Aug 2004.
- [81] Claudia R Ruprecht and Antonio Lanzavecchia. Toll-like receptor stimulation as a third signal required for activation of human naive b cells. *Eur J Immunol*, 36(4):810–816, Apr 2006.
- [82] Sudhanshu Agrawal, Anshu Agrawal, Barbara Doughty, Andrew Gerwitz, John Blenis, Thomas Van Dyke, and Bali Pulendran. Cutting edge: different toll-like receptor agonists instruct dendritic cells to induce distinct th responses via differential modulation of extracellular signal-regulated kinase-mitogen-activated protein kinase and c-fos. *J Immunol*, 171(10):4984–4989, Nov 2003.
- [83] Illona Gillette-Ferguson, Katrin Daehnel, Amy G Hise, Yan Sun, Eric Carlson, Eugenia Diaconu, Helen F McGarry, Mark J Taylor, and Eric Pearlman. Toll-like receptor 2 regulates cxc chemokine production and neutrophil recruitment to the cornea in onchocerca volvulus/wolbachia-induced keratitis. *Infect Immun*, 75(12):5908–5915, Dec 2007.
- [84] Amélie v Saint André, Nathan M Blackwell, Laurie R Hall, Achim Hoerauf, Norbert W Brattig, Lars Volkmann, Mark J Taylor, Louise Ford, Amy G Hise, Jonathan H Lass, Eugenia Diaconu, and Eric Pearlman. The role of endosymbiotic wolbachia

- bacteria in the pathogenesis of river blindness. *Science*, 295(5561):1892–1895, Mar 2002.
- [85] Norbert W Brattig, Chiara Bazzocchi, Carsten J Kirschning, Norbert Reiling, Dietrich W Büttner, Fabrizio Ceciliani, Frank Geisinger, Hubertus Hochrein, Martin Ernst, Hermann Wagner, Claudio Bandi, and Achim Hoerauf. The major surface protein of wolbachia endosymbionts in filarial nematodes elicits immune responses through tlr2 and tlr4. *J Immunol*, 173(1):437–445, Jul 2004.
- [86] Amy G Hise, Katrin Daehnel, Illona Gillette-Ferguson, Eun Cho, Helen F McGarry, Mark J Taylor, Douglas T Golenbock, Katherine A Fitzgerald, James W Kazura, and Eric Pearlman. Innate immune responses to endosymbiotic wolbachia bacteria in *brugia malayi* and *onchocerca volvulus* are dependent on tlr2, tlr6, myd88, and mal, but not tlr4, trif, or tram. *J Immunol*, 178(2):1068–1076, Jan 2007.
- [87] Joseph D Turner, R. Stuart Langley, Kelly L Johnston, Katrin Gentil, Louise Ford, Bo Wu, Maia Graham, Faye Sharpley, Barton Slatko, Eric Pearlman, and Mark J Taylor. Wolbachia lipoprotein stimulates innate and adaptive immunity through toll-like receptors 2 and 6 (tlr2/6) to induce disease manifestations of filariasis. *J Biol Chem*, May 2009.
- [88] Subash Babu, Carla P Blauvelt, V. Kumaraswami, and Thomas B Nutman. Diminished expression and function of tlr in lymphatic filariasis: a novel mechanism of immune dysregulation. *J Immunol*, 175(2):1170–1176, Jul 2005.
- [89] Subash Babu, Carla P Blauvelt, V. Kumaraswami, and Thomas B Nutman. Cutting edge: diminished t cell tlr expression and function modulates the immune response in human filarial infection. *J Immunol*, 176(7):3885–3889, Apr 2006.
- [90] Joseph D Turner, R. Stuart Langley, Kelly L Johnston, Gill Egerton, Samuel Wanji, and Mark J Taylor. Wolbachia endosymbiotic bacteria of *brugia malayi* mediate macrophage tolerance to tlr- and cd40-specific stimuli in a myd88/tlr2-dependent manner. *J Immunol*, 177(2):1240–1249, Jul 2006.
- [91] Helen S Goodridge, Fraser A Marshall, Kathryn J Else, Katrina M Houston, Caitlin Egan, Lamyaa Al-Riyami, Foo-Yew Liew, William Harnett, and Margaret M Harnett. Immunomodulation via novel use of tlr4 by the filarial nematode phosphorylcholine-containing secreted product, es-62. *J Immunol*, 174(1):284–293, Jan 2005.
- [92] Timothy R D J Radstake, Mieke F Roelofs, Yvonne M Jenniskens, Birgitte Oppers-Walgreen, Piet L C M van Riel, Pilar Barrera, Leo A B Joosten, and Wim B van den Berg. Expression of toll-like receptors 2 and 4 in rheumatoid synovial tissue and

- regulation by proinflammatory cytokines interleukin-12 and interleukin-18 via interferon-gamma. *Arthritis Rheum*, 50(12):3856–3865, Dec 2004.
- [93] K. Harada, K. Isse, and Y. Nakanuma. Interferon gamma accelerates nf-kappab activation of biliary epithelial cells induced by toll-like receptor and ligand interaction. *J Clin Pathol*, 59(2):184–190, Feb 2006.
- [94] Stephan Spiller, Greg Elson, Ruth Ferstl, Stefan Dreher, Thomas Mueller, Marina Freudenberg, Bruno Daubeuf, Hermann Wagner, and Carsten J Kirschning. Tlr4-induced ifn-gamma production increases tlr2 sensitivity and drives gram-negative sepsis in mice. *J Exp Med*, 205(8):1747–1754, Aug 2008.
- [95] Yves Delneste, Peggy Charbonnier, Nathalie Herbault, Giovanni Magistrelli, Gersende Caron, Jean-Yves Bonnefoy, and Pascale Jeannin. Interferon-gamma switches monocyte differentiation from dendritic cells to macrophages. *Blood*, 101(1):143–150, Jan 2003.
- [96] Q. Tang and R. L. Hendricks. Interferon gamma regulates platelet endothelial cell adhesion molecule 1 expression and neutrophil infiltration into herpes simplex virus-infected mouse corneas. *J Exp Med*, 184(4):1435–1447, Oct 1996.
- [97] Yue Wu, Paul Stabach, Michael Michaud, and Joseph A Madri. Neutrophils lacking platelet-endothelial cell adhesion molecule-1 exhibit loss of directionality and motility in cxcr2-mediated chemotaxis. *J Immunol*, 175(6):3484–3491, Sep 2005.
- [98] Rachel M McLoughlin, Jean C Lee, Dennis L Kasper, and Arthur O Tzianabos. Ifn-gamma regulated chemokine production determines the outcome of staphylococcus aureus infection. *J Immunol*, 181(2):1323–1332, Jul 2008.
- [99] R. L. Gendron, C. Y. Liu, H. Paradis, L. C. Adams, and W. W. Kao. Mk/t-1, an immortalized fibroblast cell line derived using cultures of mouse corneal stroma. *Mol Vis*, 7:107–113, May 2001.
- [100] André Boonstra, Ricardo Rajsbaum, Mary Holman, Rute Marques, Carine Asselin-Paturel, João Pedro Pereira, Elizabeth E M Bates, Shizuo Akira, Paulo Vieira, Yong-Jun Liu, Giorgio Trinchieri, and Anne O’Garra. Macrophages and myeloid dendritic cells, but not plasmacytoid dendritic cells, produce il-10 in response to myd88- and trif-dependent tlr signals, and tlr-independent signals. *J Immunol*, 177(11):7551–7558, Dec 2006.
- [101] Illona Gillette-Ferguson, Amy G Hise, Helen F McGarry, Joseph Turner, Andrew Esposito, Yan Sun, Eugenia Diaconu, Mark J Taylor, and Eric Pearlman. Wolbachia-induced neutrophil activation in a mouse model of ocular onchocerciasis (river blindness). *Infect Immun*, 72(10):5687–5692, Oct 2004.

- [102] E. Pearlman, J. W. Kazura, F. E. Hazlett, and W. H. Boom. Modulation of murine cytokine responses to mycobacterial antigens by helminth-induced t helper 2 cell responses. *J Immunol*, 151(9):4857–4864, Nov 1993.
- [103] C. M. Snapper, C. Peschel, and W. E. Paul. Ifn-gamma stimulates igg2a secretion by murine b cells stimulated with bacterial lipopolysaccharide. *J Immunol*, 140(7):2121–2127, Apr 1988.
- [104] S. Huang, W. Hendriks, A. Althage, S. Hemmi, H. Bluethmann, R. Kamijo, J. Vilcek, R. M. Zinkernagel, and M. Aguet. Immune response in mice that lack the interferon-gamma receptor. *Science*, 259(5102):1742–1745, Mar 1993.
- [105] Y. Kawano, T. Noma, and J. Yata. Regulation of human igg subclass production by cytokines. ifn-gamma and il-6 act antagonistically in the induction of human igg1 but additively in the induction of igg2. *J Immunol*, 153(11):4948–4958, Dec 1994.
- [106] R. K. Mehlotra, L. R. Hall, A. W. Higgins, I. A. Dreshaj, M. A. Haxhiu, J. W. Kazura, and E. Pearlman. Interleukin-12 suppresses filaria-induced pulmonary eosinophilia, deposition of major basic protein and airway hyperresponsiveness. *Parasite Immunol*, 20(10):455–462, Oct 1998.
- [107] Pedram Hamrah, Ying Liu, Qiang Zhang, and M. Reza Dana. The corneal stroma is endowed with a significant number of resident dendritic cells. *Invest Ophthalmol Vis Sci*, 44(2):581–589, Feb 2003.
- [108] Pedram Hamrah and M. Reza Dana. Corneal antigen-presenting cells. *Chem Immunol Allergy*, 92:58–70, 2007.
- [109] Norimitsu Kadowaki. Dendritic cells: a conductor of t cell differentiation. *Allergol Int*, 56(3):193–199, Sep 2007.
- [110] F. Re and J. L. Strominger. Toll-like receptor 2 (tlr2) and tlr4 differentially activate human dendritic cells. *J Biol Chem*, 276(40):37692–37699, Oct 2001.
- [111] Gabriele Grunig, Alice Banz, and Rene de Waal Malefyt. Molecular regulation of th2 immunity by dendritic cells. *Pharmacol Ther*, 106(1):75–96, Apr 2005.
- [112] Andrew S MacDonald, Amy D Straw, Nicole M Dalton, and Edward J Pearce. Cutting edge: Th2 response induction by dendritic cells: a role for cd40. *J Immunol*, 168(2):537–540, Jan 2002.
- [113] W. Lu, G. L. Egerton, A. E. Bianco, and S. A. Williams. Thioredoxin peroxidase from onchocerca volvulus: a major hydrogen peroxide detoxifying enzyme in filarial parasites. *Mol Biochem Parasitol*, 91(2):221–235, Mar 1998.

- [114] S. Schrum, A. Bialonski, T. Marti, and P. F. Zipfel. Identification of a peroxidoxin protein (ovpxn-2) of the human parasitic nematode *onchocerca volvulus* by sequential protein fractionation. *Mol Biochem Parasitol*, 94(1):131–135, Jul 1998.
- [115] I. Ghosh, S. W. Eisinger, N. Raghavan, and A. L. Scott. Thioredoxin peroxidases from *brugia malayi*. *Mol Biochem Parasitol*, 91(2):207–220, Mar 1998.
- [116] N. C. Smith and C. Bryant. The effect of antioxidants on the rejection of *nippostrongylus brasiliensis*. *Parasite Immunol*, 11(2):161–167, Mar 1989.
- [117] E. Pearlman, F. P. Heinzl, F. E. Hazlett, and J. W. Kazura. Il-12 modulation of t helper responses to the filarial helminth, *brugia malayi*. *J Immunol*, 154(9):4658–4664, May 1995.
- [118] Takahiro Nakamura, Fumihiko Ishikawa, Koh hei Sonoda, Toshio Hisatomi, Hong Qiao, Jun Yamada, Mitsuhiro Fukata, Tatsuro Ishibashi, Mine Harada, and Shigeru Kinoshita. Characterization and distribution of bone marrow-derived cells in mouse cornea. *Invest Ophthalmol Vis Sci*, 46(2):497–503, Feb 2005.
- [119] C. Marcos-Atxutegi, L. H. Kramer, I. Fernandez, L. Simoncini, M. Genchi, G. Prieto, and F. Simón. Th1 response in balb/c mice immunized with *dirofilaria immitis* soluble antigens: a possible role for *wolbachia*? *Vet Parasitol*, 112(1-2):117–130, Feb 2003.
- [120] Maurizio Casiraghi, Odile Bain, Ricardo Guerrero, Coralie Martin, Vanessa Pocacqua, Scott L Gardner, Alberto Franceschi, and Claudio Bandi. Mapping the presence of *wolbachia pipientis* on the phylogeny of filarial nematodes: evidence for symbiont loss during evolution. *Int J Parasitol*, 34(2):191–203, Feb 2004.
- [121] Chantima Porksakorn, Surang Nuchprayoon, Kiwon Park, and Alan L Scott. Proinflammatory cytokine gene expression by murine macrophages in response to *brugia malayi* *wolbachia* surface protein. *Mediators Inflamm*, 2007:84318, 2007.
- [122] Ute Buwitt-Beckmann, Holger Heine, Karl-Heinz Wiesmüller, Günther Jung, Roland Brock, Shizuo Akira, and Artur J Ulmer. Tlr1- and tlr6-independent recognition of bacterial lipopeptides. *J Biol Chem*, 281(14):9049–9057, Apr 2006.
- [123] Paola Massari, Philipp Henneke, Yu Ho, Eicke Latz, Douglas T Golenbock, and Lee M Wetzler. Cutting edge: Immune stimulation by neisserial porins is toll-like receptor 2 and myd88 dependent. *J Immunol*, 168(4):1533–1537, Feb 2002.
- [124] Paola Massari, Alberto Visintin, Jay Gunawardana, Kristen A Halmen, Carol A King, Douglas T Golenbock, and Lee M Wetzler. Meningococcal porin porb binds to tlr2 and requires tlr1 for signaling. *J Immunol*, 176(4):2373–2380, Feb 2006.

- [125] Amlan Biswas, Pallavi Banerjee, Gayatri Mukherjee, and Tapas Biswas. Porin of shigella dysenteriae activates mouse peritoneal macrophage through toll-like receptors 2 and 6 to induce polarized type i response. *Mol Immunol*, 44(5):812–820, Feb 2007.
- [126] Kiyoshi Takatsu and Hiroshi Nakajima. Il-5 and eosinophilia. *Curr Opin Immunol*, 20(3):288–294, Jun 2008.
- [127] H. C. Oettgen. Regulation of the ige isotype switch: new insights on cytokine signals and the functions of epsilon germline transcripts. *Curr Opin Immunol*, 12(6):618–623, Dec 2000.

Curriculum vitae

Scientific Career

- Since 02/2008 Postdoctoral Fellow in Prof. Achim Hoerauf's group, University of Bonn, Department of Medical Parasitology, Bonn, Germany
Research Area: Interactions between the endosymbiont bacterium *Wolbachia* and its filarial host
- 01/2005 – 11/2007 Postdoctoral Fellow in Dr. Eric Pearlman's lab, Case Western Reserve University, Cleveland, OH, USA
Research Area: Immunology of filarial infection
- 09/2000 – 09/2001 Graduate Student in Dr. Philip M Silverman's lab, Oklahoma Medical Research Foundation, Oklahoma City, OK, USA
Research Area: Horizontal Gene Transfer in *E. coli*

Bibliography

Publications

Original Publication

1. **Daehnel, K.**, Harris, R., Maddera, L. and Silverman, P., Fluorescence assays for F-pili and their application. *Microbiology* 2005. **151**:3541-3548.
2. Hise, A. G., **Daehnel, K.**, Gillette-Ferguson, I., Cho, E., McGarry, H. F., Taylor, M. J., Golenbock, D. T., Fitzgerald, K. A., Kazura, J. W. and Pearlman, E., Innate Immune Responses to Endosymbiotic *Wolbachia* Bacteria in *Brugia malayi* and *Onchocerca volvulus* Are Dependent on TLR2, TLR6, MyD88, and Mal, but Not TLR4, TRIF, or TRAM. *J Immunol* 2007. **178**:1068-1076.
3. **Daehnel, K.**, Gillette-Ferguson, I., Hise, A. G., Diaconu, E., Harling, M. J., Heinzl, F. P. and Pearlman, E., Toll-like Receptor (TLR) 2 mediates *Filaria*-induced Dendritic Cell Activation and IFN γ production, but not IL-5 production or eosinophil migration to the cornea in a murine model of river blindness. *Parasite Immunol* 2007. **29**:463-473.
4. Gillette-Ferguson, I., **Daehnel, K. (co-first author)**, Hise, A. G., Sun, Y., Carlson, E., Diaconu, E., McGarry, H. F., Taylor, M. J., and Pearlman, E., Toll-like receptor 2 regulates CXC chemokine production and neutrophil recruitment to the cornea in *Onchocerca volvulus*/*Wolbachia*-induced keratitis. *Infect Immun* 2007. **75**:5908-5915.
5. Portillo, J. A., Van Grol, J., Zheng, L., Okenka, G., **Gentil, K.**, Garland, A., Carlson, E. C., Kern, T. S., and Subauste, C. S., CD40 mediates retinal inflammation and neurovascular degeneration. *J Immunol* 2008. **181**:8719-8726.
6. **Gentil, K.**, Pearlman, E., IFN γ mediates neutrophil infiltration into the corneal stroma in a mouse model of *Onchocerca volvulus* keratitis. *Infect Immun* 2009. **77**:1606-1612.

7. Turner J.D., Langley, R. S. Johnston, K. L., **Gentil, K.**, Ford, L., Wu, B., Graham, M., Sharpley, F., Slatko, B., Pearlman, E., Taylor, M. J. *Wolbachia* lipoprotein stimulates innate and adaptive immunity through toll-like receptors 2 and 6 (TLR2/6) to induce disease manifestations of filariasis. *J Biol Chem* 2009.

Reviews

1. **Daehnel, K.**, Hise, A. G., Gillette-Ferguson, I., and Pearlman, E., *Wolbachia* and *Onchocerca volvulus*: Pathogenesis of River Blindness. 2007. Bookchapter in *Wolbachia: a but's life in another bug*. Hoerauf, A., Rao, R. U. (ed). (Karger press)
2. Ghedin, E., **Daehnel, K.**, Foster, J., Slatko, B., Lustigman, S., The symbiotic relationship between filarial parasitic nematodes and their *Wolbachia* endosymbionts – a resource for a new generation of control measures. *Symbiosis* 2008.

Dissertation

A mutagenic approach to F pilus structure and function. Universität Göttingen, Abteilung für Mikrobiologie, June 2002.

Honors and Awards

- | | |
|-------------------|---|
| 07/2009 | International Eosinophil Society meeting, Brugge, Belgium
Travel Award |
| 02/2009 | Symposium Infektion und Immunabwehr, Rothenfels, Germany
Presentation Award |
| 11/2006 | Society of Leukocyte Biology meeting, San Antonio, TX, USA
Finalist in the Young Investigator Award Competition |
| 06/2006 – 05/2007 | Scholarship German Research Foundation (DFG DA1024/1-1),
Project: "Role of Toll-like receptors in dendritic cell maturation and T
cell activation in response to <i>Wolbachia</i> and filarial antigens." |
| 1999 – 2004 | Fellow of the German National Merit Foundation |
| 2003 | Fellow of the Carlo-Schmid-Program for internships in International
Organizations, funded by the German Academic Exchange Service and
the German National Merit Foundation |

Köln, 07.08.2009